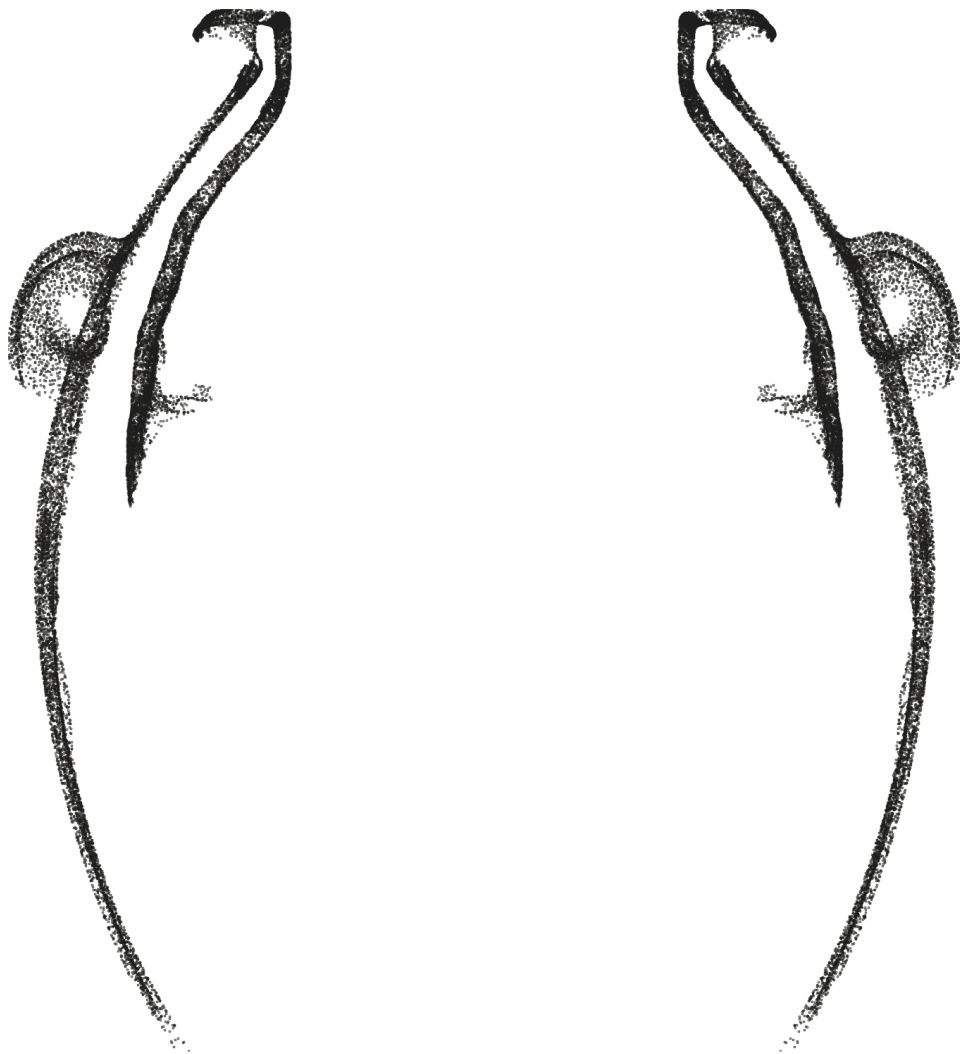


MV016c - Tall Shouldered Jar

An Exploration of Precision



Author: Stine Gerdes, arcsai.org

License: Creative Commons BY-NC-SA 4.0

Date: 2025-07-21

Version: 01.20



Petrie Museum, CC BY-NC-SA

Contents

Artifact Information	2
Alignment In The Cartesian Coordinate System	3
Statistics used throughout the report	5
Precision	6
Circularity	6
Concentricity	30
Coaxiality	43
Surface Variability	47
Precision Score Of The Artifact	56
Analysis Roadmap	58
Appendix A - Comparison Of Circularity Measurements (Z-plane vs. surface-perpendicular)	59
Appendix B - Comparison Of Concentricity Measurements (Z-plane vs. surface-perpendicular)	69

Artifact Information

Artifact Data

Collection	Petrie Museum of Egyptian Archaeology
Provenance ¹	Petrie Museum of Egyptian Archaeology (London), recovered by Flinders Petrie
Provenience ²	Naqada Tomb T 16 (Naqada II) - Petrie Excavation
Attribution	Naqada II

Museum information

Ref.	LDUCE-UC4356
Description	Stone vase, basalt, barrel shaped, type 55. From Naqada Tomb T 16
URL	https://collections.ucl.ac.uk/Details/collect/6564

Maijers vessel classification³

Short classification	Tall Shouldered Jar
Long classification	The vessel is created in a closed form classified as a tall jar with a shouldered shape, it has a footed base and a raised blunt rim.

Physical properties

Precision score ⁴	2.27
Height (approximate)	144 mm 5.67 in
Width (approximate)	108 mm 4.25 in
Material	Basalt
Mohs Hardness ⁵	6 - 7 (Basalt)
Weight	

Scan information

Source	Max Fomitchev-Zamilov, 3D Scans of the Naqada Period Stone Vessels from the Petrie Museum of Egyptian and Sudanese Archeology, 2025.
Source file name	UC4356-lo-30deg.stl
Scan method	CMM
Scanner	Keyence VL -500
Rated scan accuracy	10 µm 0.41 thou
Scan date	2025-05-12
Scanned by	Max Fomitchev-Zamilov

Mesh decimation	None, raw scan file used in the analysis
Number of vertices	270 066
Mesh density ⁶	206 µm 8.12 thou
Max vertex distance	1372 µm 54.000 thou
Min vertex distance	8 µm 0.328 thou
Vertices per cm ²	313 (approximated)
Vertices per in ²	2019 (approximated)

¹The verifiable chain of custody of an artifact

²The location or site where an artifact was recovered

³Vessel artifact classification developed by W. Arnold Maijer and described in his publication Masters of Stone, ISBN 978-90-829212-0-5

⁴The precision score metric is described in Precision Score Of The Artifact, p. 57

⁵The Mohs scale is an ordinal scale, from 1 to 10, describing the materials resistance to abrasion (the ability of harder material to scratch softer material)

⁶Median distance between vertices

Alignment In The Cartesian Coordinate System

For precise and valid measurements of the vessel's geometry to be possible, the points of the scanned dataset must first and foremost be placed optimally in a Cartesian coordinate system. Several alignment methods and algorithms have been tested on a number of different vessels to determine the best way to achieve optimal alignment.

Any misalignment of the artifact will increase the error of the precision measurements, due to the distortion/wobble effect caused by the misaligned object. To visualize this distortion, we can consider a representation of the three-dimensional point cloud data, folded to a two-dimensional plane. This folded representation is obtained by rotating all scanned points around an assumed center axis to $y = 0, x > 0$, thus resulting in a two-dimensional profile representation of all scanned vertices in the object.

Figure 1 illustrates this effect on a ideal ellipsoid. In the first image, the ellipsoid is perfectly aligned, resulting in a narrow and precise two-dimensional folded profile. As misalignments are introduced, the two-dimensional profile increases in width, visually showing the distortion, causing the error in the precision measurements to increase. While easy to understand visually, this distortion can also be objectively quantified, and as such used to compare the fitness of different assumed center axes against each other, and further to create an automated and solid process for optimal Cartesian alignment of the scan data.

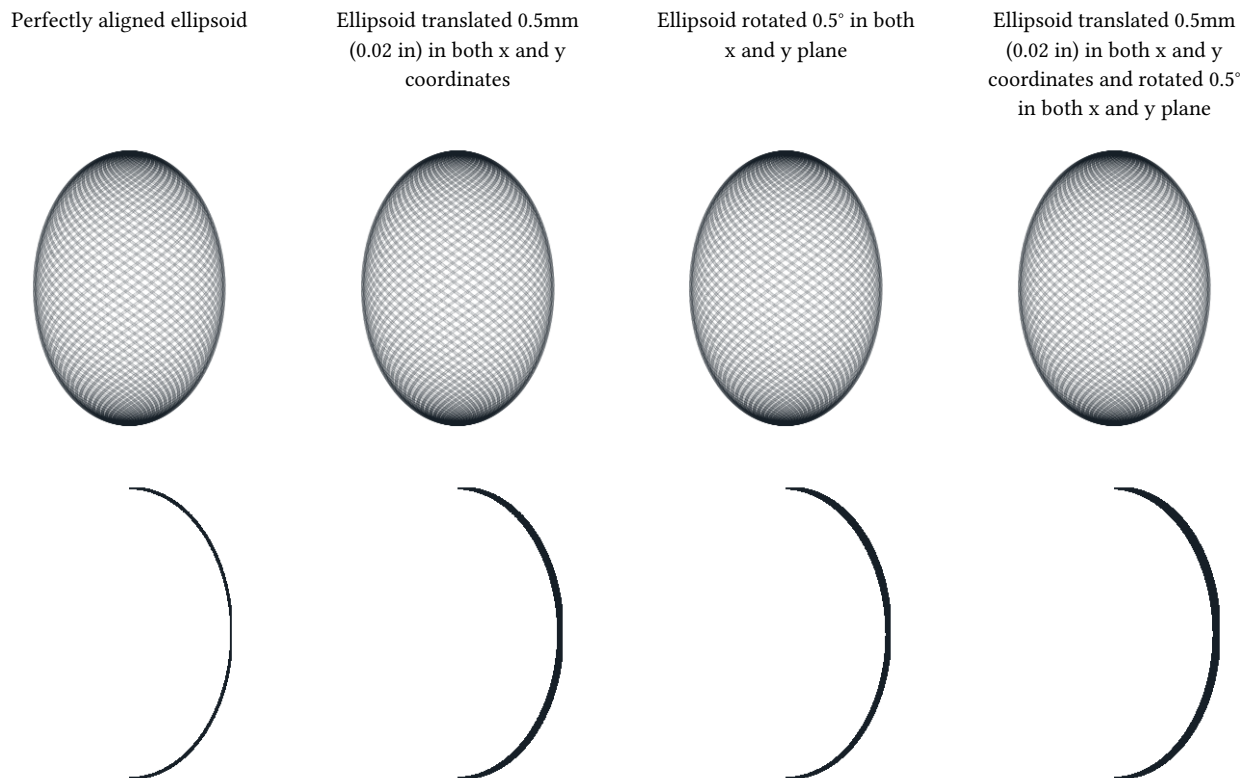


Figure 1: Distortion caused by a misalignment of the artifact

In contemporary metrology analysis of modern production objects, it is common to align the object in a Cartesian coordinate system by fitting a flat surface of the object to a reference plane in the coordinate system, cylindrical features to an ideal cylinder etc., or by using specific markers placed on the object in the design process. This methodology, however, is inadequate for the ancient objects in question. Most scanned artifacts, do not have a valid flat surface which could be aligned to a plane in the Cartesian coordinate system; most surfaces seem to be curved. Some artifacts do have a flat base, however this is often a worn area of the artifact and practical tests have shown that alignment to such surfaces will not produce optimal alignment of the scan data.

As conventional methods of alignment do not always yield good results with these types of artifacts, a more adequate method of alignment has been developed to enable precise measurements and statistical analysis of the scan data.

To find the optimal position of the vessel in the coordinate system, a range of rotation and translation tests are carried out to find the best fit of the central axis.

Based on the assumption that the analyzed object was created using a rotational process, and thus have symmetry around a central axis, the alignment of the artifact is carried out in a two-step process. An overview of this process is given below.

The artifact is placed in a Cartesian coordinate system, in an initially unaligned state. The first step in the alignment process estimates the central rotational axis of the vessel, by analyzing the coaxiality of thin cross-section slices of the vessel. The slices will be as thin as possible based on the mesh density of the scan, while still ensuring enough data points in each slice to be statistically valid.

For each slice, circular regression⁷ (estimate of best fit circle) is used to estimate the center point of this slice. Combined over the total Z-axis range of the vessel, these center points provide us with an indicator of the incline and position of the vessel's central axis.

The next step will optimize the center axis alignment by progressively minimizing the deviation (perpendicular to the surface curvature) of the two-dimensional profile, see Figure 1. By ascertaining and comparing the resulting fit of many thousands of different potential rotations, the best fit alignment of the scan data can be estimated, and an optimal center axis (in relation to the data points) can be reconstructed. The actual three-dimensional point-cloud is then aligned to this axis, by rotating and translating the scanned data points to match the Z-axis of the Cartesian coordinate system.

To enable extensive analysis of the full surface of the artifact, the mesh is split into exterior and interior surfaces. The exterior surface is aligned independently of interior data points, providing a baseline for exterior quality assessment. The interior surface is represented by two alignments:

- Aligned with the exterior mesh to analyze concentricity, and
- Aligned separately to assess its precision and compare the true tilt/displacement between interior and exterior surfaces.

⁷Circle regression algorithm used: Kenichi Kanatani, Prasanna Rangarajan, "Hyper least squares fitting of circles and ellipses" Computational Statistics & Data Analysis, Vol. 55, pages 2197-2208, (2011)

Statistics used throughout the report

This section provides an overview of the key statistical and model-evaluation metrics employed throughout the report to analyze dataset variability, model fit, and predictive accuracy.

Each measure is introduced with its mathematical formulation, practical interpretation, and explicit reference to how it is calculated in the context of the evaluated models and residuals. Together, these metrics quantify:

- Data variability (e.g., MAD, Standard Deviation, Range).
- Model accuracy (e.g., MSD, RMSD).
- Robustness vs. sensitivity to extreme values and central tendencies.

Mean Squared Deviation (MSD), also known as Mean Squared Error (MSE).

$$\text{MSD} = \frac{\sum_{i=1}^n (y_i - \hat{y})^2}{n}$$

The Mean Squared Deviation (MSD) measures the average magnitude of squared differences between observed (y_i) and predicted (\hat{y}) values, calculated as the mean of squared residuals, and is used as a measure of discrepancy in regression and model-fitting contexts.

This measure amplifies the influence of larger deviations through squaring, emphasizes imperfections in the observed data, but retains sensitivity to outliers.

Root Mean Squared Deviation (RMSD), also known as Root Mean Squared Error (RMSE).

$$\text{RMSD} = \sqrt{\frac{\sum_{i=1}^n (y_i - \hat{y})^2}{n}}$$

The Root Mean Square Deviation (RMSD) measures the magnitude of differences between observed (y_i) and predicted (\hat{y}) values by calculating the square root of the average of squared residuals.

RMSD is a commonly used measure of discrepancy in regression and model-fitting contexts. It quantifies the average magnitude of residuals while retaining sensitivity to larger deviations (via squaring), making it particularly useful for evaluating model accuracy.

Standard Deviation (SD)

$$s = \sqrt{\frac{\sum_{i=1}^n (y_i - \bar{y})^2}{n - 1}}$$

The Standard Deviation measures the spread of data (y_i) around the mean (\bar{y}) by calculating the square root of the average of squared differences between each value and the mean.

It is sensitive to outliers as it amplifies their influence through squaring, in contrast to MAD.

Throughout this report, the Standard Deviation is calculated using the absolute residuals from regression models.

Median Absolute Deviation (MedianAD)

$$\text{MedianAD} = \text{median}(|y_i - \text{median}(y)|)$$

The Median Absolute Deviation (MAD) measures the spread of data around the median by calculating the median of absolute differences between each value and the median.

MAD is a robust measure of spread, analogous to the interquartile range (a robust measure centered on the middle 50% of data), and differs from the standard deviation in that it minimizes the impact of outliers.

Throughout this report, the MAD is calculated using the absolute values of residuals from regression models.

Range

$$\max(y_i) - \min(y_i)$$

The Range measures the spread of a dataset by calculating the difference between the maximum and minimum values.

The Range is a simple measure of spread, capturing the full extent of variability. Range is very sensitive to extreme values, as it is entirely determined by the two most extreme data points.

Throughout this report, the Range is calculated using the full range of residuals from regression models.

Precision

To explore the manufacturing precision of the artifact in depth, the following analysis have been carried out:

- Circularity around the axis of symmetry is examined in detail at selected cross-sections.
- Overall circularity around the axis of symmetry is measured for the full height of the vessel (areas of the vessel with extensive damage are not taken into account for this metric).
- Concentricity of the vessel between selected cross-sections are examined in detail to determine if the existence of an axis of rotation in the manufacture of the object can be established.
- The coaxiality of the vessel is analyzed to explore the precision of the central axis of the object.
- The surface variability is analyzed and visualized on through a heatmap.

Circularity

Circularity is the measurement of how round the surface of an object is, optionally in reference to a datum axis. The *circularity tolerance* is the radial distance of two circles, each with their centers in the datum axis, and each of them conforming, respectively, to the minimum and maximum deviations of the data-set to a true circle, see Figure 2.

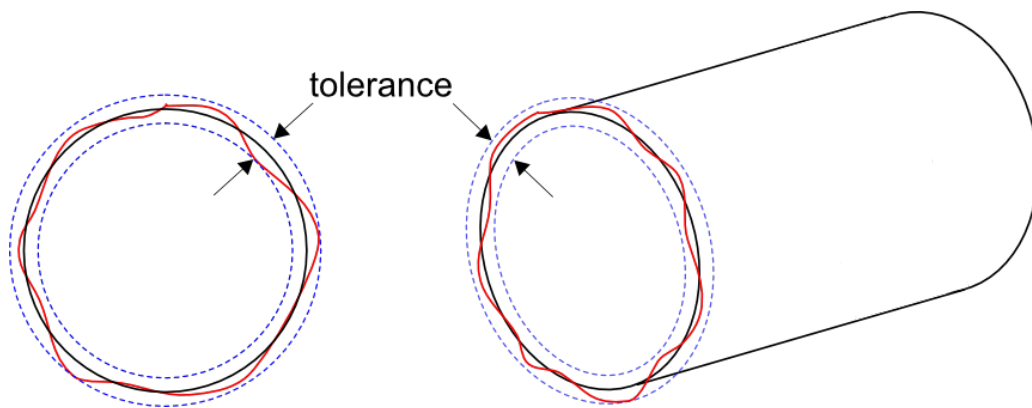


Figure 2: Circularity tolerance.

Circularity is examined at different cross-sections of the vessel, using the established Z-axis as the datum axis (axis of symmetry). The distance between the scanned points in the local datum plane is measured to determine the range between the two concentric circles encompassing the measured points, see Figure 3.

Referencing all of the individual circularity measurements to the global (reconstructed) axis of symmetry of the object, allows us to ascertain not only circularity of local features of the object, but how well circularity was *maintained* over the entire manufacturing process. This is an important distinction, which may be able to provide valuable insights into requirements of the construction methods. For reference, and seeing that the variance in local circularity also holds interest, measurements of circularity of the vessel without reference to the axis of symmetry can additionally be found in the Concentricity, p. 31.



Figure 3: Circularity measurements.

If the circularity is determined from slices of the vessel exclusively in the *Z-plane* (actually measuring the cylindricity of a very thin slices of the vessel, in an attempt to approximate circularity), this would - in some areas - introduce significant distortion (increasing measurement errors) in the samples, due to the curvature of the vessel's surface.

Each sample slice of the vessel is therefore obtained perpendicular to the surface curvature, see Figure 6 to Figure 16. The measurements are taken conservatively without filtration of potential outliers.

To explore the potential distortion caused by obtaining samples in the Z-plane only, please refer to Appendix A, where measurements in the Z-plane and measurements perpendicular to surface curvature are compared side by side.

Detailed circularity measurements of selected points

Circularity measurements across a range of selected slices of the vessel (see Table 1) have been analyzed in-depth, and detailed plots of each measurement is provided. Furthermore, full circularity measurements are shown for each available scanned surface including a detailed plot to visualize the circularity of all areas of the vessel.

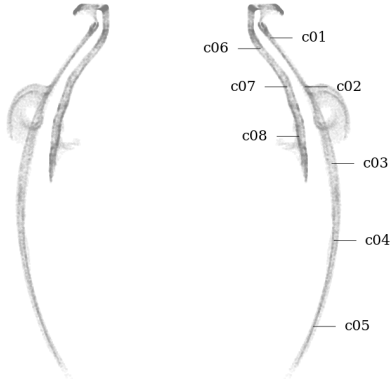


Figure 4: Circularity measurement sample locations, full mesh aligned with exterior surface

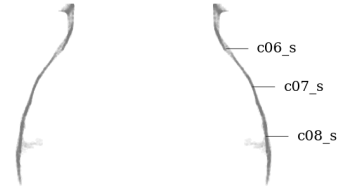


Figure 5: Circularity measurement sample location, separately aligned interior mesh

Metric

Tag	Area	Measured deviation ⁸	Residuals				Sample size	Slice		
			Range	RMSD ⁹	MAD ¹⁰	SD		Height	Z coord.	Radius ¹¹
		mm	mm	mm	mm	mm		mm	mm	mm
c01	exterior	Ø61.619±0.703	1.238	0.419	0.134	0.179	90	0.200	130.027	30.810
c02	exterior	Ø84.997±1.159	1.984	0.565	0.141	0.270	96	0.200	113.564	42.499
c03	exterior	Ø102.924±2.178	3.561	0.982	0.392	0.463	147	0.200	87.878	51.462
c04	exterior	Ø104.396±1.413	2.551	0.735	0.293	0.370	188	0.200	61.934	52.198
c05	exterior	Ø90.543±1.001	1.726	0.430	0.210	0.289	116	0.200	33.154	45.272
c06	interior	Ø55.143±0.987	1.900	0.711	0.167	0.249	151	0.200	126.417	27.572
c06_s	interior sep.	Ø55.278±0.859	1.452	0.496	0.131	0.219	176	0.200	126.417	27.639
c07	interior	Ø73.070±1.324	2.566	0.799	0.272	0.348	251	0.200	113.564	36.535
c07_s	interior sep.	Ø73.161±0.204	0.374	0.105	0.045	0.056	216	0.200	113.564	36.581
c08	interior	Ø81.112±1.976	2.898	0.827	0.171	0.476	366	0.200	97.005	40.556
c08_s	interior sep.	Ø82.136±0.628	1.187	0.274	0.104	0.159	376	0.200	97.005	41.068

Imperial

Tag	Area	Measured deviation ⁸	Residuals				Sample size	Slice		
			Range	RMSD ⁹	MAD ¹⁰	SD		Height	Z coord.	Radius ¹¹
		in	in	in	in	in		in	in	in
c01	exterior	Ø2.4260±0.0277	0.0487	0.0165	0.0053	0.0071	90	0.0079	5.1192	1.2130
c02	exterior	Ø3.3463±0.0456	0.0781	0.0223	0.0056	0.0106	96	0.0079	4.4710	1.6732
c03	exterior	Ø4.0521±0.0858	0.1402	0.0387	0.0155	0.0182	147	0.0079	3.4598	2.0261
c04	exterior	Ø4.1101±0.0556	0.1004	0.0289	0.0115	0.0146	188	0.0079	2.4383	2.0550
c05	exterior	Ø3.5647±0.0394	0.0679	0.0169	0.0083	0.0114	116	0.0079	1.3053	1.7823
c06	interior	Ø2.1710±0.0388	0.0748	0.0280	0.0066	0.0098	151	0.0079	4.9771	1.0855
c06_s	interior sep.	Ø2.1763±0.0338	0.0572	0.0195	0.0052	0.0086	176	0.0079	4.9771	1.0881
c07	interior	Ø2.8768±0.0521	0.1010	0.0315	0.0107	0.0137	251	0.0079	4.4710	1.4384
c07_s	interior sep.	Ø2.8804±0.0080	0.0147	0.0041	0.0018	0.0022	216	0.0079	4.4710	1.4402
c08	interior	Ø3.1934±0.0778	0.1141	0.0325	0.0068	0.0187	366	0.0079	3.8191	1.5967
c08_s	interior sep.	Ø3.2337±0.0247	0.0467	0.0108	0.0041	0.0062	376	0.0079	3.8191	1.6169

Table 1: Detailed circularity measurements at selected samples of MV016c.

Figure 6 to Figure 16 shows a detailed plots of each circularity measurement.

⁸Sample diameter Ø± maximum measured deviation from measured radius

⁹Root mean square deviation (RMSD) also called Root mean square error (RMSE)

¹⁰Median absolute deviation

¹¹Median sample radius from z-axis

Graphical overview of circularity measurement c01

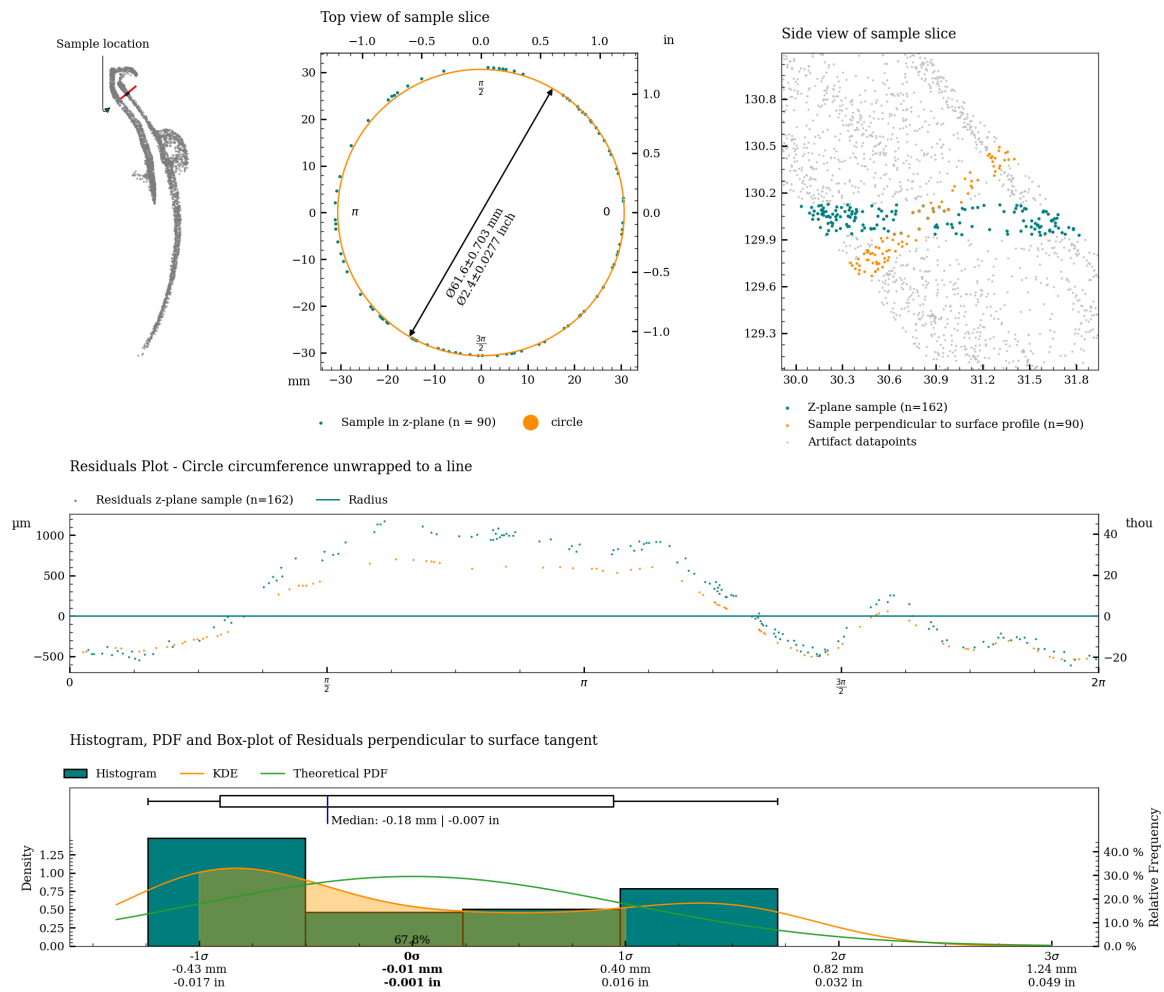


Figure 6: Charts with statistics for the measurement of c01.

Graphical overview of circularity measurement c02

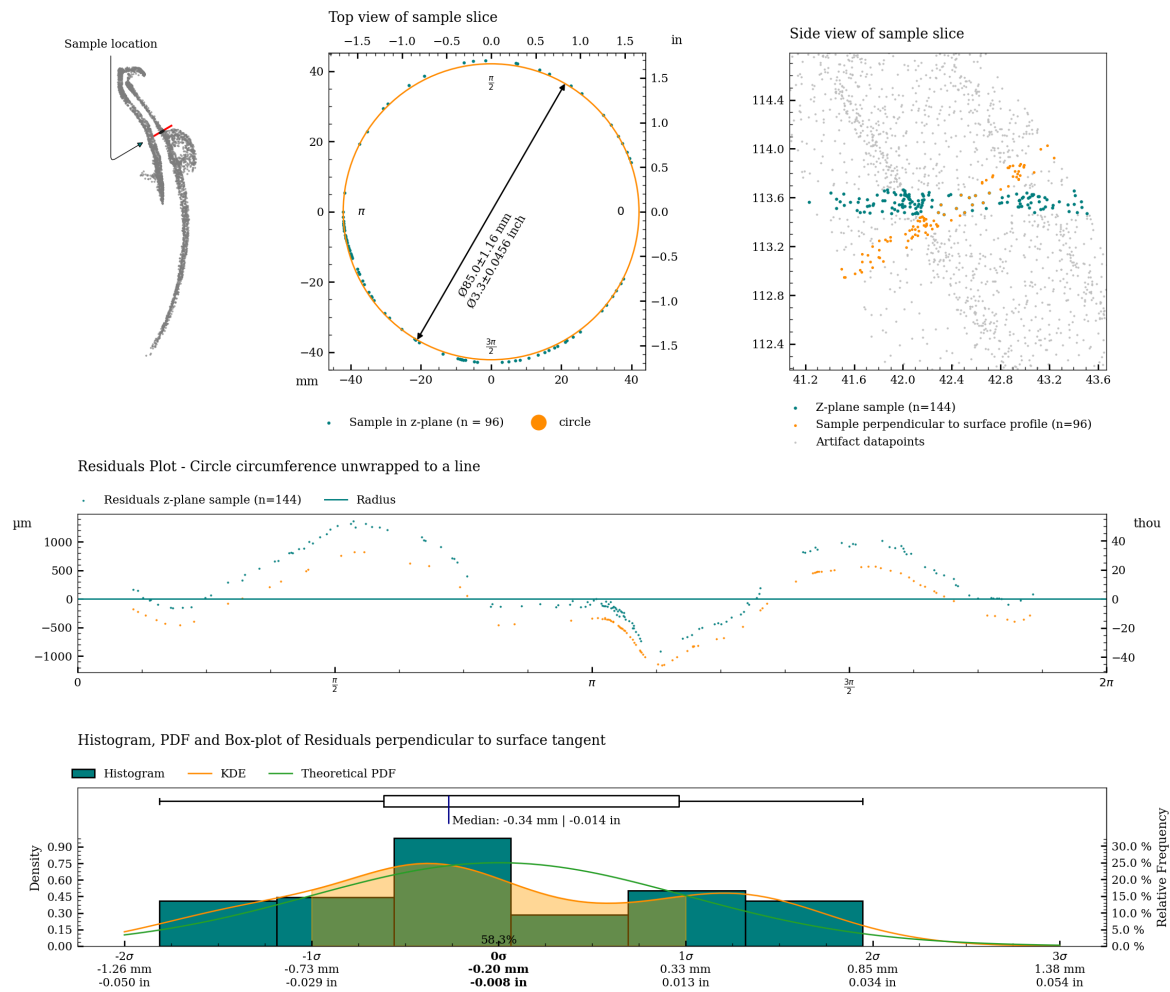


Figure 7: Charts with statistics for the measurement of c02.

Graphical overview of circularity measurement c03

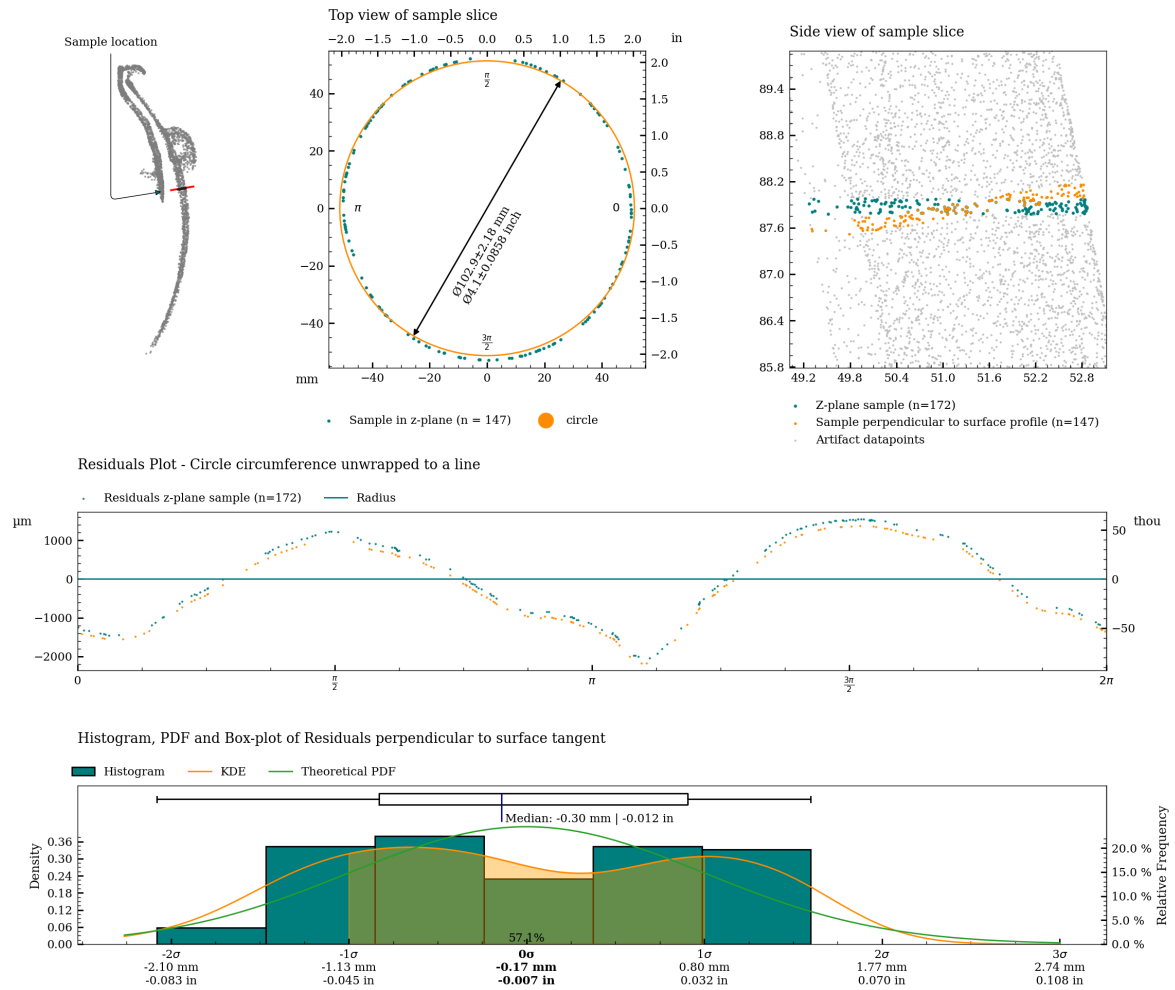


Figure 8: Charts with statistics for the measurement of c03.

Graphical overview of circularity measurement c04

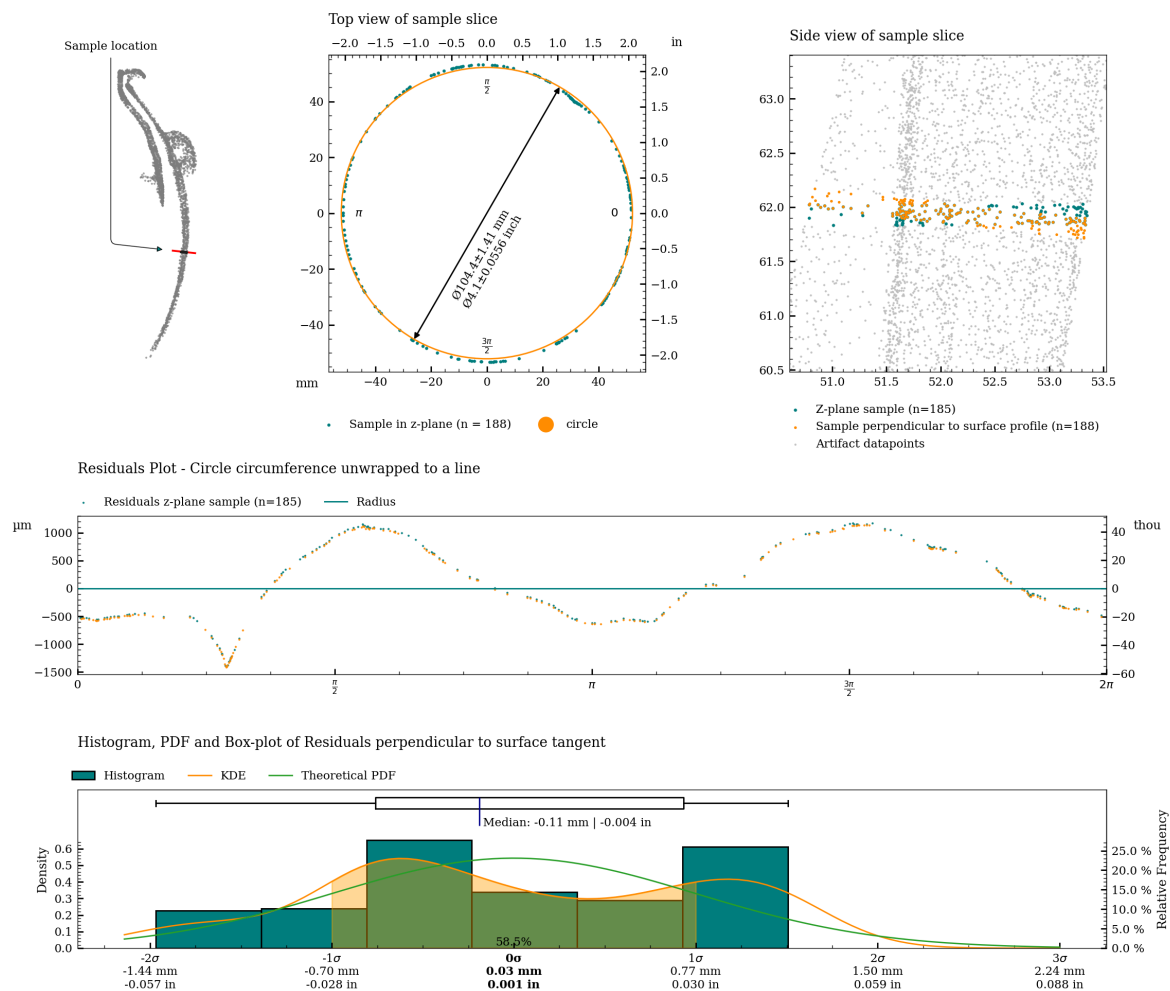


Figure 9: Charts with statistics for the measurement of c04.

Graphical overview of circularity measurement c05

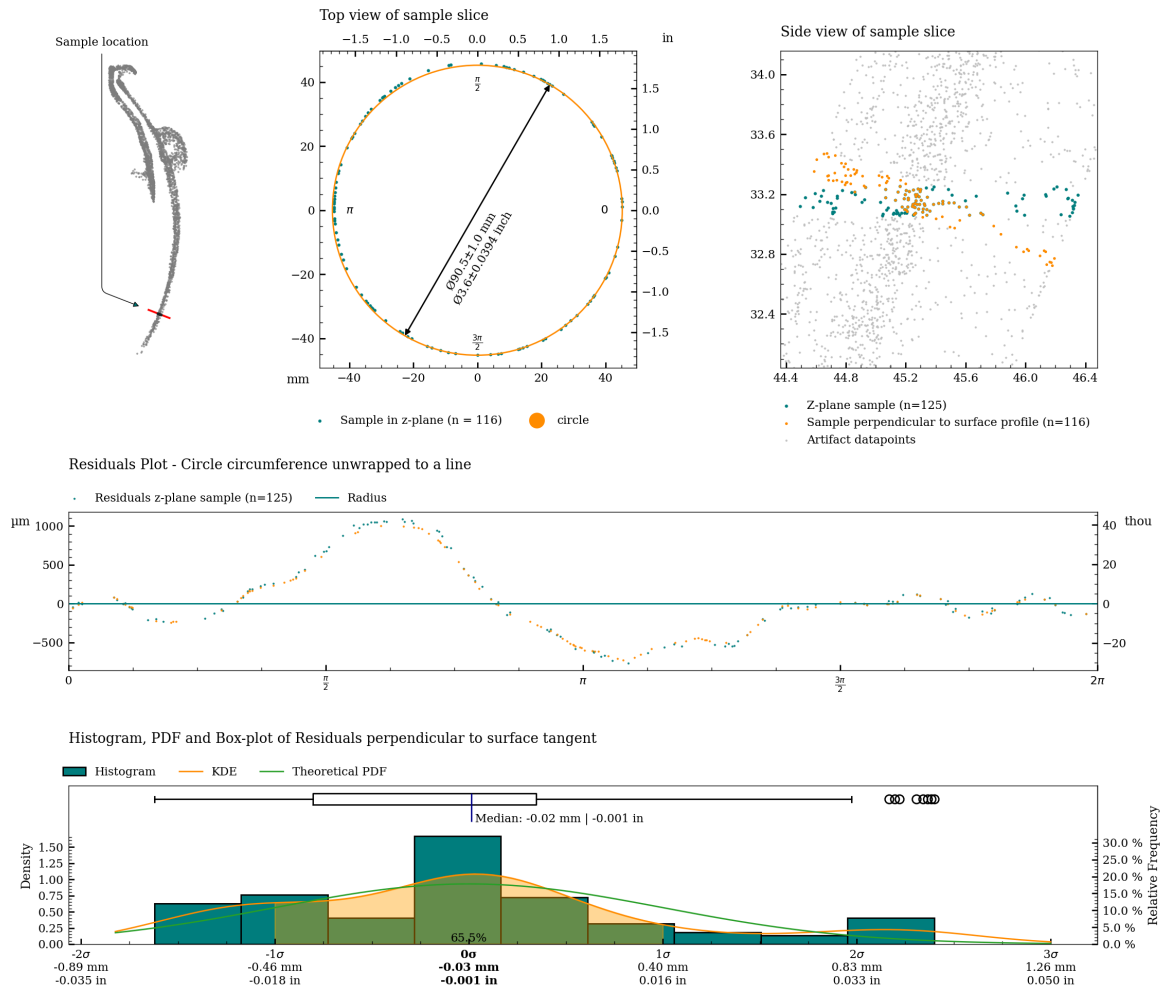


Figure 10: Charts with statistics for the measurement of c05.

Graphical overview of circularity measurement c06

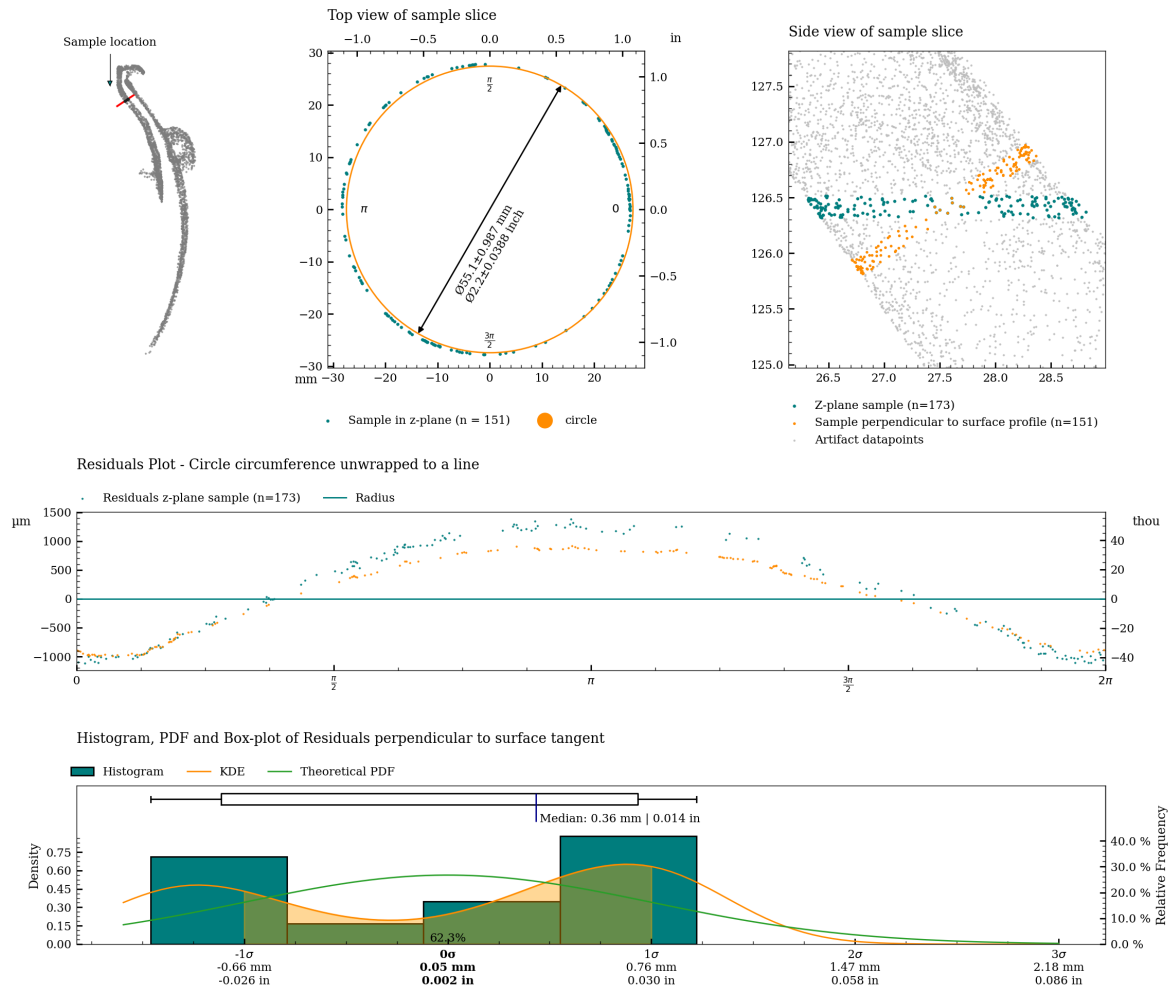


Figure 11: Charts with statistics for the measurement of c06.

Graphical overview of circularity measurement c06_s

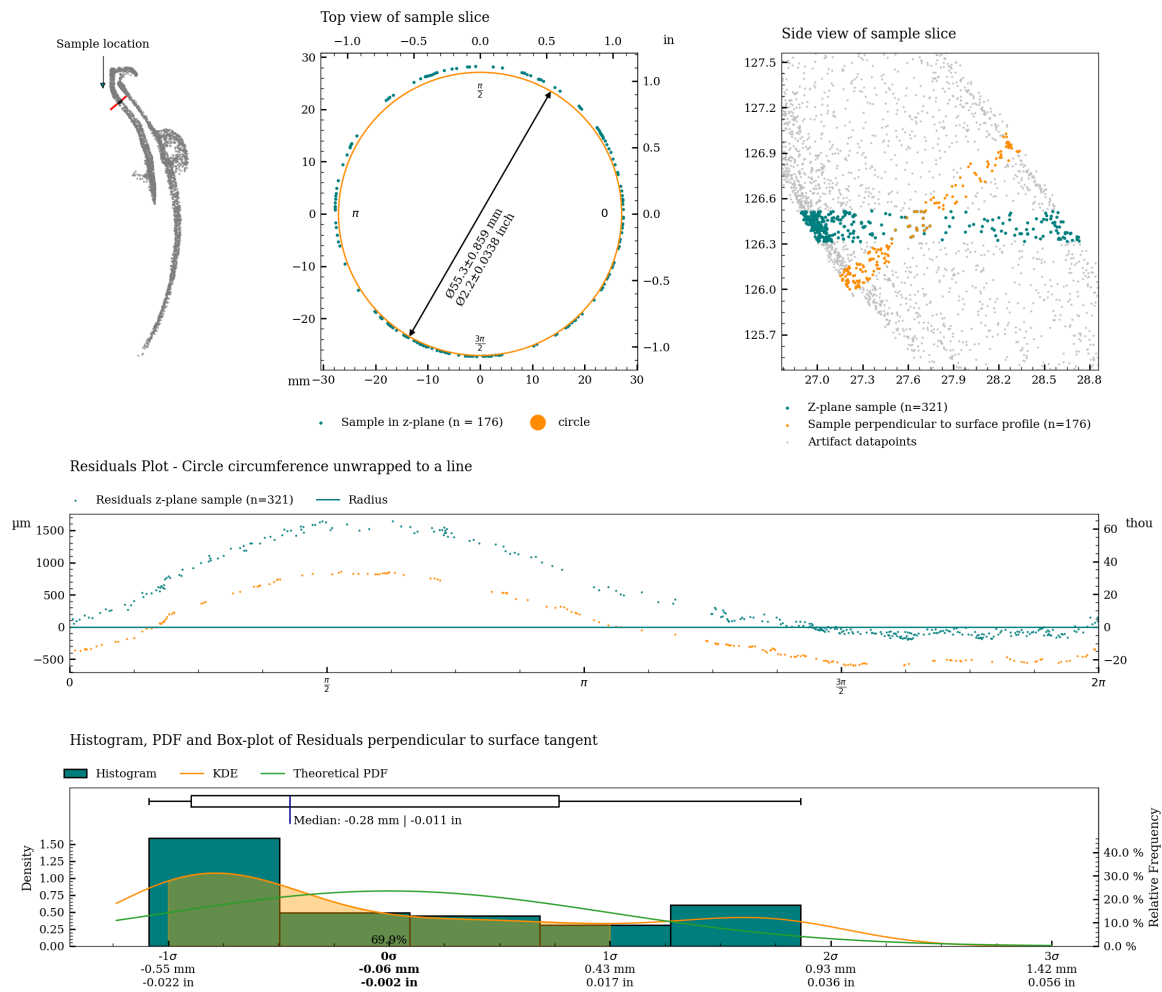


Figure 12: Charts with statistics for the measurement of c06_s.

Graphical overview of circularity measurement c07

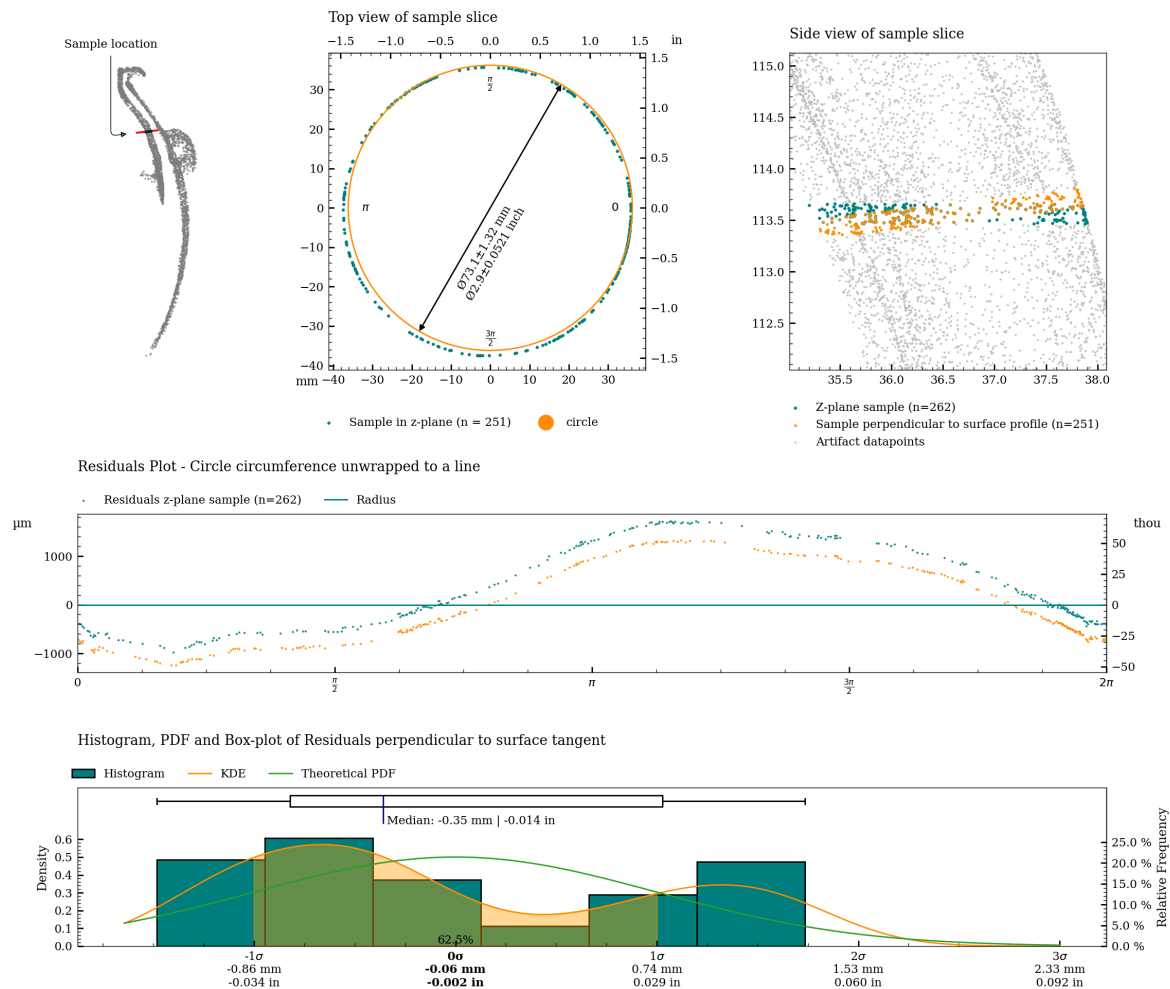


Figure 13: Charts with statistics for the measurement of c07.

Graphical overview of circularity measurement c07_s

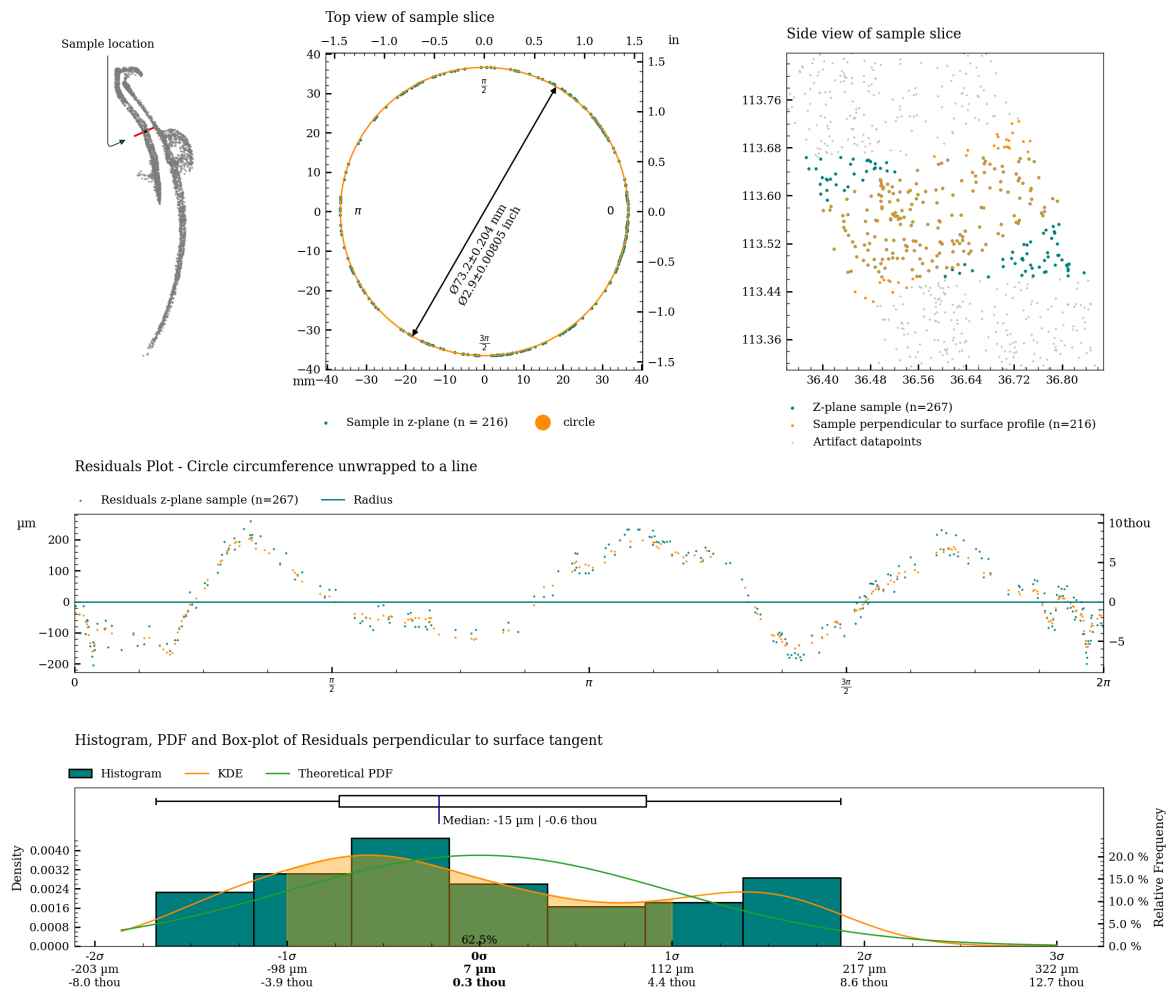


Figure 14: Charts with statistics for the measurement of c07_s.

Graphical overview of circularity measurement c08

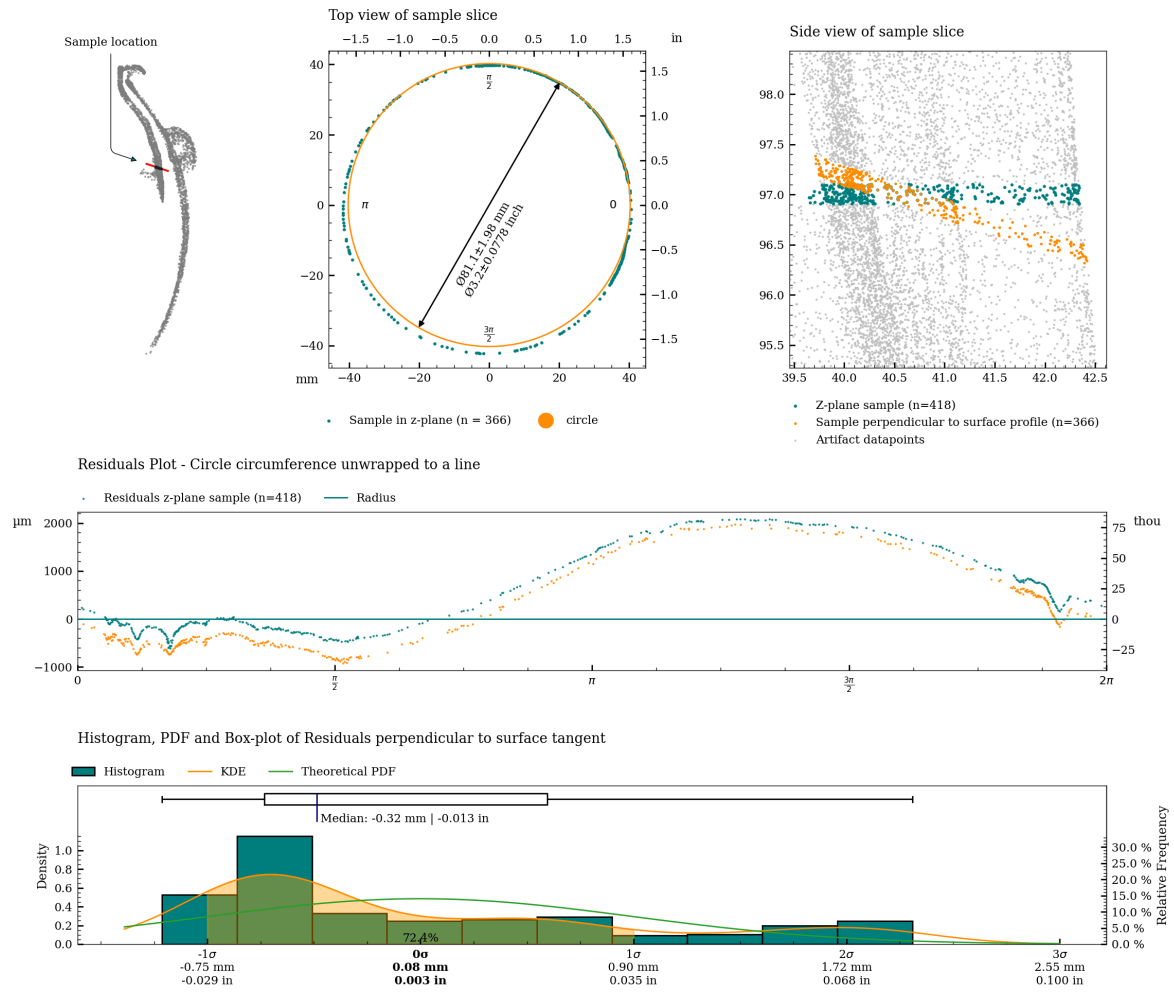


Figure 15: Charts with statistics for the measurement of c08.

Graphical overview of circularity measurement c08_s

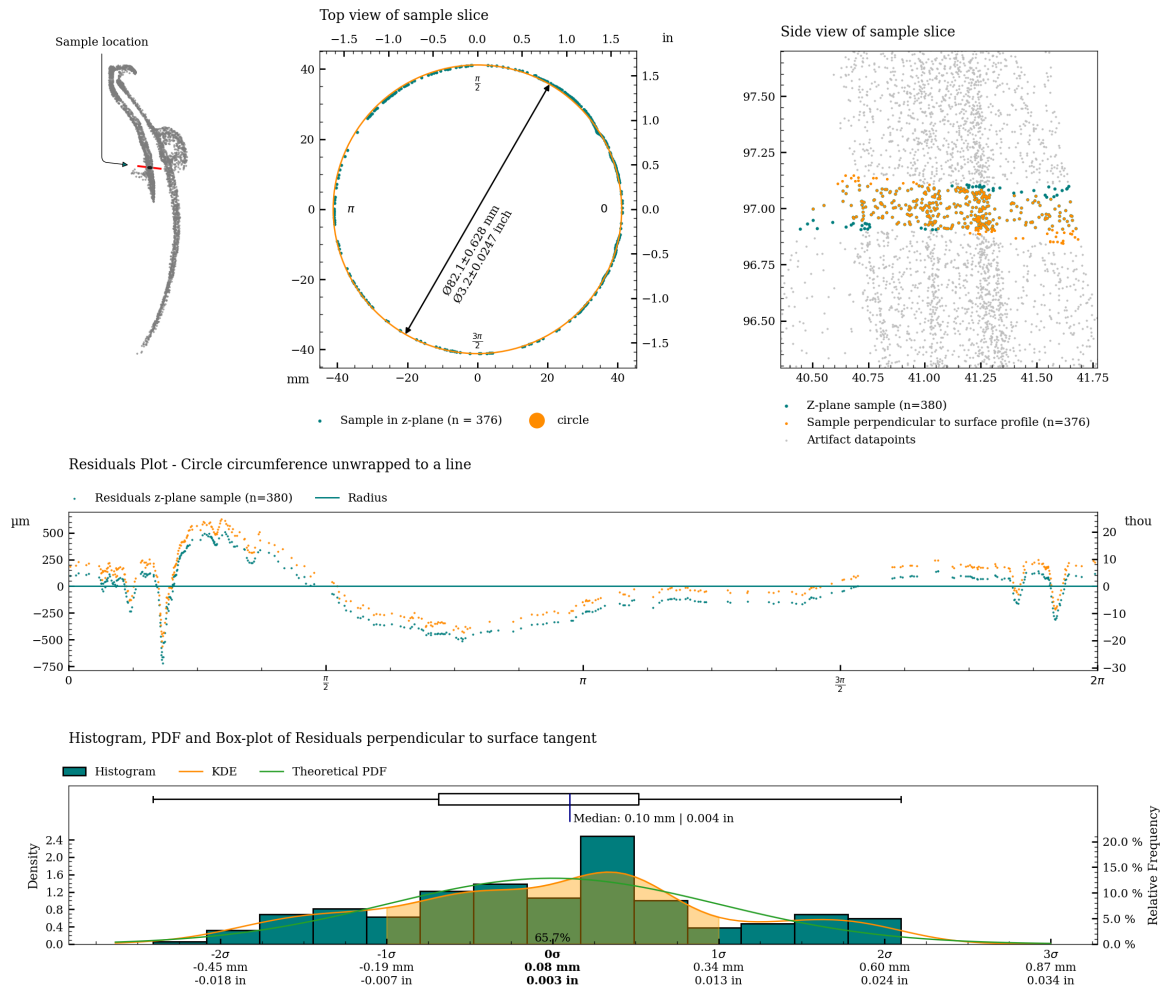


Figure 16: Charts with statistics for the measurement of c08_s.

Table 2 shows statistical measures of the circularity of the vessel, measured along the full height (areas on the artifact scan containing damaged parts have been removed to the best extent possible to reduce the influence of the measurement).

Metric											
Area	Range			Standard Deviation			RMSD			Slices	Slice height
	Median	Min.	Max.	Median	Min.	Max.	Median	Min.	Max.		
	mm	mm	mm	mm	mm	mm	mm	mm	mm		
Exterior	2.343	1.185	3.571	0.318	0.132	0.548	0.672	0.215	1.063	405	0.200
Interior	2.270	1.277	9.686	0.298	0.173	1.428	0.670	0.330	2.249	192	0.200
Interior separate	1.009	0.362	8.364	0.129	0.046	1.341	0.241	0.081	2.168	221	0.200

Imperial											
Area	Range			Standard Deviation			RMSD			Slices	Slice height
	Median	Min.	Max.	Median	Min.	Max.	Median	Min.	Max.		
	in	in	in	in	in	in	in	in	in		
Exterior	2.343	1.185	3.571	0.318	0.132	0.548	0.672	0.215	1.063	405	0.200
Interior	2.270	1.277	9.686	0.298	0.173	1.428	0.670	0.330	2.249	192	0.200
Interior separate	1.009	0.362	8.364	0.129	0.046	1.341	0.241	0.081	2.168	221	0.200

Table 2: Perpendicular Circularity analysis of MV016c.

Circularity analysis of exterior surface

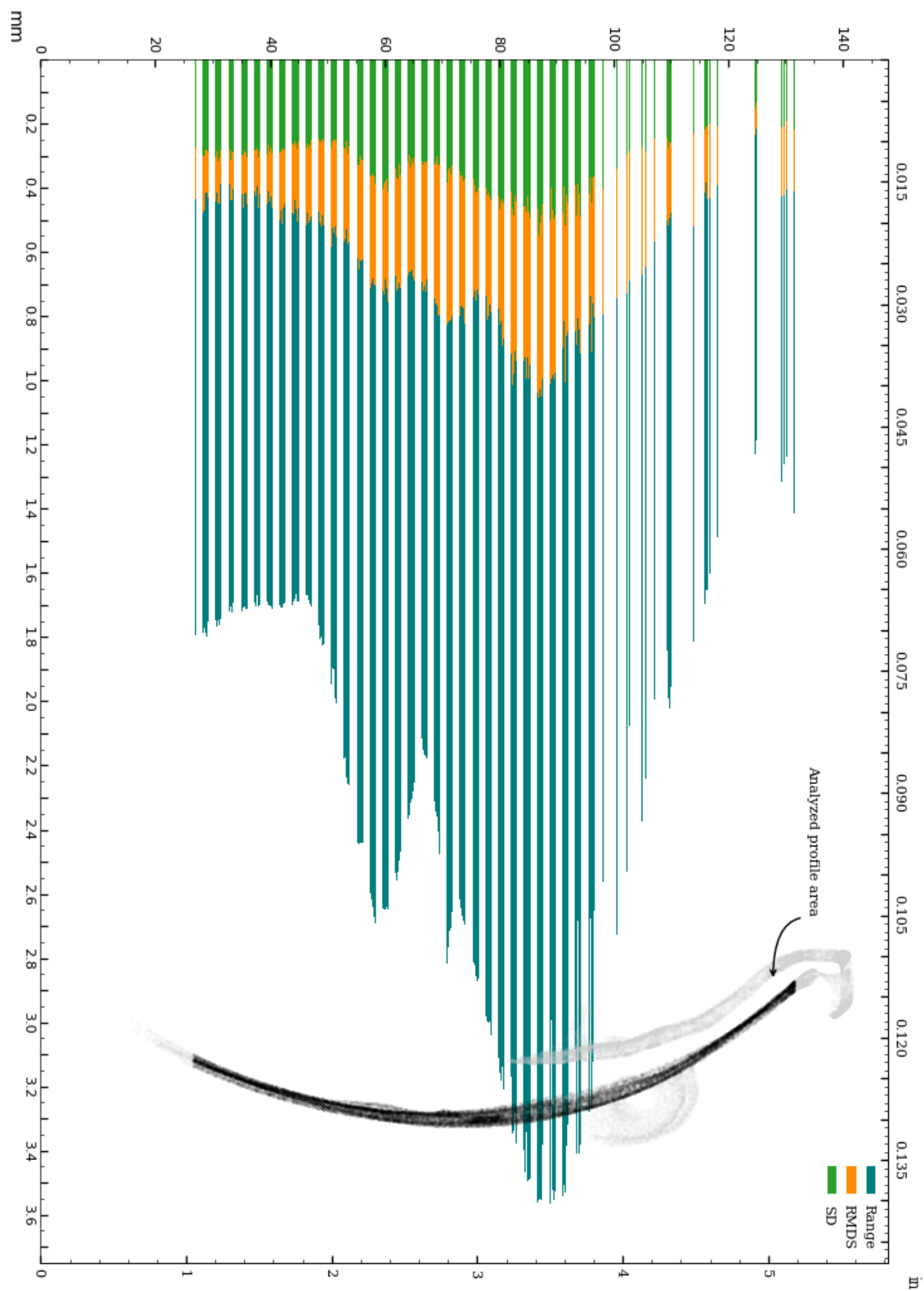


Figure 17: Circularity of exterior surface.

Circularity analysis of exterior surface, Standard Deviation and Root Mean Squared Deviation

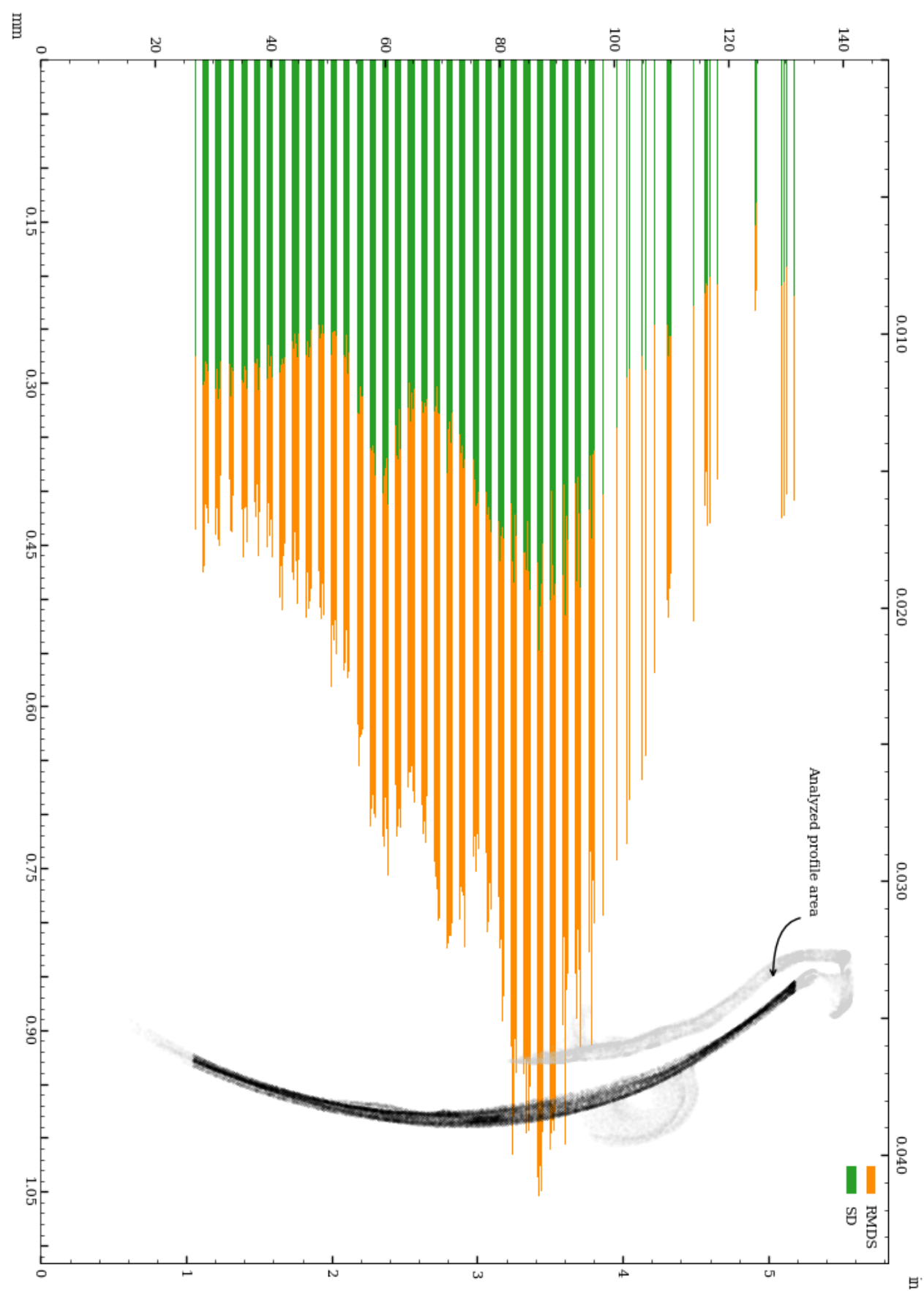


Figure 18: Vessel circularity of exterior surface, standard deviation and median absolute deviation.

The distributions of the circularity measurements across 405 slices of the exterior surface are shown below.

Range measurement distribution across 405 slices of exterior surface

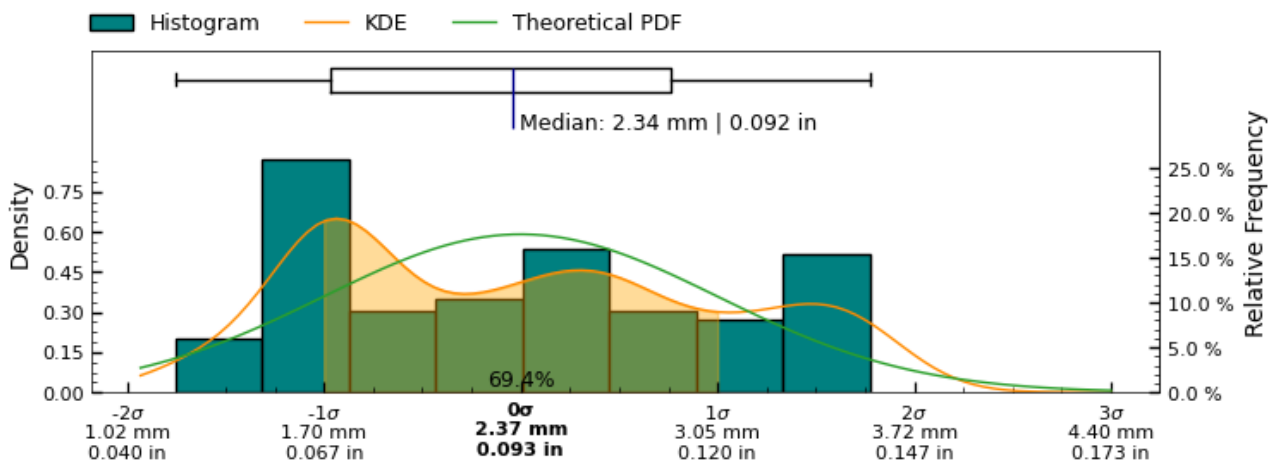


Figure 19: Range measurement distribution across measured slices of exterior surface

Standard Deviation measurement distribution across 405 slices of exterior surface

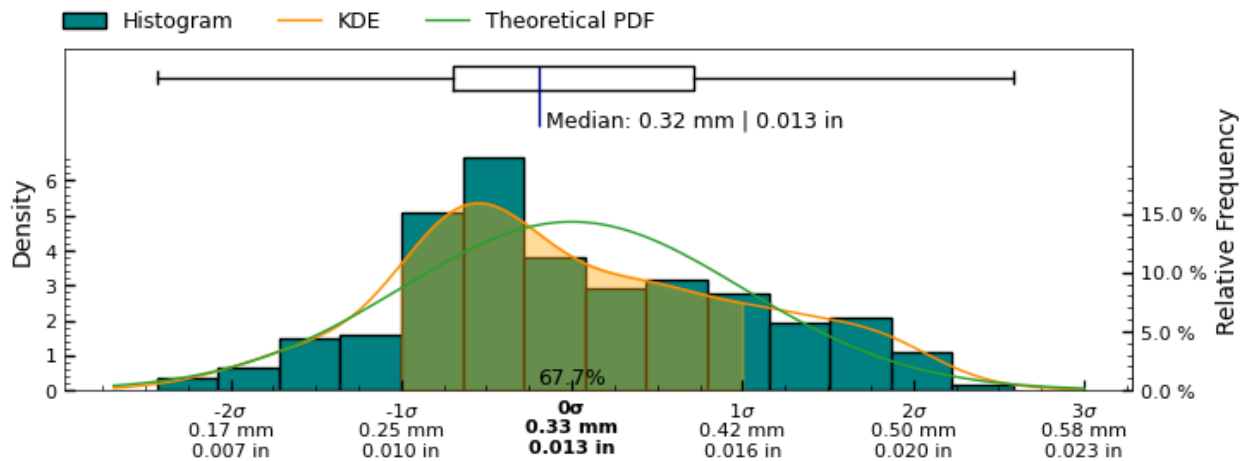


Figure 20: Standard Deviation measurement distribution across measured slices of " + exterior + " surface

Root Mean Squared Deviation measurement distribution across 405 slices of exterior surface

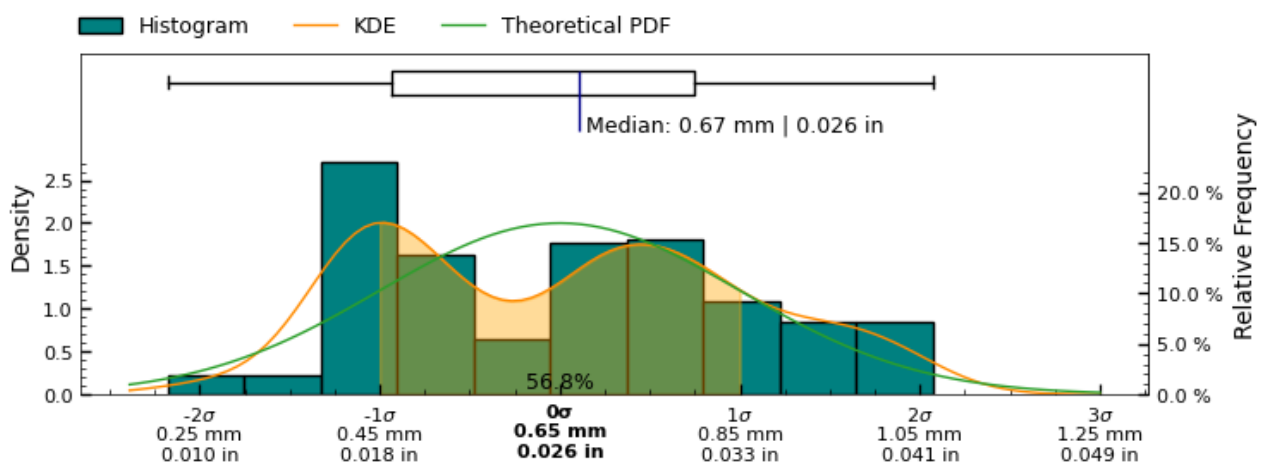


Figure 21: Root Mean Squared Deviation measurement distribution across measured slices of exterior surface

Circularity analysis of interior surface

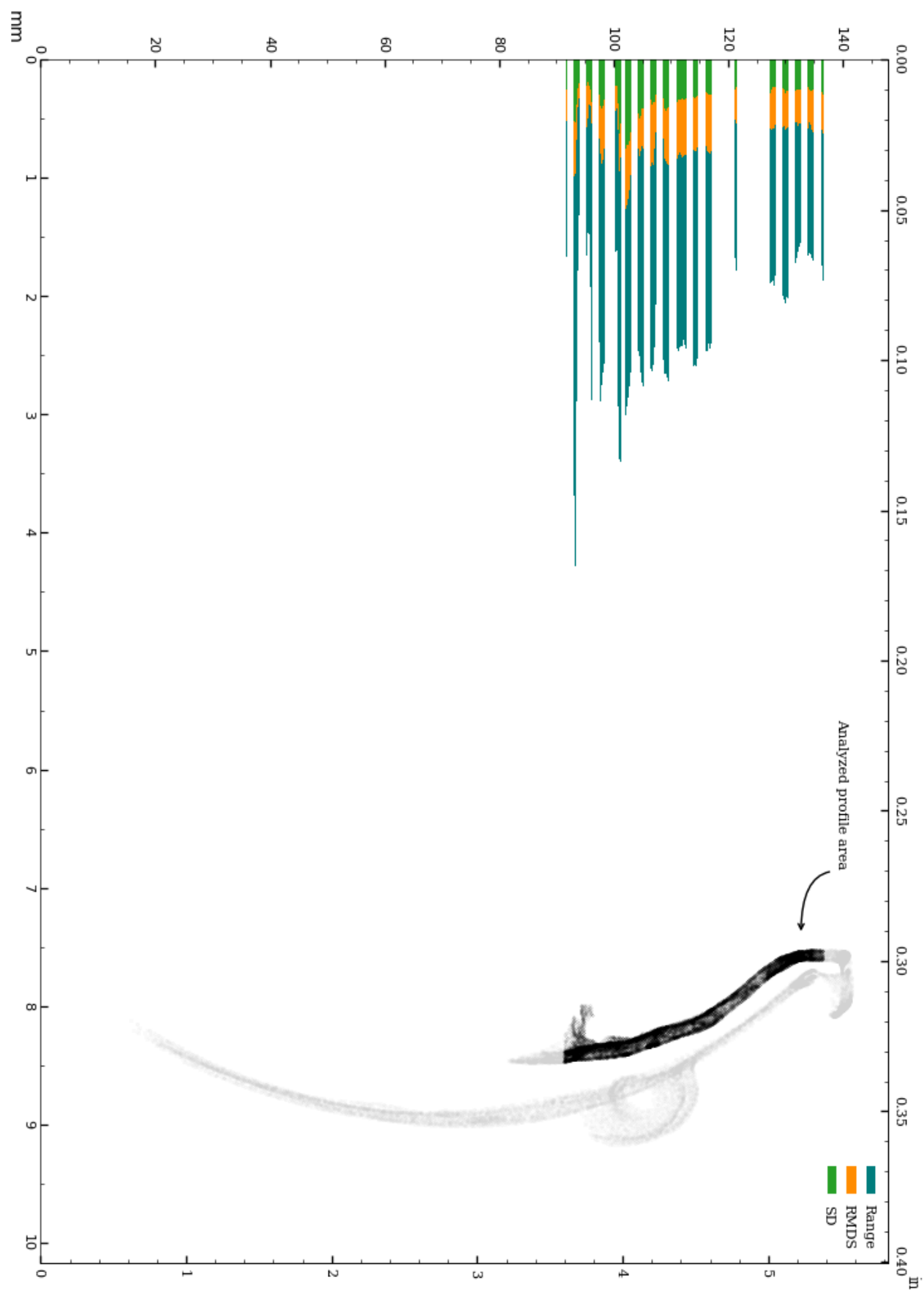


Figure 22: Circularity of interior surface.

Circularity analysis of interior surface, Standard Deviation and Root Mean Squared Deviation

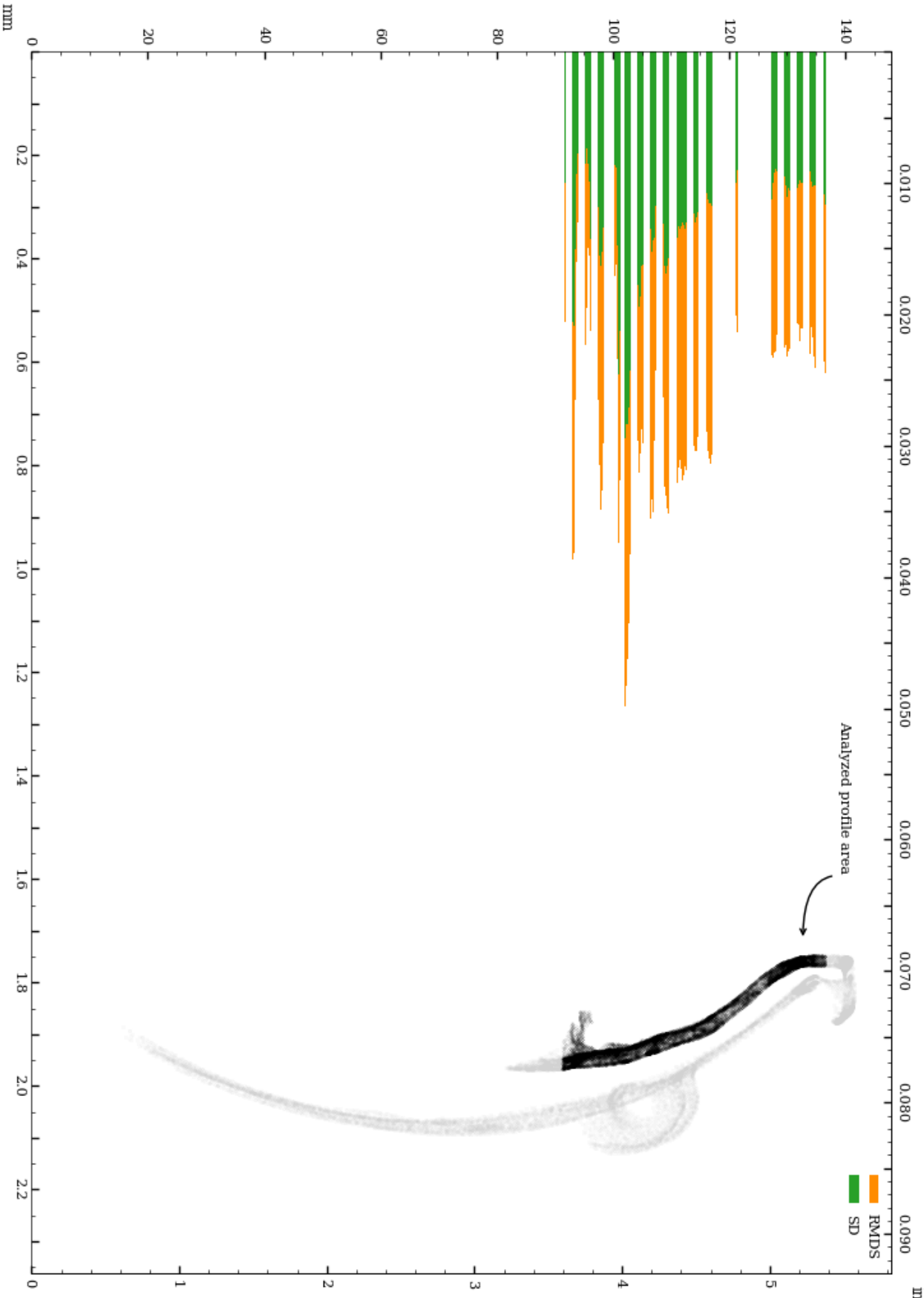


Figure 23: Vessel circularity of interior surface, standard deviation and median absolute deviation.

The distributions of the circularity measurements across 192 slices of the interior surface are shown below.

Range measurement distribution across 192 slices of interior surface

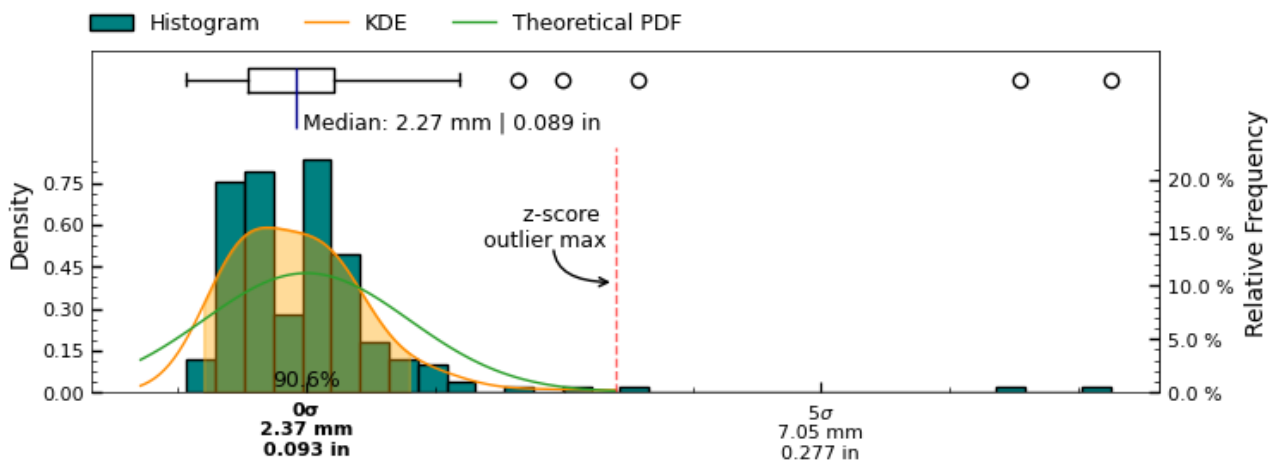


Figure 24: Range measurement distribution across measured slices of interior surface

Standard Deviation measurement distribution across 192 slices of interior surface

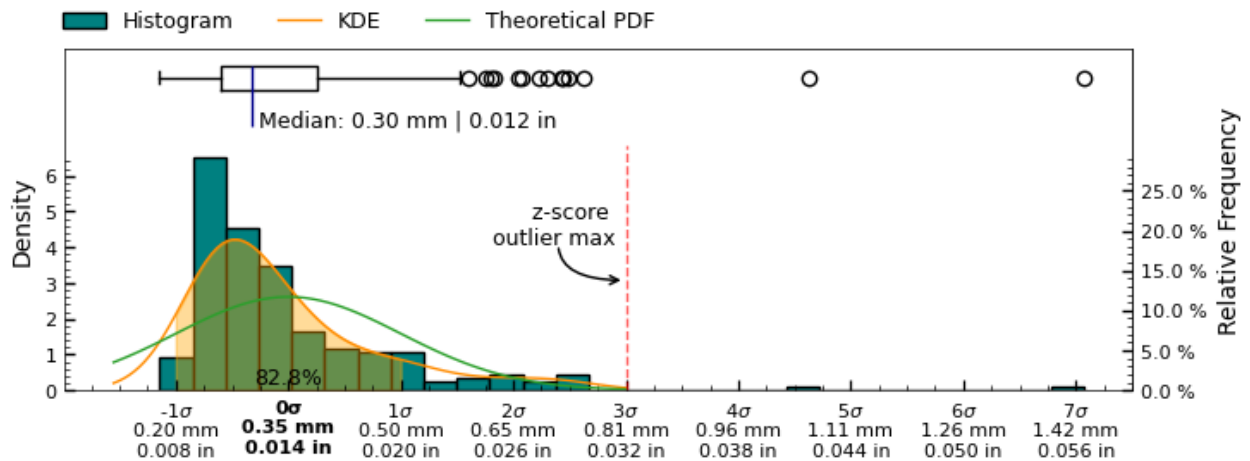


Figure 25: Standard Deviation measurement distribution across measured slices of "+ interior +" surface

Root Mean Squared Deviation measurement distribution across 192 slices of interior surface

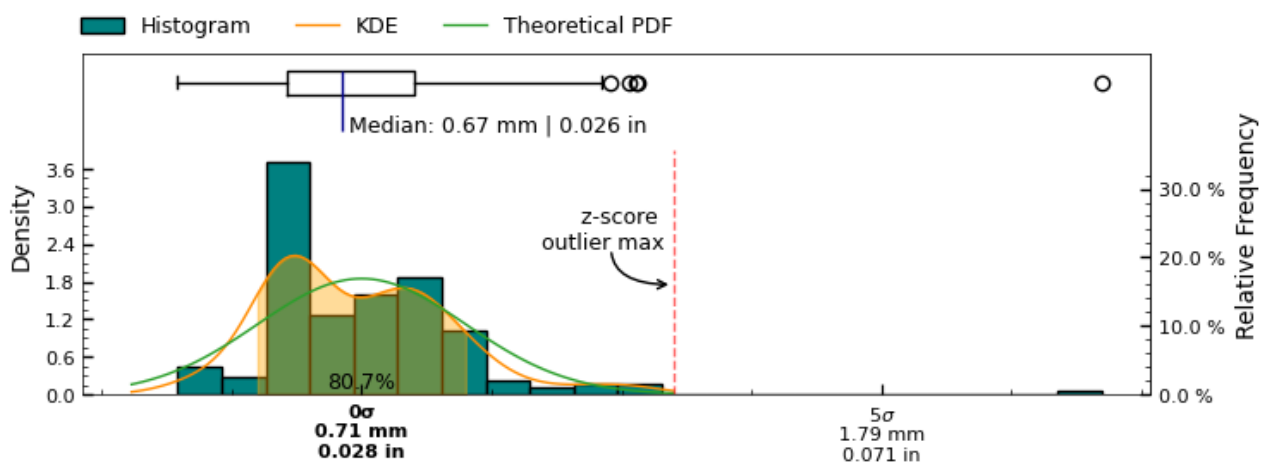


Figure 26: Root Mean Squared Deviation measurement distribution across measured slices of interior surface

Circularity analysis of interior separately aligned surface

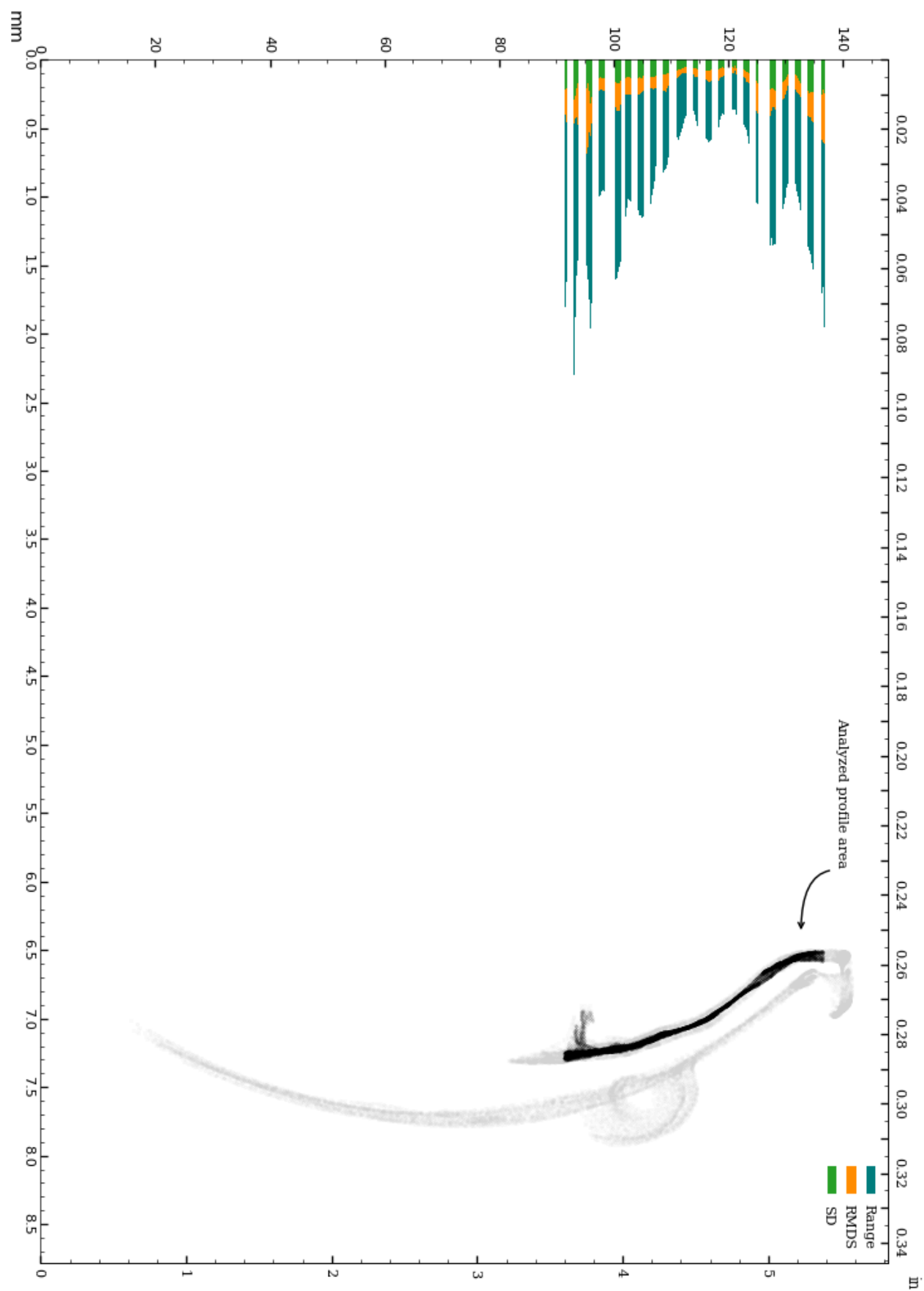


Figure 27: Circularity of interior_separate surface.

Circularity analysis of interior separately aligned surface, Standard Deviation and Root Mean Squared Deviation

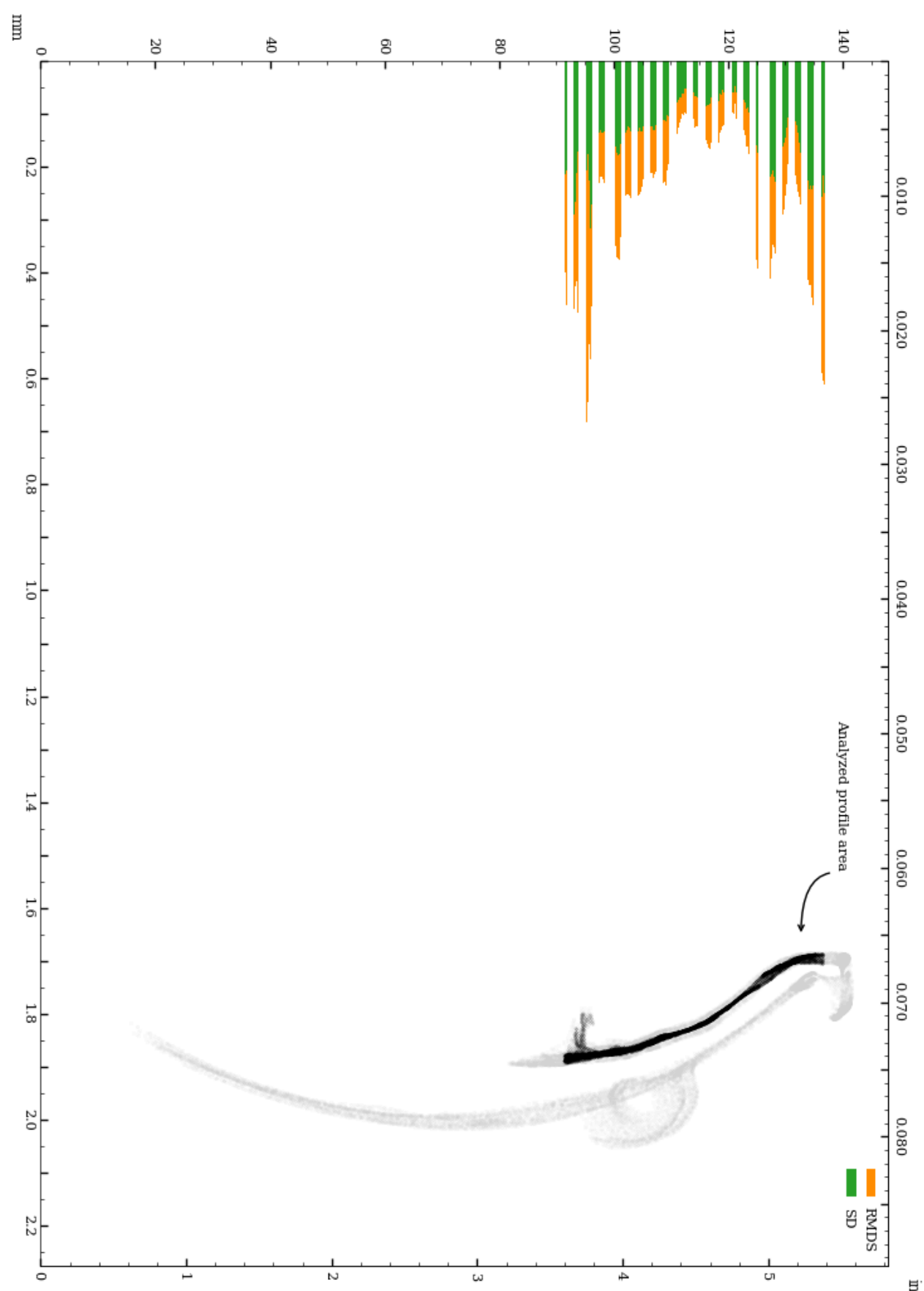


Figure 28: Vessel circularity of interior_separate surface, standard deviation and median absolute deviation.

The distributions of the circularity measurements across 221 slices of the interior_separate surface are shown below.

Range measurement distribution across 221 slices of interior separately aligned surface

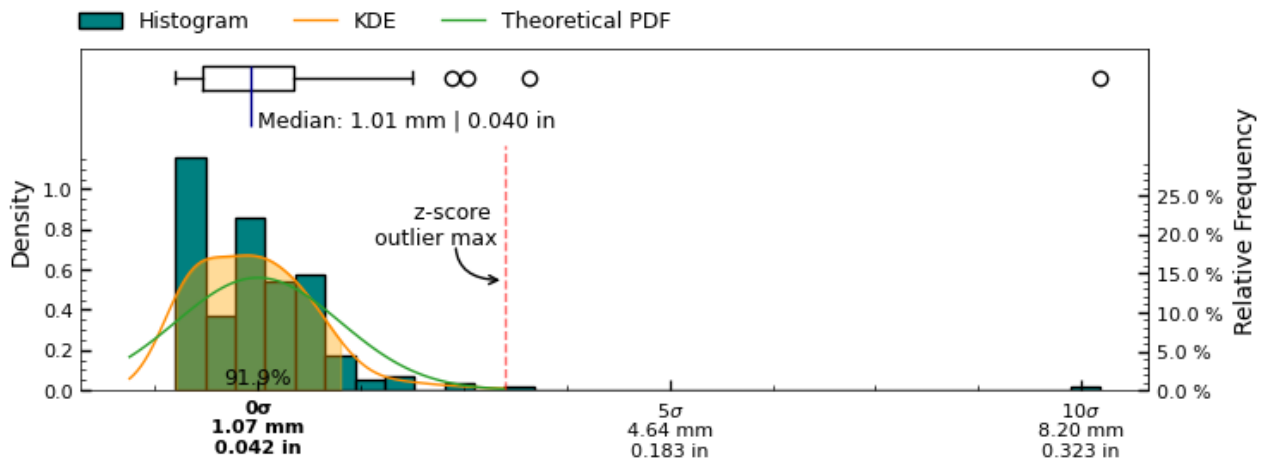


Figure 29: Range measurement distribution across measured slices of interior_separate surface

Standard Deviation measurement distribution across 221 slices of interior separately aligned surface

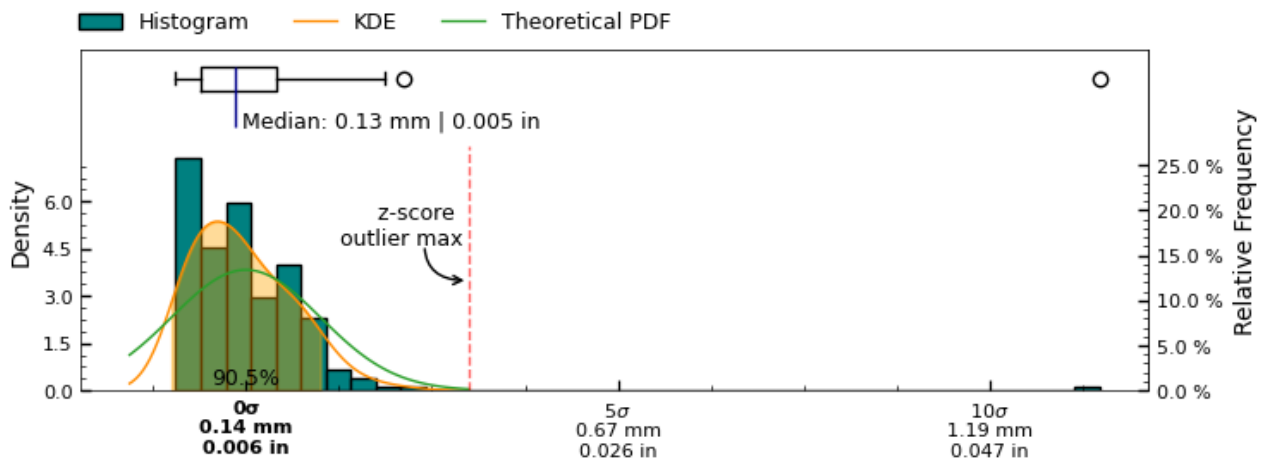


Figure 30: Standard Deviation measurement distribution across measured slices of " + interior_separate + " surface

Root Mean Squared Deviation measurement distribution across 221 slices of interior separately aligned surface

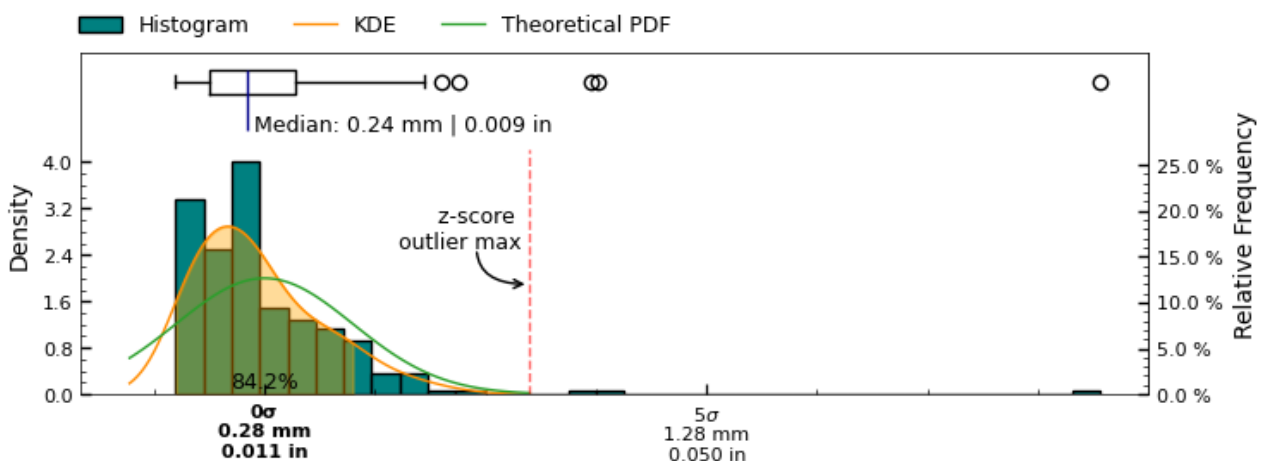


Figure 31: Root Mean Squared Deviation measurement distribution across measured slices of interior separately aligned surface

Concentricity

The concentricity metric describes the deviation in the center-point of the referenced features. As such, it is a measure to determine if several features of the object share the same center point/axis, and how closely. See Figure 32 for a visual representation of this metric.

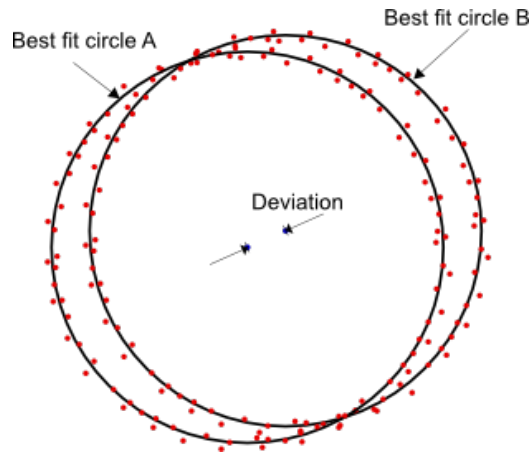


Figure 32: Concentricity measures the deviation (distance) between the center of two circles.

Determination of concentricity has been carried out by establishing the best fit circles of sample slices, using RANSAC (Random sample consensus) algorithm for outlier detection of a least squares circle regression on the scanned data-points at each cross-section, to estimate centers of each cross-section.

The concentricity between both the interior and exterior circular cross-sections is explored for cross-section measurements with the same Z-coordinates.

Additionally, the concentricity between each cross-section measurement defined in Figure 4 and the datum axis $(x, y) = (0, 0)$ has been calculated to establish the deviation of the feature center from the datum axis.

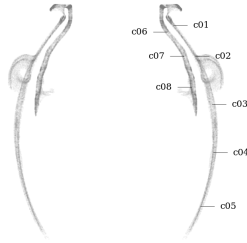


Figure 33: Circularity measurement sample locations, full mesh aligned to exterior surface

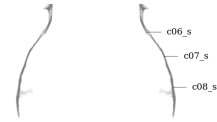


Figure 34: Circularity measurement sample location, separately aligned interior mesh

Metric

Tag	Reference	Deviation	Sample size	Circle fit residuals analysis for sample listed in Tag column						Center (x,y)
				Range full	Range inliers	RMSD full	RMDS inliers	SD full	SD inliers	
		mm		mm	mm	mm	mm	mm	mm	µm
c01	z-axis	0.463	90	1.496	1.496	0.418	0.418	0.213	0.213	−403, 229
c02	z-axis	0.318	96	1.994	1.994	0.548	0.548	0.264	0.264	318, 5
c03	z-axis	0.345	147	3.621	3.621	1.035	1.035	0.550	0.550	134, −318
c04	z-axis	0.385	188	3.144	3.144	0.867	0.867	0.467	0.467	−289, −254
c05	z-axis	0.341	116	2.263	2.263	0.637	0.637	0.336	0.336	129, 316
c06	z-axis	0.776	151	1.904	1.904	0.711	0.711	0.270	0.270	−776, −2
c06_s	z-axis	0.541	176	2.194	2.194	0.755	0.755	0.345	0.345	−229, 490
c07	z-axis	1.222	251	5.196	5.196	1.686	1.686	0.717	0.717	−769, −950
c07_s	z-axis	0.032	216	0.394	0.394	0.108	0.108	0.054	0.054	−31, −10
c08	z-axis	1.244	366	5.646	5.646	2.005	2.005	0.824	0.824	−569, −1107
c08_s	z-axis	0.210	376	1.188	1.120	0.296	0.293	0.166	0.165	206, 40
c02	c07_s	0.349								349, 16
c06	c06_s	0.736								−547, −493
c08	c08_s	1.384								−775, −1147

Imperial

Tag	Reference	Deviation	Sample size	Circle fit residuals analysis for sample listed in Tag column						Center (x,y)
				Range full	Range inliers	RMSD full	RMDS inliers	SD full	SD inliers	
		in		in	in	in	in	in	in	thou
c01	z-axis	0.0182	90	0.0589	0.0589	0.0165	0.0165	0.0084	0.0084	−15.9, 9.0
c02	z-axis	0.0125	96	0.0785	0.0785	0.0216	0.0216	0.0104	0.0104	12.5, 0.2
c03	z-axis	0.0136	147	0.1426	0.1426	0.0408	0.0408	0.0216	0.0216	5.3, −12.5
c04	z-axis	0.0151	188	0.1238	0.1238	0.0342	0.0342	0.0184	0.0184	−11.4, −10.0
c05	z-axis	0.0134	116	0.0891	0.0891	0.0251	0.0251	0.0132	0.0132	5.1, 12.4
c06	z-axis	0.0305	151	0.0750	0.0750	0.0280	0.0280	0.0106	0.0106	−30.5, −0.1
c06_s	z-axis	0.0213	176	0.0864	0.0864	0.0297	0.0297	0.0136	0.0136	−9.0, 19.3
c07	z-axis	0.0481	251	0.2046	0.2046	0.0664	0.0664	0.0282	0.0282	−30.3, −37.4
c07_s	z-axis	0.0013	216	0.0155	0.0155	0.0042	0.0042	0.0021	0.0021	−1.2, −0.4
c08	z-axis	0.0490	366	0.2223	0.2223	0.0789	0.0789	0.0324	0.0324	−22.4, −43.6
c08_s	z-axis	0.0083	376	0.0468	0.0441	0.0117	0.0116	0.0065	0.0065	8.1, 1.6
c02	c07_s	0.0137								13.7, 0.6
c06	c06_s	0.0290								−21.5, −19.4
c08	c08_s	0.0545								−30.5, −45.2

Table 3: Concentricity analysis of MV016c.

Concentricity analysis of c01

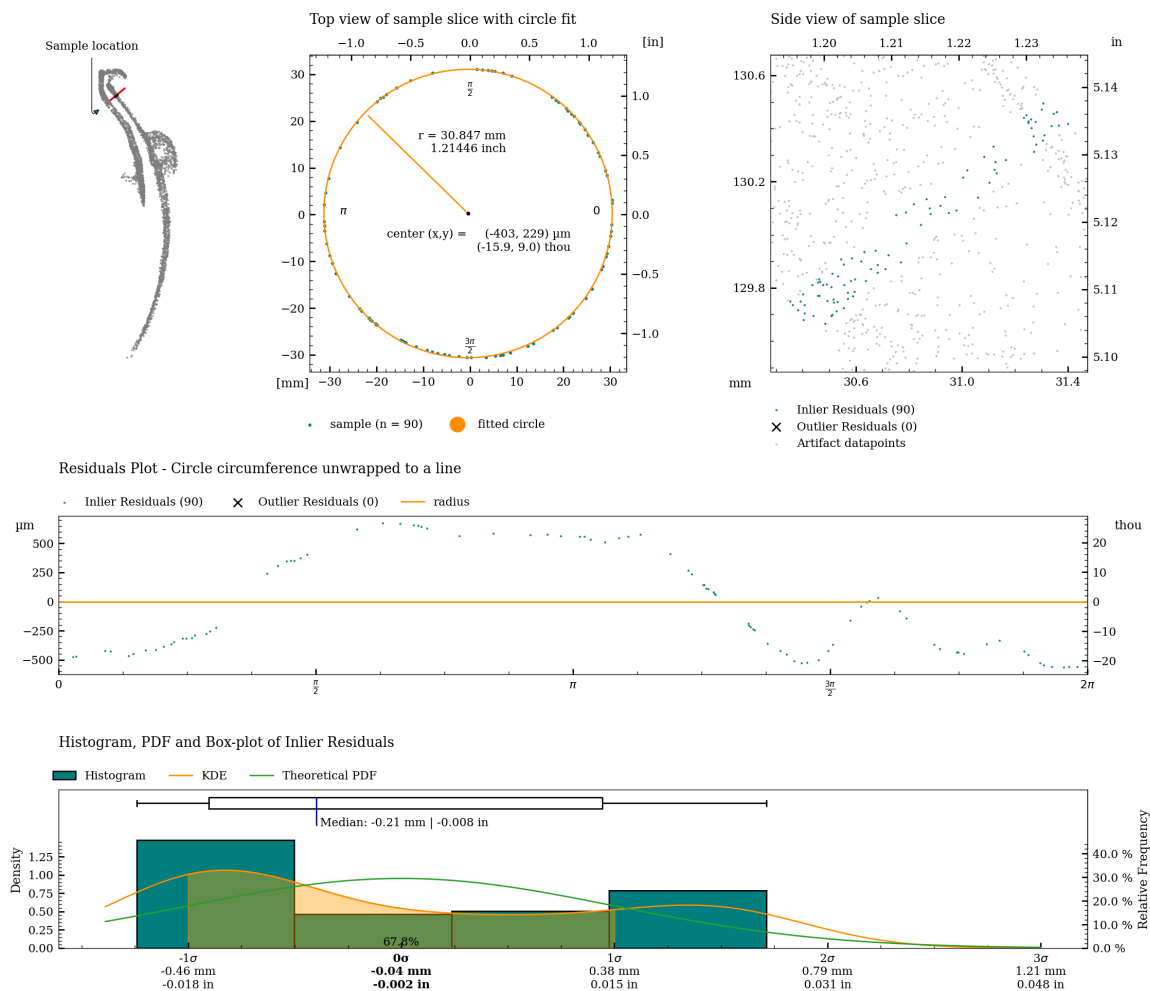


Figure 35: Detailed plot of concentricity measurement for c01.

Concentricity analysis of c02

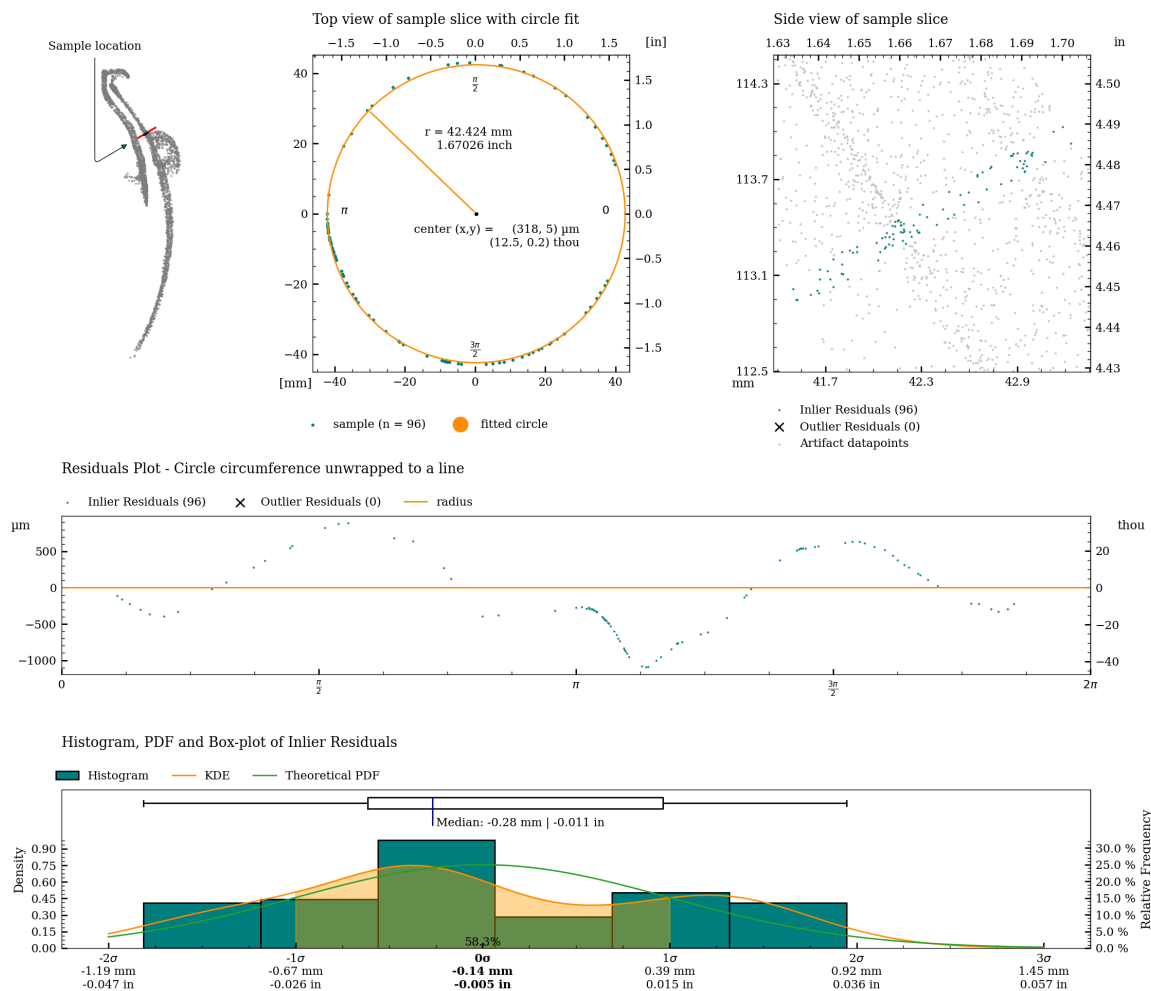


Figure 36: Detailed plot of concentricity measurement for c02.

Concentricity analysis of c03

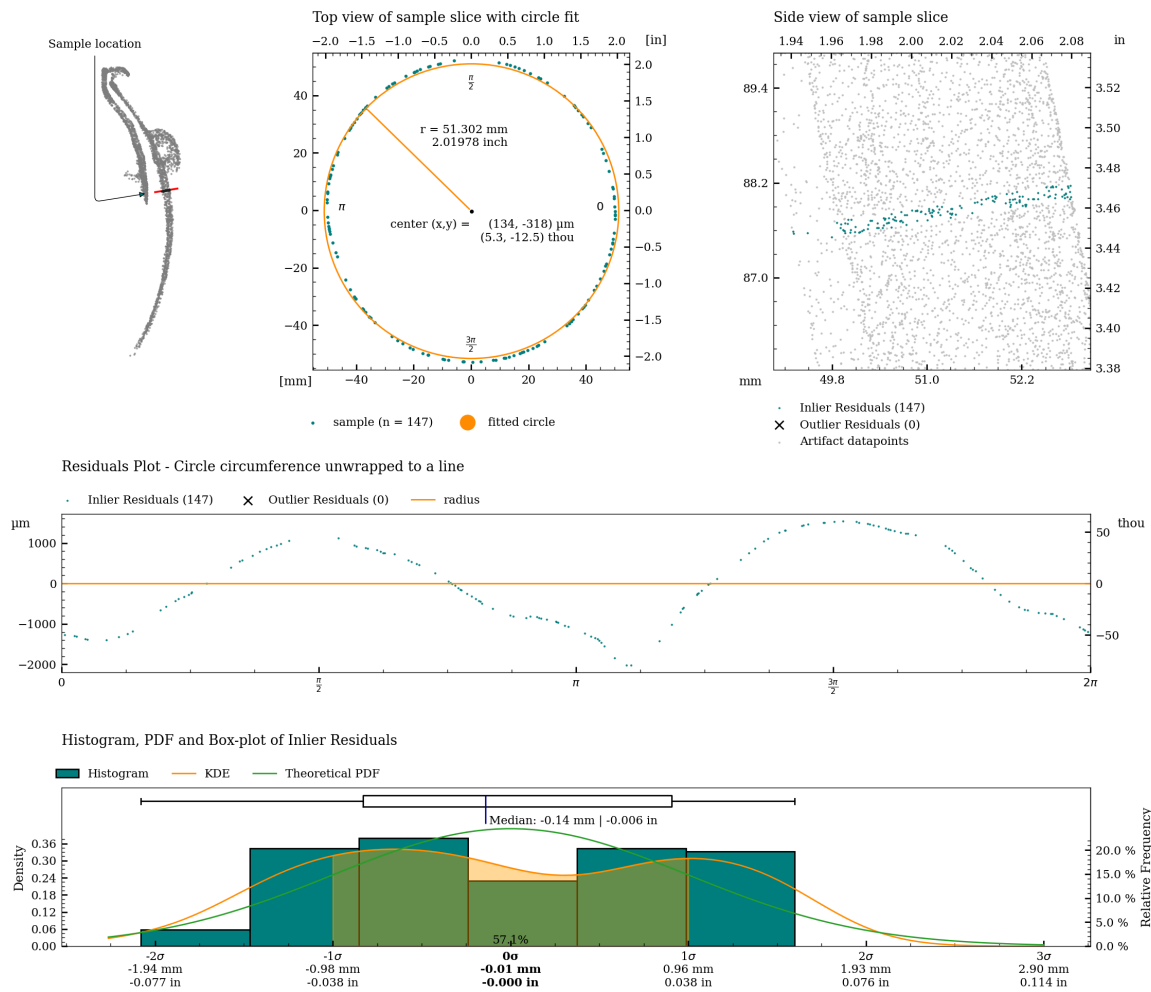


Figure 37: Detailed plot of concentricity measurement for c03.

Concentricity analysis of c04

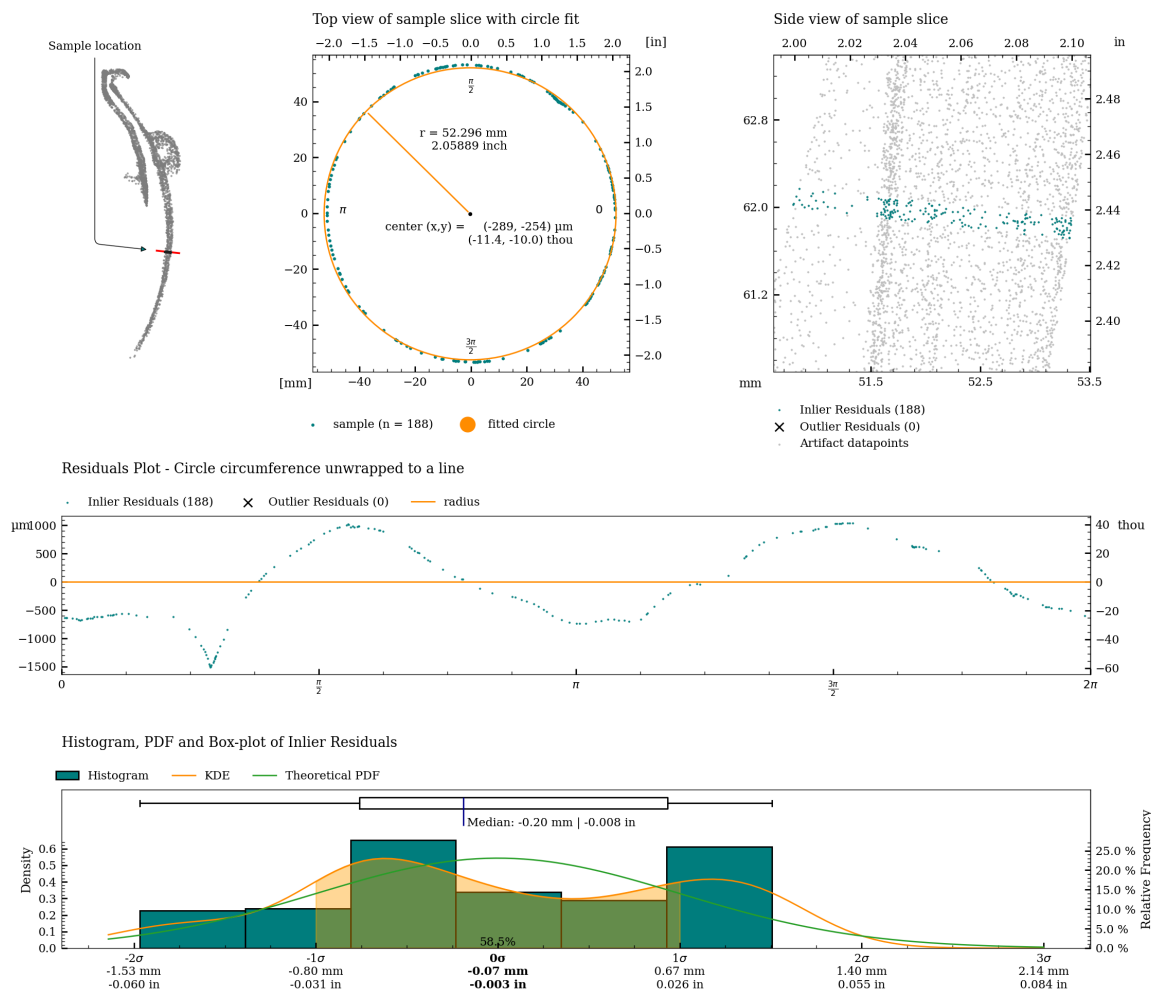


Figure 38: Detailed plot of concentricity measurement for c04.

Concentricity analysis of c05

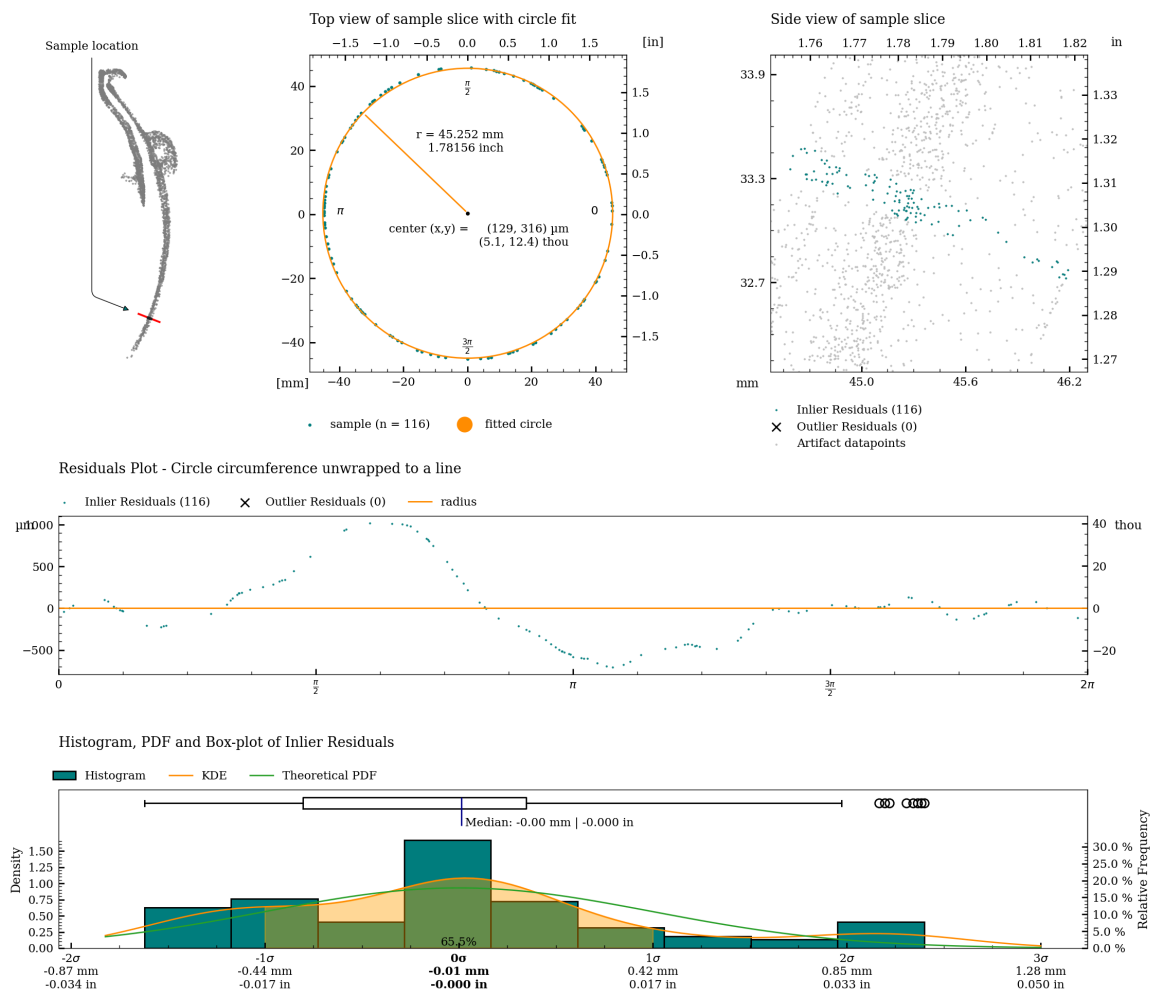


Figure 39: Detailed plot of concentricity measurement for c05.

Concentricity analysis of c06

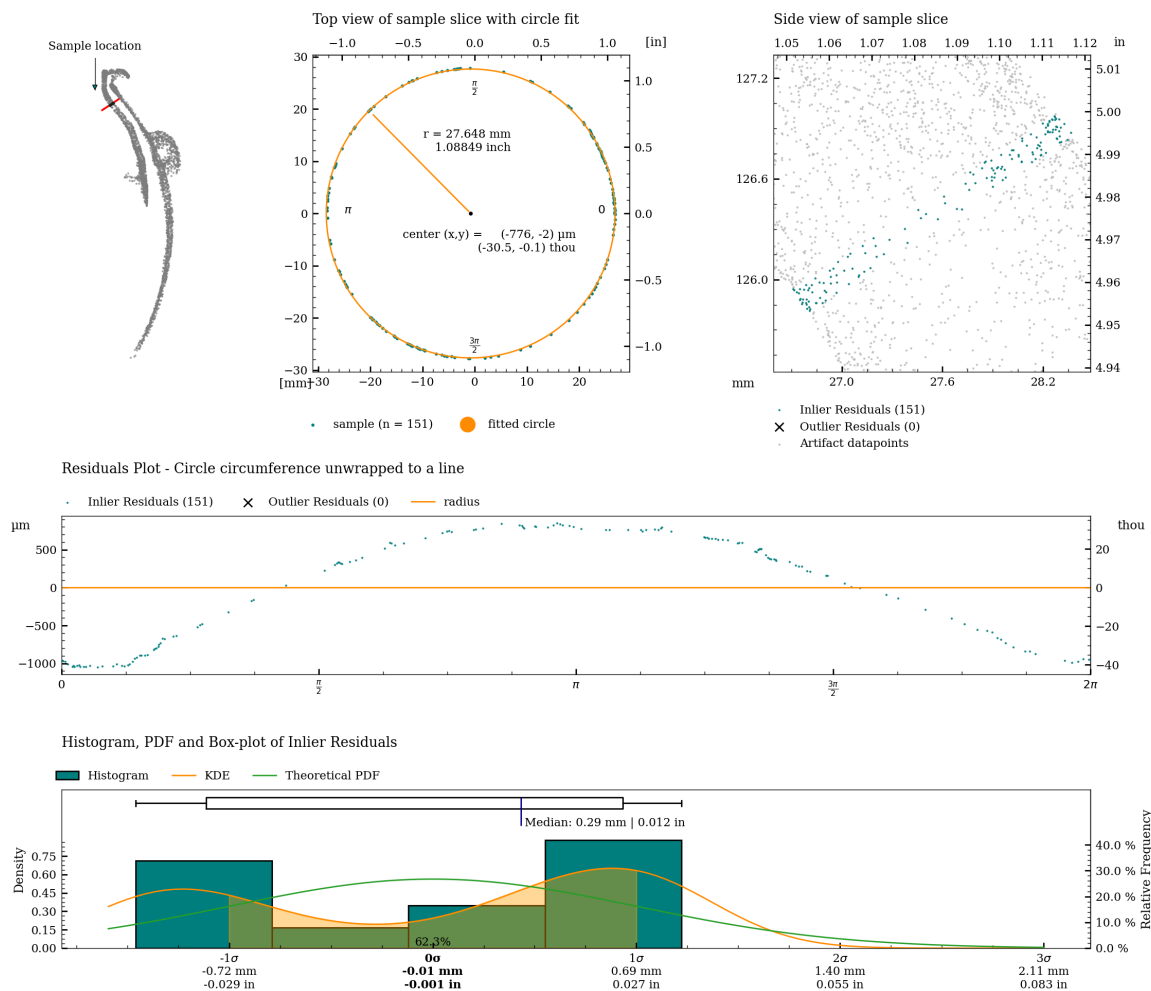


Figure 40: Detailed plot of concentricity measurement for c06.

Concentricity analysis of c06_s

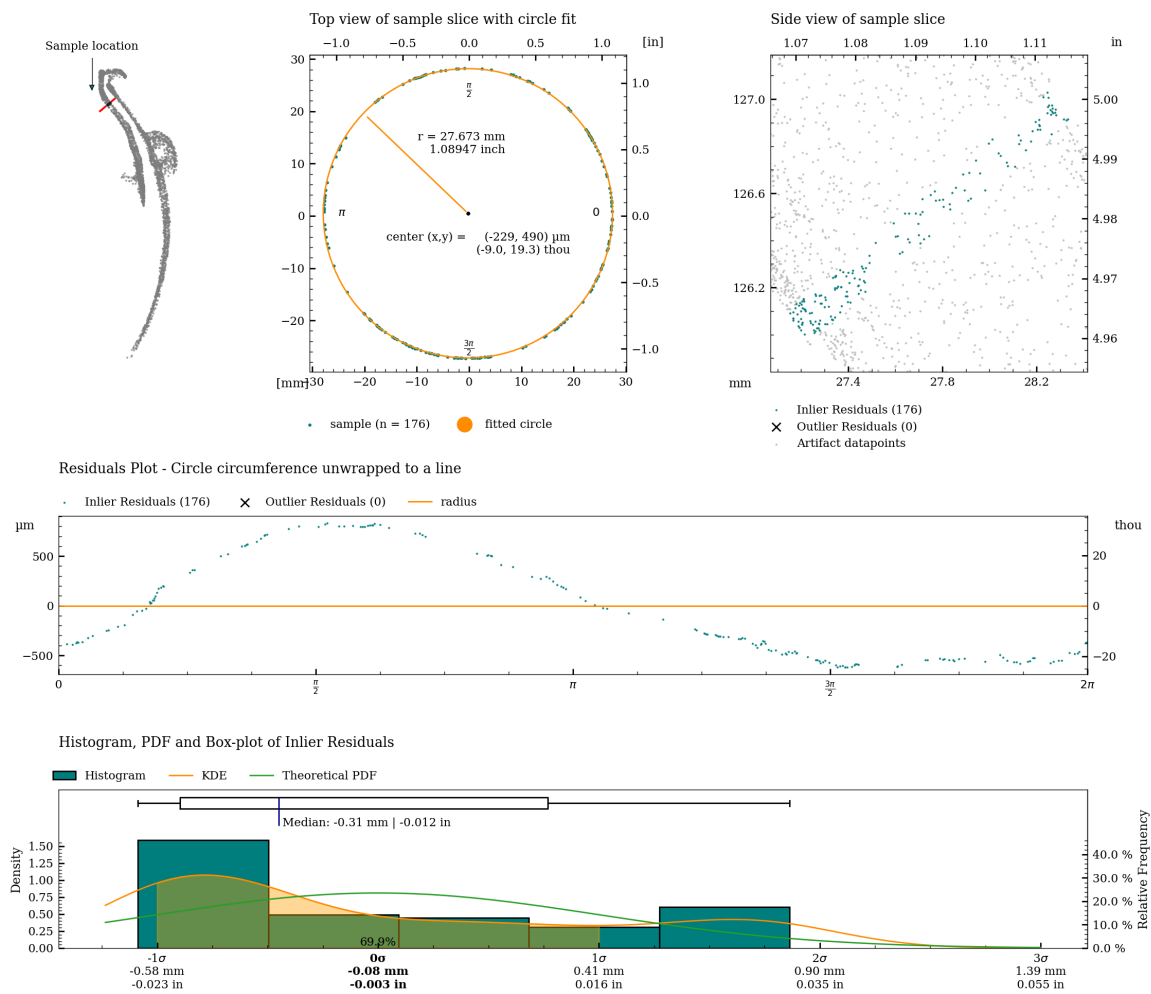


Figure 41: Detailed plot of concentricity measurement for c06_s.

Concentricity analysis of c07

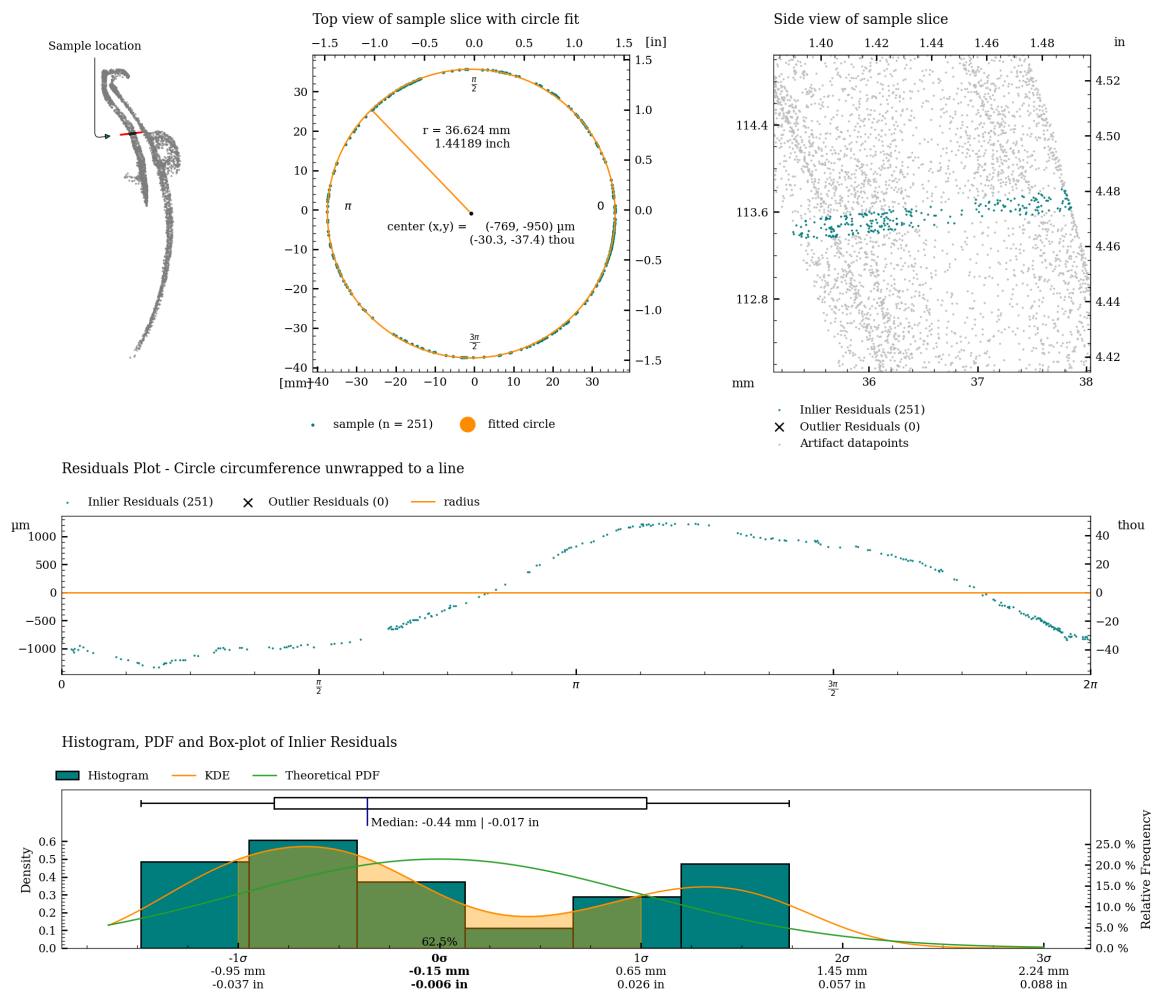


Figure 42: Detailed plot of concentricity measurement for c07.

Concentricity analysis of c07_s

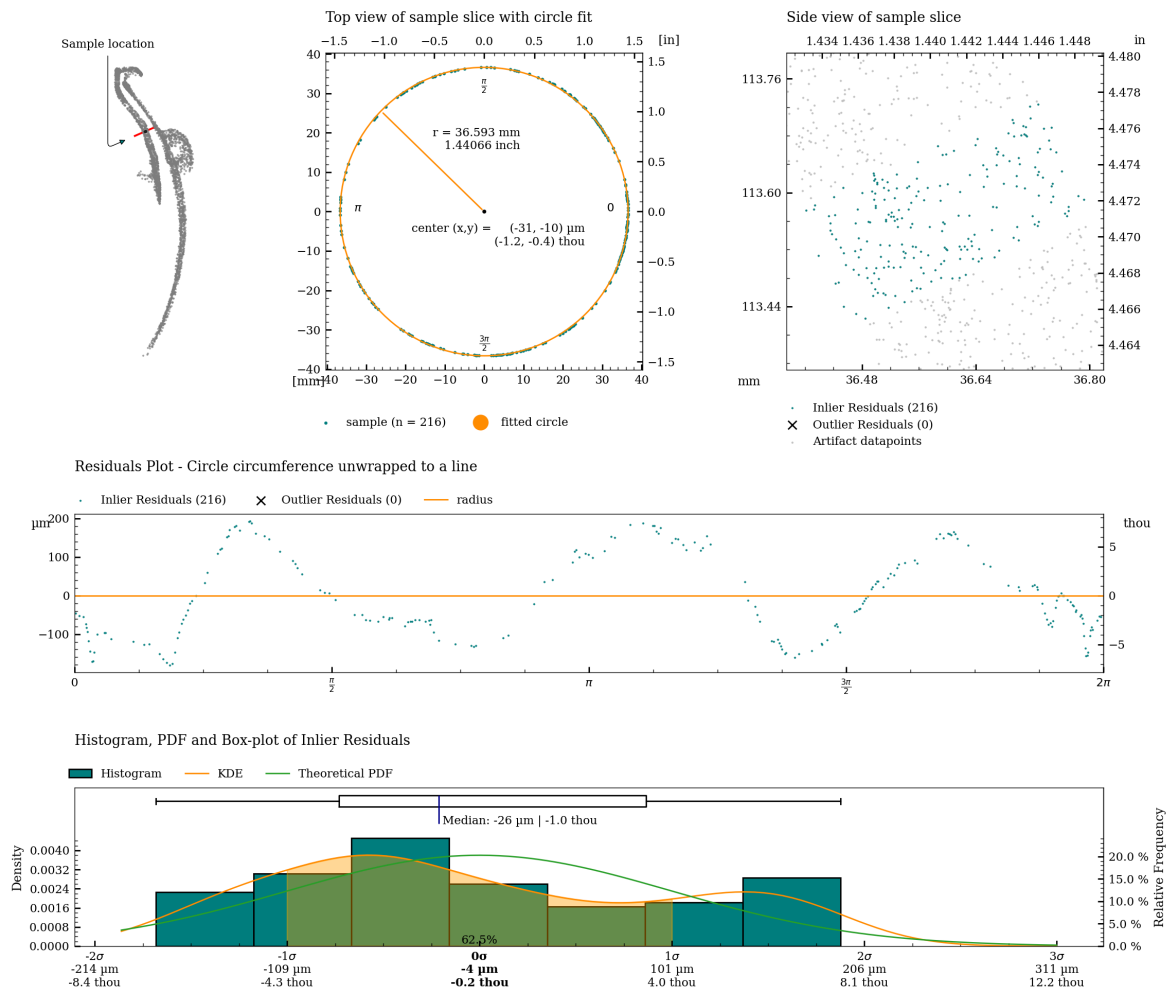


Figure 43: Detailed plot of concentricity measurement for c07_s.

Concentricity analysis of c08

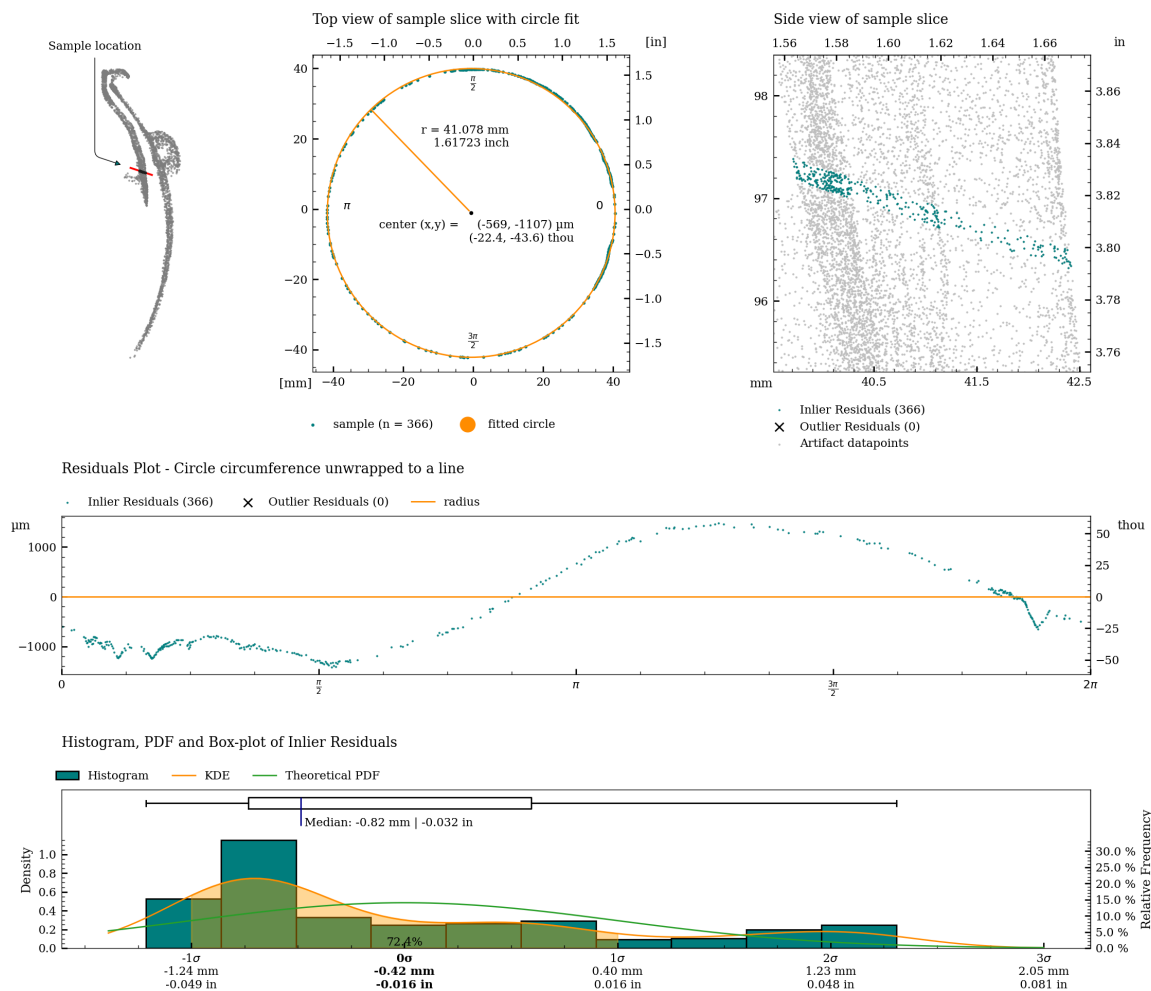


Figure 44: Detailed plot of concentricity measurement for c08.

Concentricity analysis of c08_s

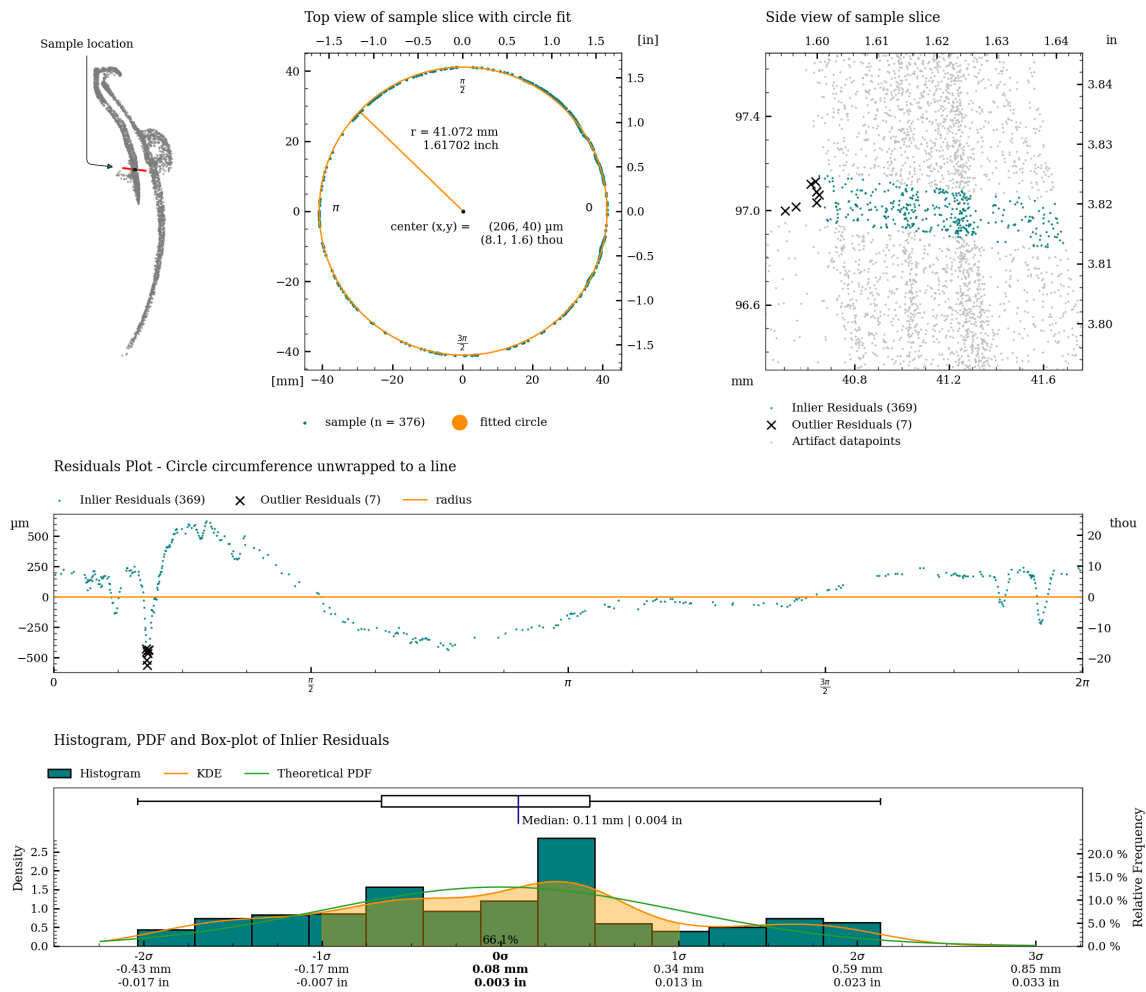


Figure 45: Detailed plot of concentricity measurement for c08_s.

Coaxiality

Coaxiality refers to the straightness and consistency of a central line running through the center of the vase. It measures how aligned the core of the vase remains along its vertical axis.

The coaxiality measurements are calculated using RANSAC (Random sample consensus) algorithm for outlier detection on least squares circle regression on cross-sections of the vessel (excluding potential handles), to estimate the best fit circle centers for each slice of the vessel. A best-fit line connects these centers, showing whether the vessels's shape twists or remains straight. This concept helps describe the symmetry and structural uniformity in a visual and analytical way.

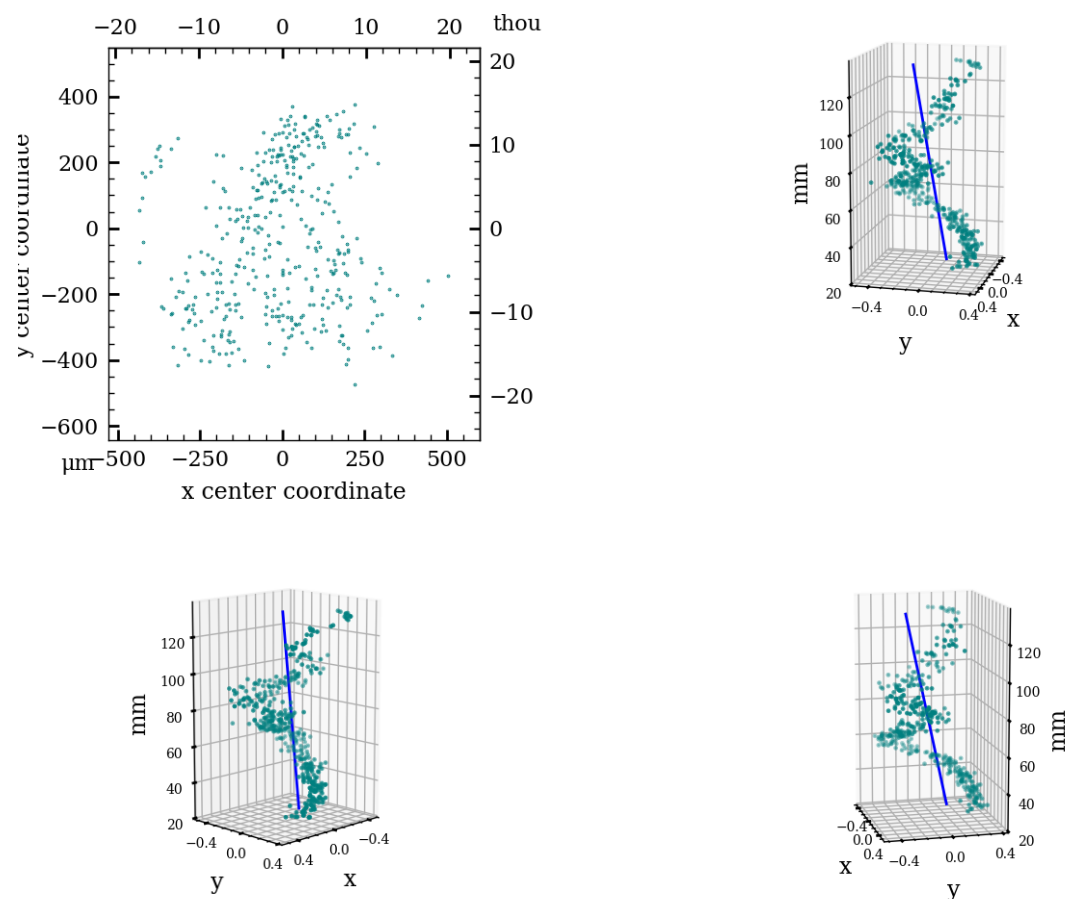
Coaxiality is measured for:

- The exterior surface (excluding handles)
- The interior surface

	Exterior		Interior		Interior separate	
Analyzed Slices	405		192		221	
Median sample size	145		253		275	
Slice Height	200 μm	7.9 thou	200 μm	7.9 thou	200 μm	7.9 thou
Statistics with Z-axis as Reference						
Median Absolute Deviation (MAD)	261 μm	10.3 thou	1038 μm	40.8 thou	212 μm	8.3 thou
Standard Deviation (SD)	110 μm	4.3 thou	249 μm	9.8 thou	194 μm	7.6 thou
Root Mean Square Deviation (RMSD)	284 μm	11.2 thou	1015 μm	40.0 thou	323 μm	12.7 thou
Statistics with Best Fit Central Axis as Reference						
Best fit Central Axis Equation (in metric coordinate system with unit [mm])	x = 0.067 + t-0.00116 y = 0.166 + t-0.00288 z = 0.000 + t1.00000		x = -0.279 + t-0.00253 y = -2.776 + t0.01771 z = 0.000 + t0.99984		x = 0.262 + t0.00153 y = 0.366 + t0.00335 z = 0.000 + t-0.99999	
Axis tilt	-0.067°		-0.142°		0.087°	
Median Absolute Deviation (MAD)	238 μm	9.4 thou	206 μm	8.1 thou	171 μm	6.7 thou
Standard Deviation (SD)	109 μm	4.3 thou	182 μm	7.2 thou	182 μm	7.2 thou
Root Mean Square Deviation (RMSD)	269 μm	10.6 thou	308 μm	12.1 thou	308 μm	12.1 thou

Table 4: Coaxiality analysis of vessel MV016c.

Coaxiality plots, exterior surface



Coaxiality residuals from fitted axis, exterior surface

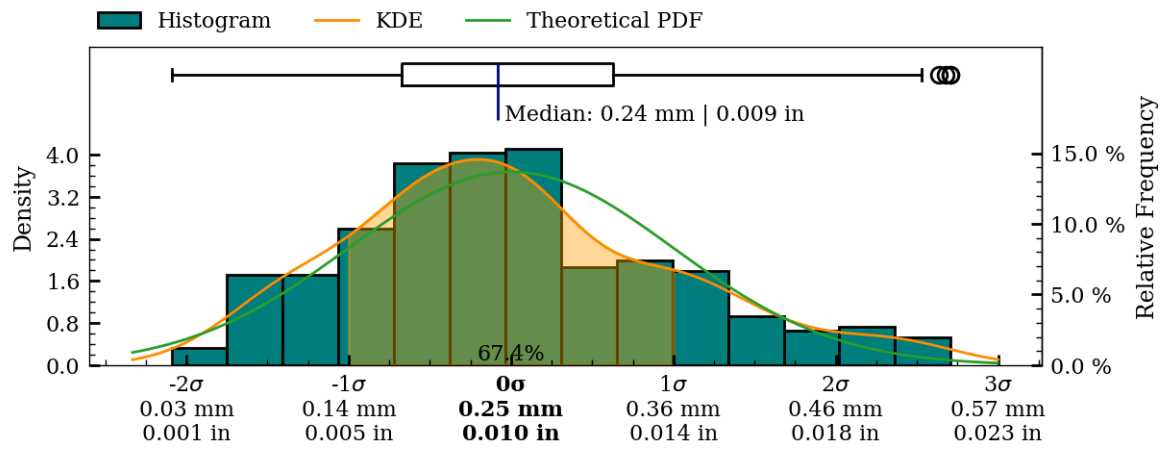
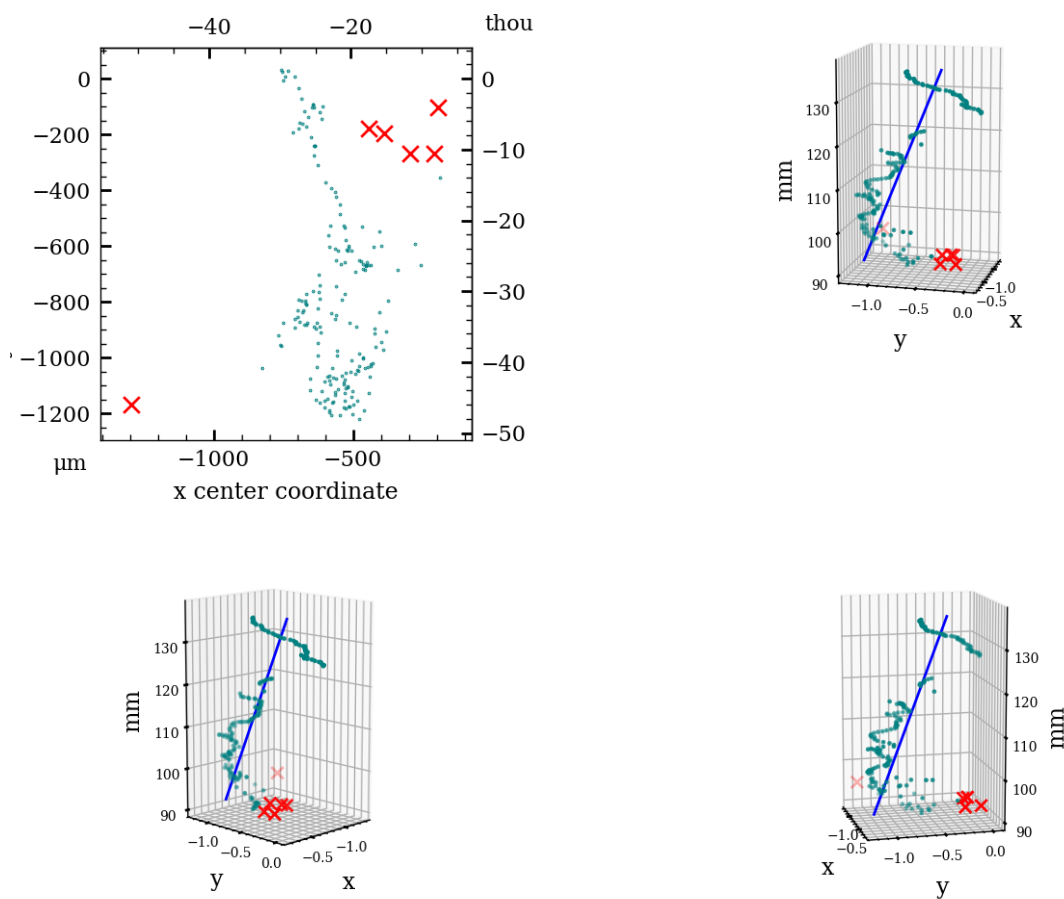


Figure 46: Coaxiality residual plots of exterior surface, MV016c.

Coaxiality plots, interior surface



Coaxiality residuals from fitted axis, interior surface

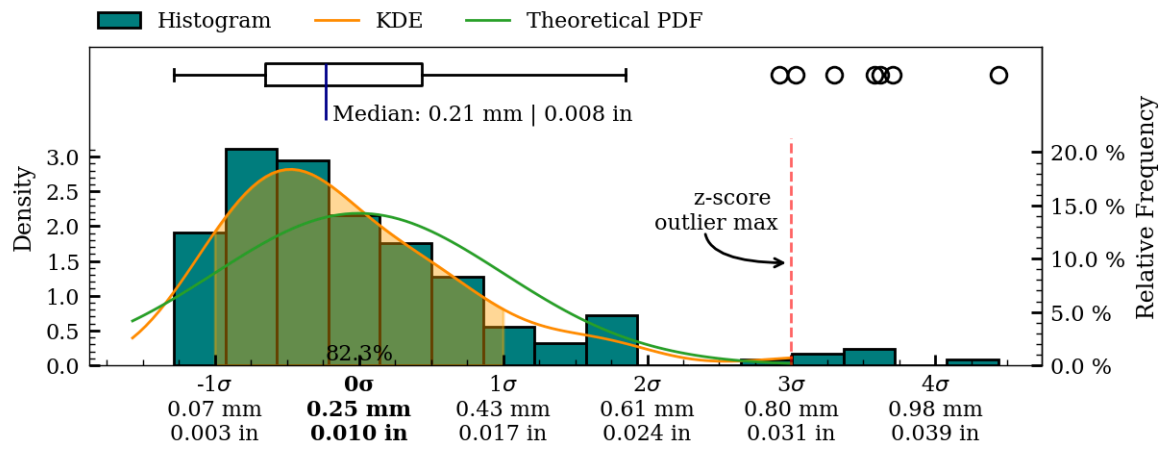
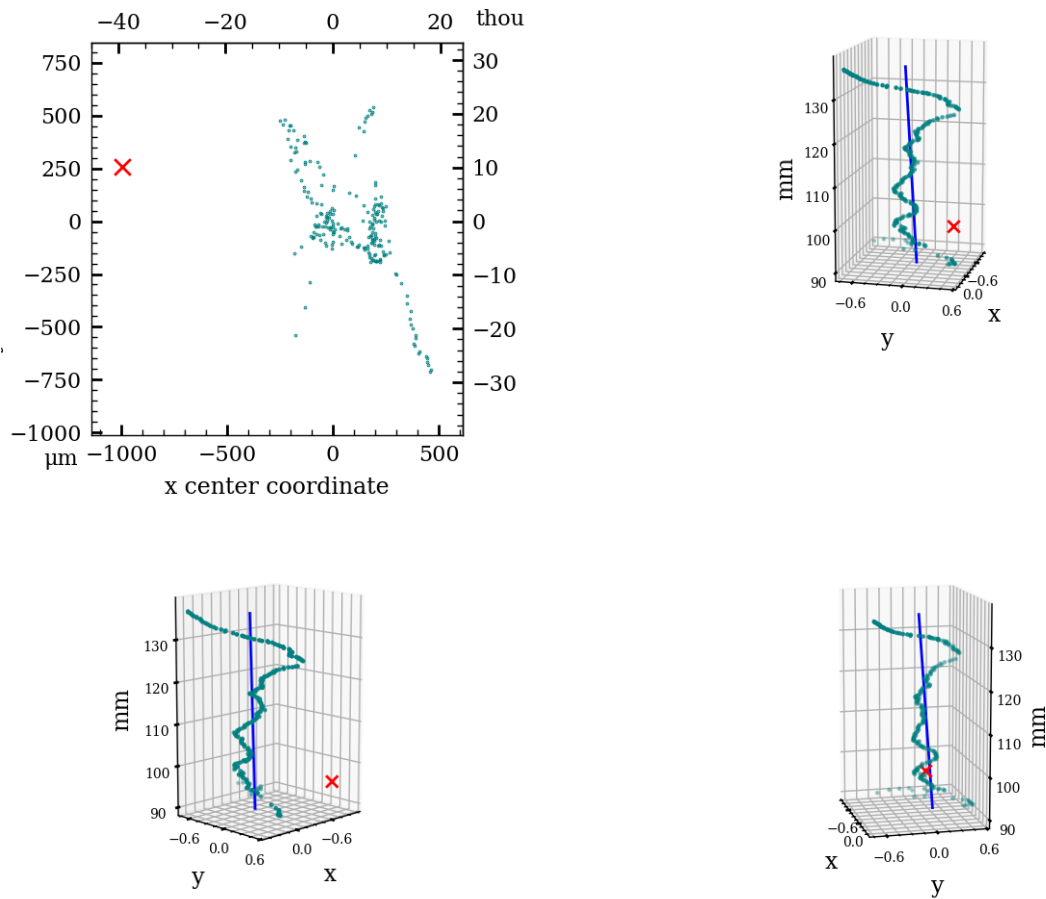


Figure 47: Coaxiality residual plots of interior surface, MV016c.

Coaxiality plots, interior separately aligned surface



Coaxiality residuals from fitted axis, interior separately aligned surface

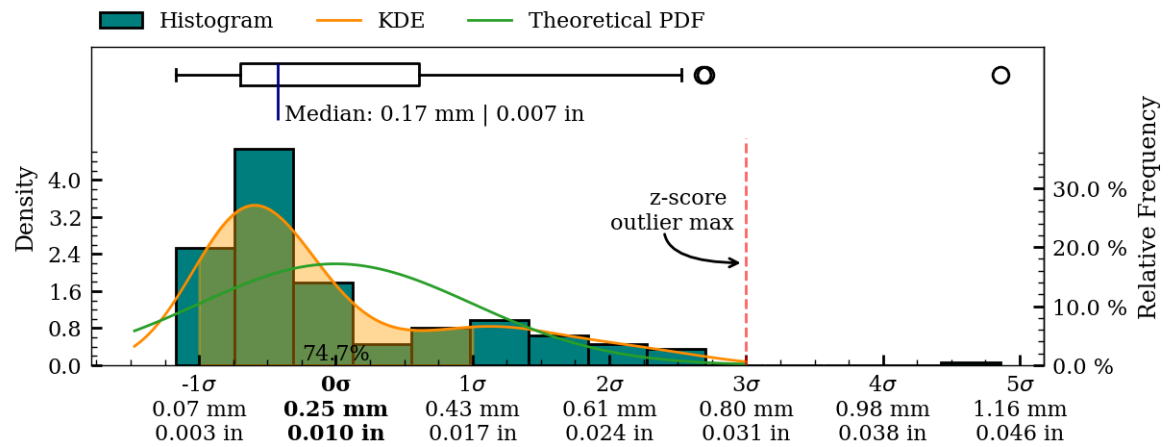


Figure 48: Coaxiality residual plots of interior_separate surface, MV016c.

Surface Variability

To illustrate the overall surface deviations of the object, a surface variability heatmap has been created. This heatmap provides an accessible overview of the topography of the manufacturing precision and surface structure of the object.

The surface variability measurements are created by fitting a number of higher-order polynomials to the two-dimensional folded profile of the scan data. This process creates an idealized mathematical representation of actual surface curvature of object, and as such provides a continuous model representation of the actual object. It is important to note that only such a non-discretized representation is sufficient to avoid introducing inconsistently varying errors in the mapping of the final surface deviation results, that the rendered heatmaps are based on.

To produce the final surface variability map, the distance from each scanned vertex to the fitted polynomial is calculated and used as the mapping function input, for applying colours to the surface of the object.

It is important to note that this variability map does not describe deviations from the original *intended* shape of the artifact (if any), as this shape (the *intended design*, so to speak) will have been lost to time. It does however provide a very informative visualization of the texture and structure of the surface and very importantly, *does* highlight potential manufacturing-relevant patterns in the surface texture (if present). Such patterns are, as an example, clearly evident on the interior surface of artifact PV001.

Exterior surface

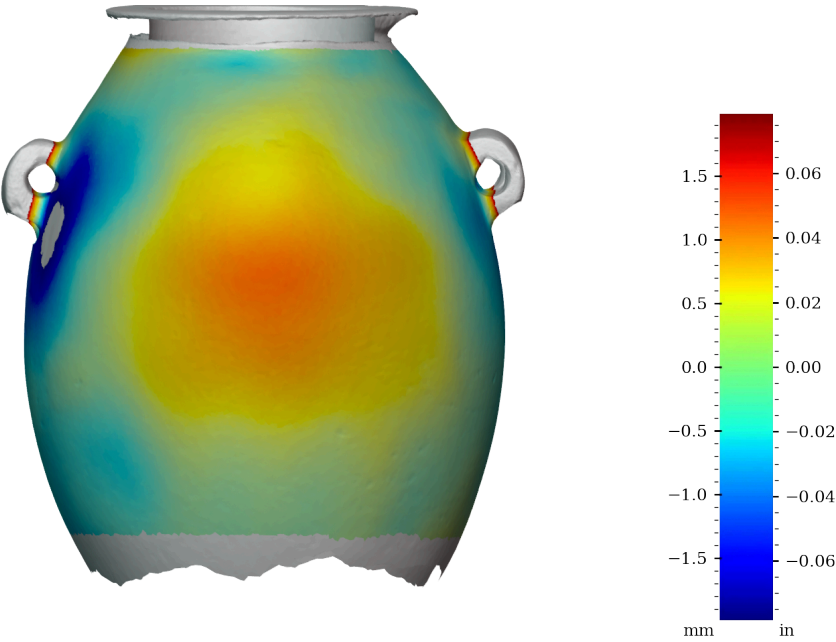


Figure 49: Surface variability heatmap of MV016c, front view

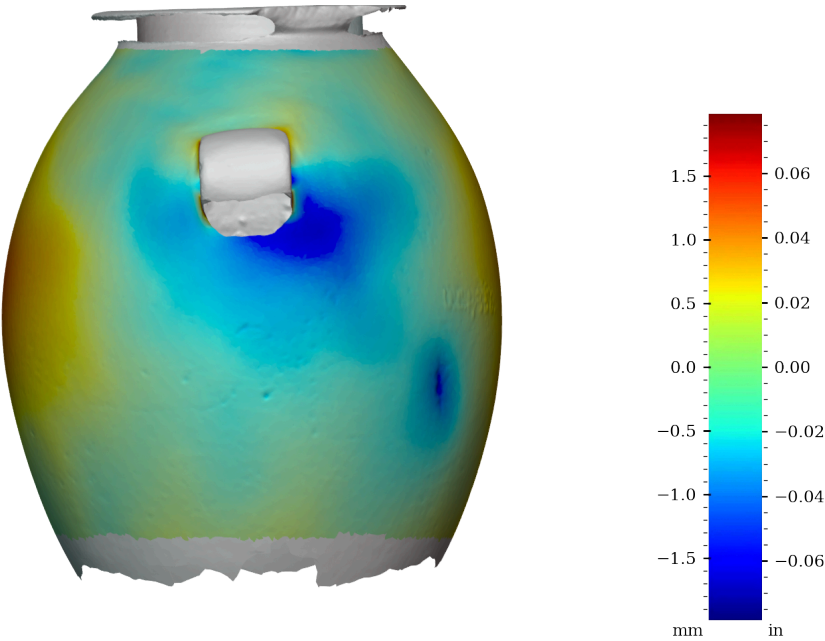


Figure 50: Surface variability heatmap of MV016c, rotated 90°

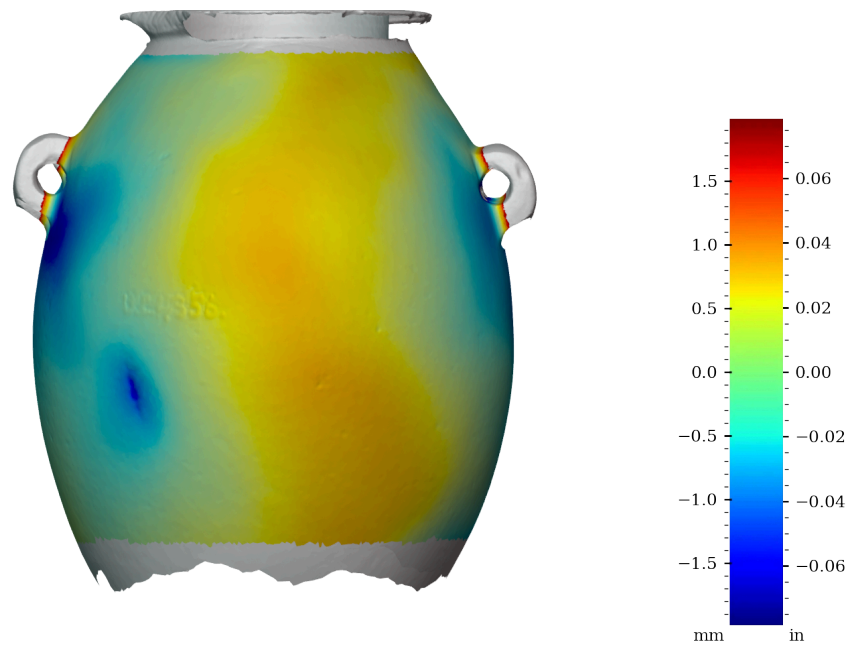


Figure 51: Surface variability heatmap of MV016c, rotated 180°

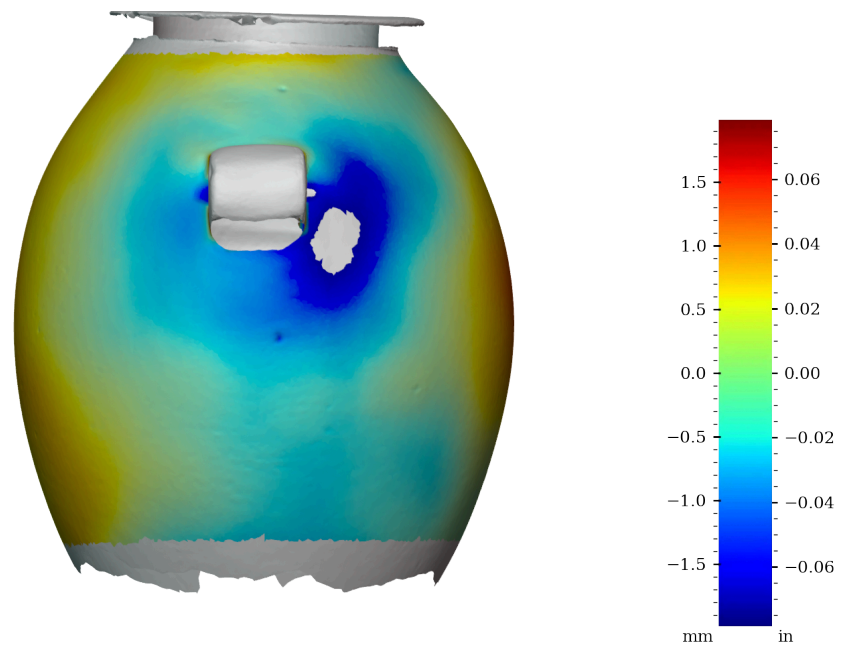


Figure 52: Surface variability heatmap of MV016c, rotated 270°

Interior surface

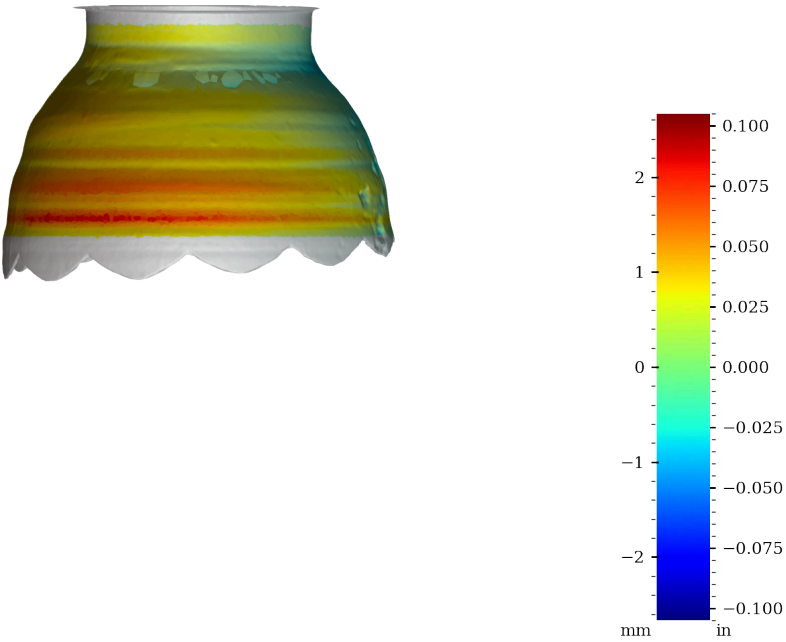


Figure 53: Surface variability heatmap of MV016c, front view

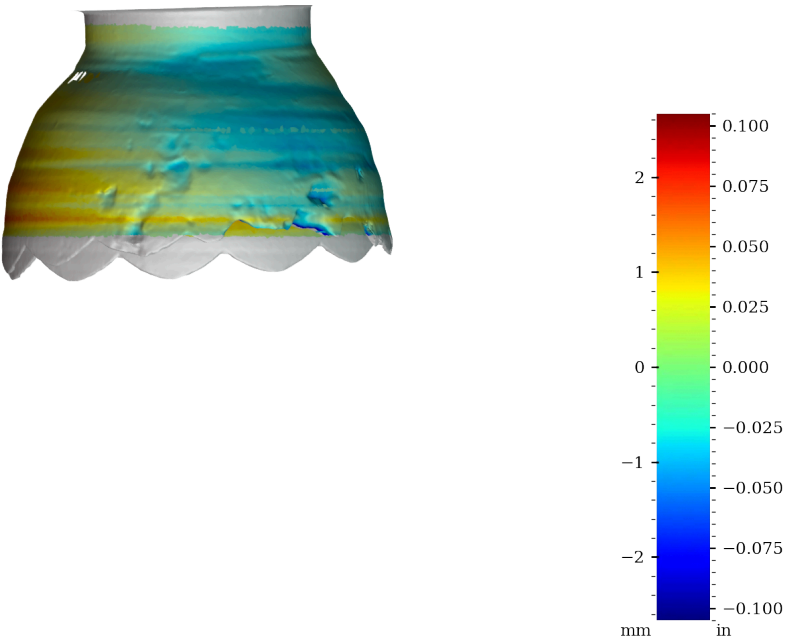


Figure 54: Surface variability heatmap of MV016c, rotated 90°

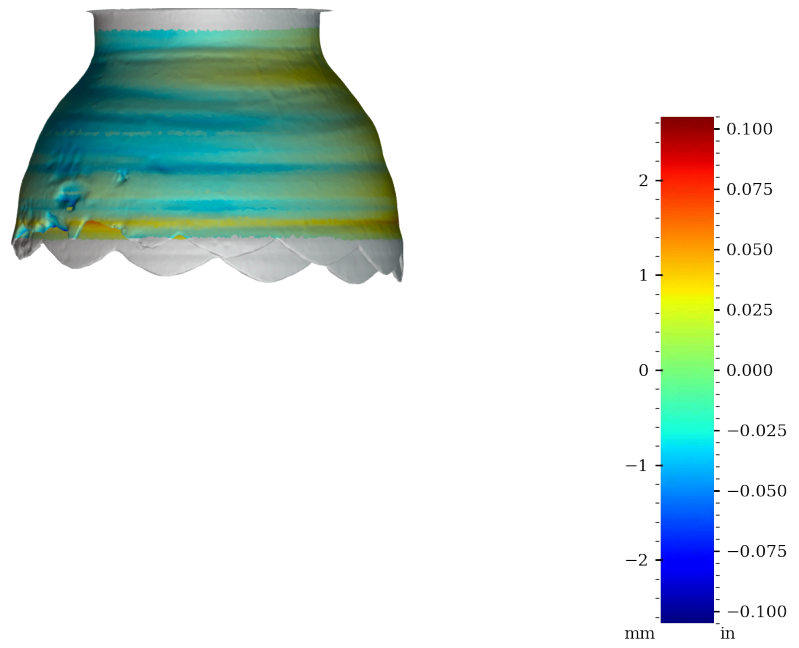


Figure 55: Surface variability heatmap of MV016c, rotated 180°

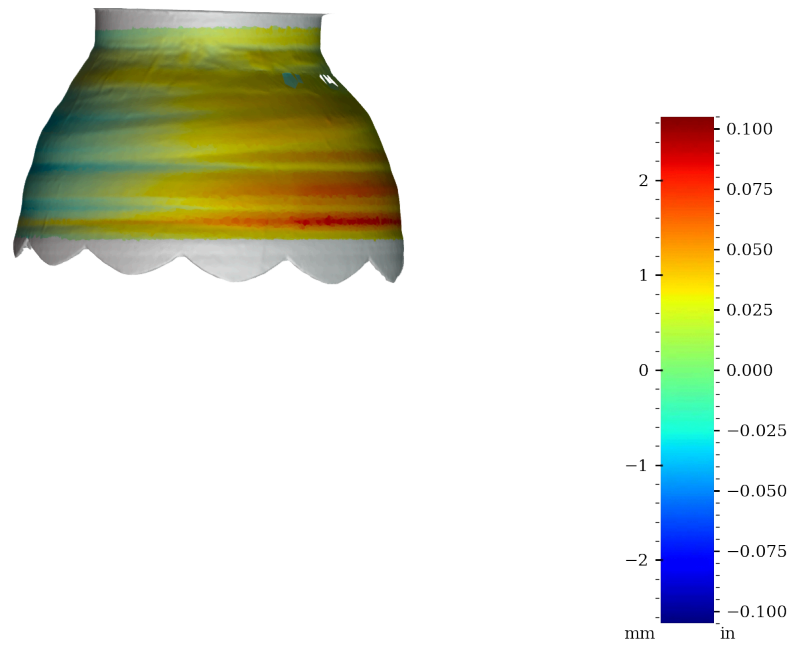


Figure 56: Surface variability heatmap of MV016c, rotated 270°

Interior surface aligned separately

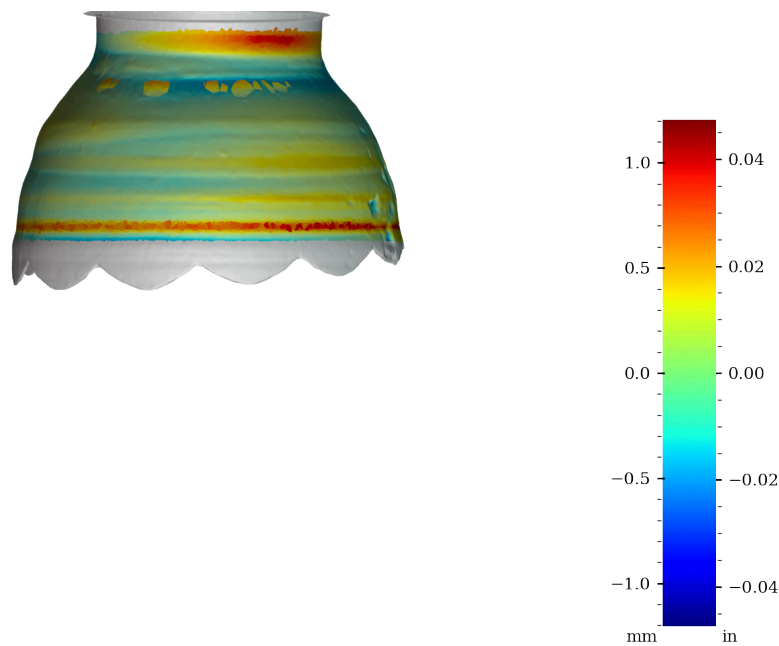


Figure 57: Surface variability heatmap of MV016c, front view

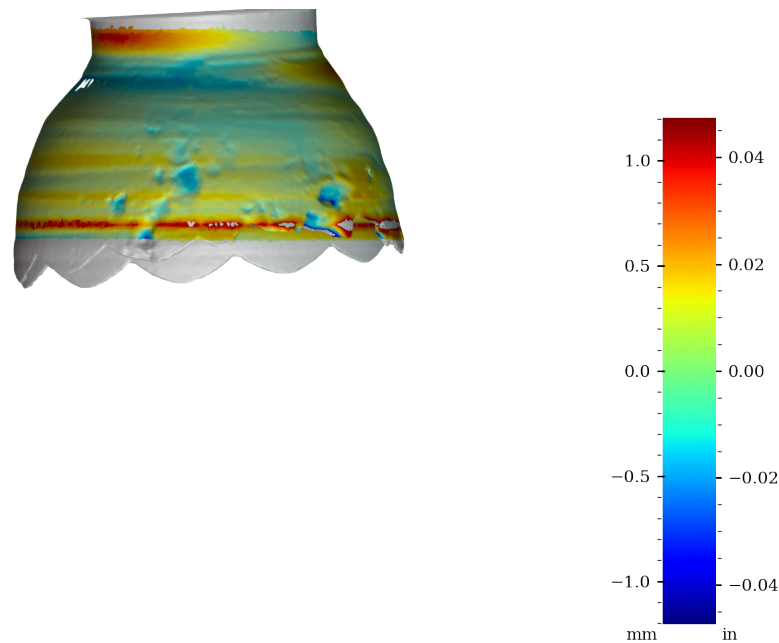


Figure 58: Surface variability heatmap of MV016c, rotated 90°

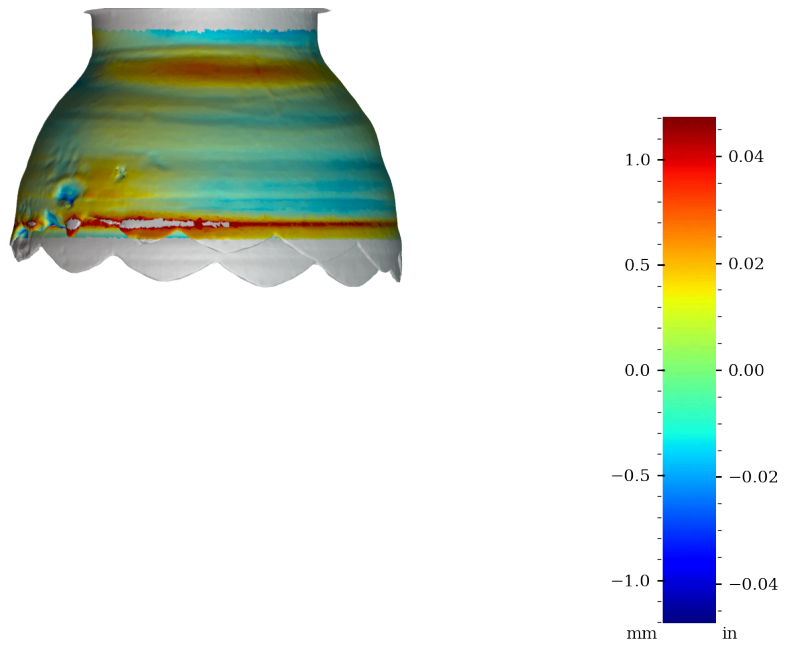


Figure 59: Surface variability heatmap of MV016c, rotated 180°

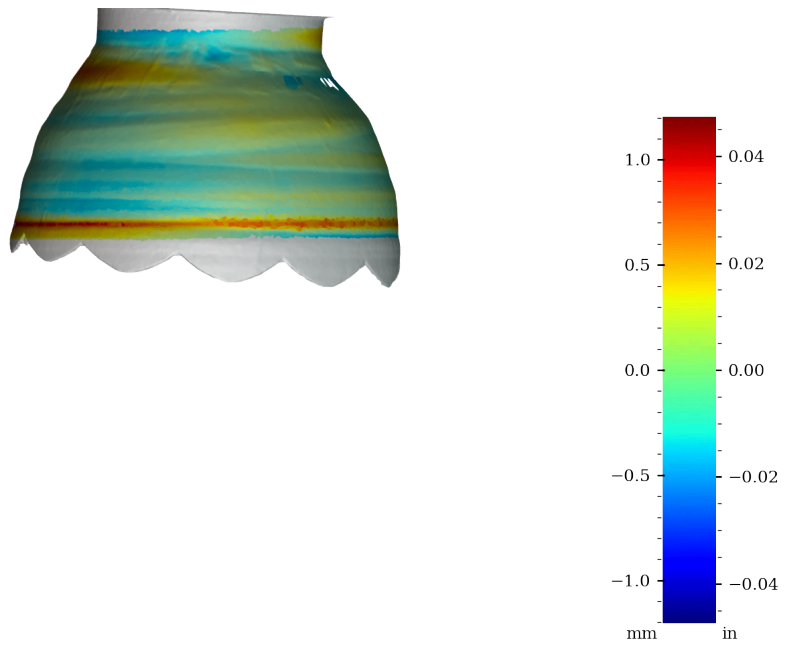


Figure 60: Surface variability heatmap of MV016c, rotated 270°

Surface variability statistics

Area	MSD	RMSD	SD	Median AD	Range	Min	Max	Sample size
	mm ²	mm	mm	mm	mm	mm	mm	
Exterior	0.4399	0.663	0.387	0.277	3.752	-2.277	1.475	81197
Interior	0.9321	0.965	0.635	0.297	9.040	-6.787	2.253	76725
Interior separate	0.3620	0.602	0.514	0.120	8.044	-6.384	1.661	77028
	in ²	in	in	in	in	in	in	
Exterior	0.000682	0.0261	0.0152	0.0109	0.1477	-0.0896	0.0581	81197
Interior	0.001445	0.0380	0.0250	0.0117	0.3559	-0.2672	0.0887	76725
Interior separate	0.000561	0.0237	0.0202	0.0047	0.3167	-0.2513	0.0654	77028

Table 5: Surface variability statistics, MV016c

Table 5 shows the statistics of the distance from the scan vertices to the best fit object model. These statistics are briefly explained below.

Histogram, KDE and Box-plot of measured surface variability - exterior surface

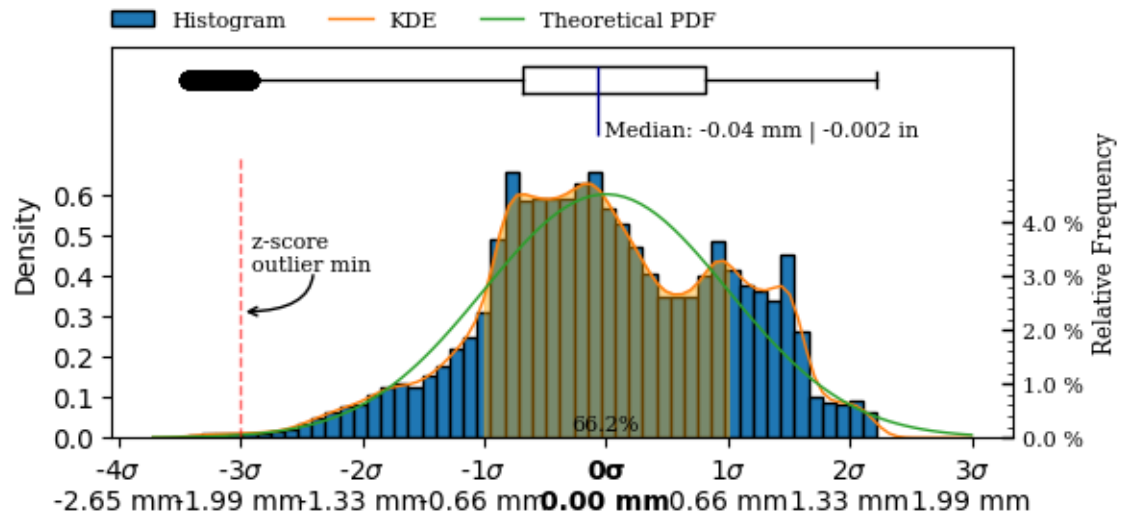


Figure 61: Exterior surface variability boxplot, kds and histogram.

Histogram, KDE and Box-plot of measured surface variability - interior surface

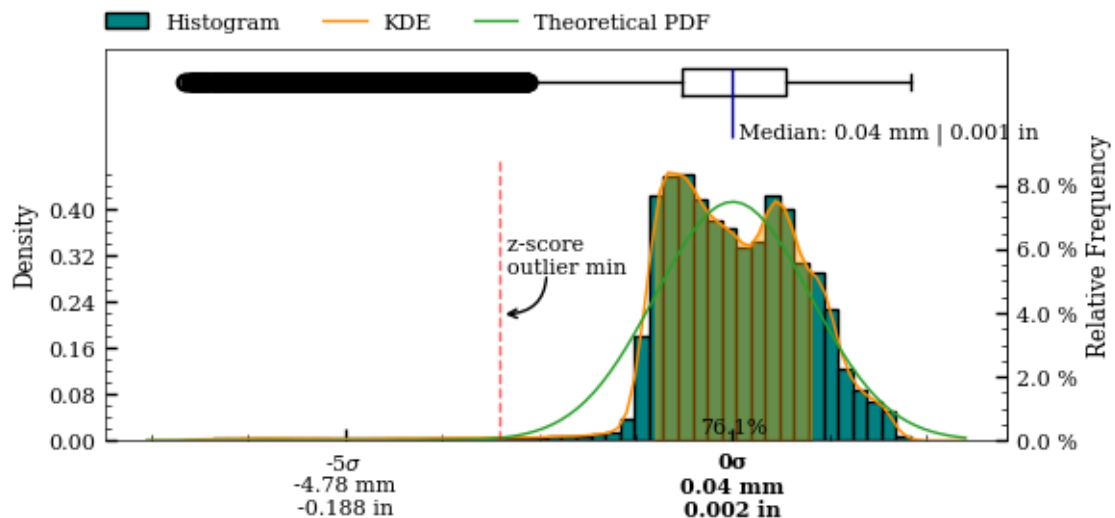


Figure 62: Interior surface variability boxplot, kds and histogram.

Histogram, KDE and Box-plot of measured surface variability - interior separately aligned surface

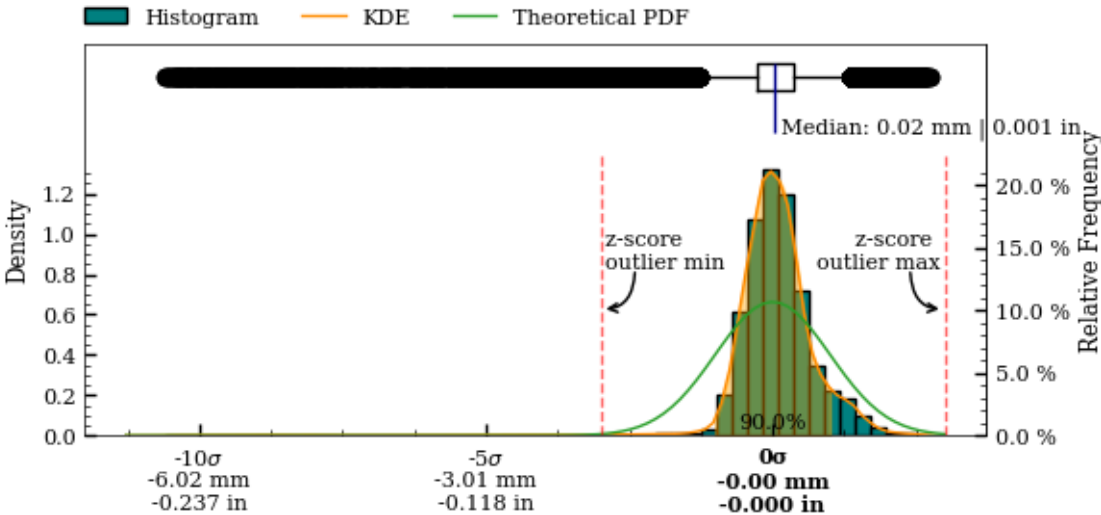


Figure 63: Interior separately aligned surface variability boxplot, kds and histogram.

Precision Score Of The Artifact

To enable valid comparison of the manufacturing precision of different artifacts, a metric that robustly quantifies the overall precision of the object is required. The considerations for such a metric will be explored in this section.

Based on these considerations, a *Precision Score* metric will be defined.

For an object to be described as having been manufactured with high precision, several qualities must be present *concurrently*, and throughout the *entire* geometry of the final object. A given object may exhibit high levels of one or more *components* of precision, but be lacking in others. For example:

- An object may present high levels of coaxiality, but lack circularity.
- An object may exhibit good circularity, but show imperfections in the surface structure.
- An object may be smoothed to perfection *without* any circularity or coaxiality.
- An object may exhibit high levels of all of the above metrics in *some* areas, but not in others.

Therefore, a precision score metric **must** account for *all* aspects of the individual, underlying precision metrics (circularity, concentricity, coaxiality and surface variability) throughout the *entire* surface area of the object.

The composite high order polynomial model, used to generate the surface variability map (described in Surface Variability, p. 48) is the best continuous mathematical representation of the object available to us (lacking any original design plans, as would normally be available in metrological analysis). This idealized model encompasses all of the above component metrics.

In the creation of the model, all scan data-points are taken into account (excluding areas with extensive damage), making it the best possible idealized representation we can achieve. When this model has been accurately created, the deviation between the model and the scanned data-points can be calculated over the non-discretized polynomials, *without* the need for an “original” CAD model (and importantly, unless such a CAD model *actually* corresponded to the original design intent, it would be an insufficient comparison basis).

Within the context of defining a valid, overall precision metric, this approach satisfies the incorporation of all of the necessary metrics:

- **Circularity:** Because the reconstructed polynomial model is revolved around the Z-plane, the idealized representation is perfectly circular, and thus incorporates the circularity component.
- **Concentricity and coaxiality:** Because the Z-axis (datum axis) is the center axis of the model, it incorporates the concentricity and coaxiality components.
- **Surface variability:** Because the model is continuous and non-discretized, it can be used accurately for all points of the scan data, and incorporates the surface variability component.

The level of precision ultimately achieved in a physical object does not share a linear relationship with its manufacturing requirements. Since continuously higher levels of final precision becomes progressively harder to achieve, an overall precision metric must take this relationship into account.

A robust statistical metric that satisfies this requirement is the *Mean Squared Deviation* (MSD or MSE). Here specifically, we can utilize the mean square of the deviations between the model (\hat{y}) and the data-points (y_i).

Combining all of the above considerations, we can express a well-defined *Precision Score* metric, that provides an immediately accessible way to understand the overall precision of an object, while being statistically valid. Since the Mean Squared Deviation tends towards zero as the overall precision increases, the inverse of the Mean Squared Deviation is taken to obtain a precision score metric that increases as precision increases¹²:

$$\text{Precision Score} = \frac{n}{\sum_{i=1}^n (y_i - \hat{y})^2}$$

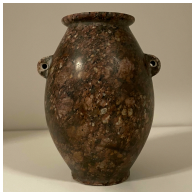
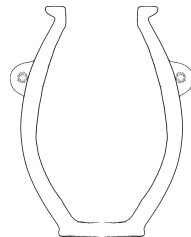

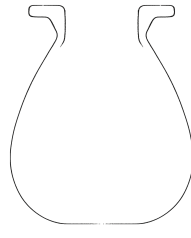

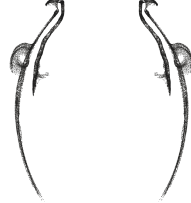




¹²The precision score unit is $\frac{1}{\text{mm}^2}$

The precision score of MV016c have been calculated separately for:

- Precision score, exterior surface: 2.27
- Precision score, separately aligned interior surface: 2.76
- Precision score, interior surface: 1.07
- Precision score, full surface: 2.49

The precision score of a Zeiss 1.00000 inch reference sphere have been calculated to 43,943 (RMSE = 0.00477 mm / 0.00010 in). The scan was obtained by Max Fomitchev-Zamilov using a Keyence VL –500 scanner with a rated accuracy of 10 microns. The precision analysis of the reference sphere scan indicates at the maximum possible precision score obtainable.

Table 6 shows the precision score of this artifact (MV016c), compared to the two most precise, and the two least precise vessels currently analyzed.

Artifact		Material	Precision Score	Link to Report
		PV001 Red Granite	1980 Full: 1177 Exterior: 1980 Interior separate: 798 Interior: 722	Report Publication
		PV006 Dark grey granite	621 Full: 610 Exterior: 621 Interior separate: 479 Interior: 152	Report Publication
		MV016c Basalt	2.27 Full: 2.49 Exterior: 2.27 Interior separate: 2.76 Interior: 1.07	Report Publication
		RV003 Marble breccia	1.46 Full: 1.49 Exterior: 1.46 Interior separate: 1.53 Interior: 0.54	Report Publication
		MV010 Calcite (Egyptian Al-abaster)	1.17 Full: 1.32 Exterior: 1.17 Interior separate: 11 Interior: 0.17	Report Publication

Analysis Roadmap

While the current iteration of this work already provides valuable results, continued future additions and improvements will enhance their utility further. This section details planned iterative updates and improvements, to both the reports themselves, and to the underlying methodology and software they are created with.

Alignment Section

- Detailed exploration of different circle regression algorithms
- If handles are present on the vessel, exploring alignment of the vessels so the handle positions match each other
- Add optimization of the perpendicular surface deviation, with the best results of the coaxial alignment
- Align by minimizing circularity results (of rotated sample slice, to compensate for sample height distortions)

Measurements of Precision

- Section detailing how measurements perpendicular to the surface curvature are obtained
- Detailed surface area analysis, exploring the residual patterns throughout subsequent sample slices of the artifact surface
- Wall thickness deviation color map
- Robust outlier identification on circularity, to better handle analysis of damaged areas of the artifacts in addition to removal of interior crystalline structure points present in CT scans
- Layout updates to the charts and tables

Visibility of Outliers and Damaged Sections

- Identification and marking of damaged parts
- Visualization of outliers on the artifact surface

Exploration of Mathematical Primitives

- Analysis of selected curvatures and flat surfaces on the vessel in both the horizontal and vertical planes
 - Circles
 - Parabolas
 - Ellipsoids
 - Hyperbolas
 - Cones
- Implementation of robust regressions models suitable for this domain, based on RANSAC.

Metrics on Primary Features

- Measurements of features in the horizontal plane
- Measurements of features in the vertical plane
- Measurements of angles
- Measurements of volume

Exploration of Potential Design Ratios

- π , φ , e , 1, 2, 3, 4 etc.

Raw Dataset Attachments

- Including all measurement and sample coordinates as CSV-files embedded in the report
- Including an STL file of the aligned object alongside the report, for easier external replication and validation of the research results

Appendix A - Comparison Of Circularity Measurements (Z-plane vs. surface-perpendicular)

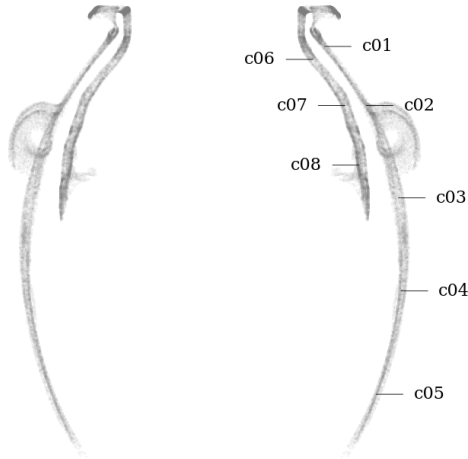


Figure 64: Circularity measurement sample locations, full mesh aligned to exterior surface

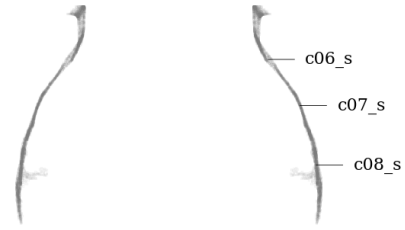


Figure 65: Circularity measurement sample location, separately aligned interior mesh

Samples perpendicular to the surface curvature

Tag	Area	Measured deviation ⁸	Residuals				Sample size	Slice		
			Range	RMSD ⁹	MAD ¹⁰	SD		Height	Z coord.	Radius ¹¹
		mm	mm	mm	mm	mm		mm	mm	mm
c01	exterior	Ø61.619±0.703	1.238	0.419	0.134	0.179	90	0.200	130.027	30.810
c02	exterior	Ø84.997±1.159	1.984	0.565	0.141	0.270	96	0.200	113.564	42.499
c03	exterior	Ø102.924±2.178	3.561	0.982	0.392	0.463	147	0.200	87.878	51.462
c04	exterior	Ø104.396±1.413	2.551	0.735	0.293	0.370	188	0.200	61.934	52.198
c05	exterior	Ø90.543±1.001	1.726	0.430	0.210	0.289	116	0.200	33.154	45.272
c06	interior	Ø55.143±0.987	1.900	0.711	0.167	0.249	151	0.200	126.417	27.572
c06_s	interior sep.	Ø55.278±0.859	1.452	0.496	0.131	0.219	176	0.200	126.417	27.639
c07	interior	Ø73.070±1.324	2.566	0.799	0.272	0.348	251	0.200	113.564	36.535
c07_s	interior sep.	Ø73.161±0.204	0.374	0.105	0.045	0.056	216	0.200	113.564	36.581
c08	interior	Ø81.112±1.976	2.898	0.827	0.171	0.476	366	0.200	97.005	40.556
c08_s	interior sep.	Ø82.136±0.628	1.187	0.274	0.104	0.159	376	0.200	97.005	41.068

Table 7: Detailed circularity measurements at selected samples in z-plane, vessel MV016c.

Samples in the Z-plane

Tag	Area	Measured deviation ⁸	Residuals				Sample size	Slice		
			Range	RMSD ⁹	MAD ¹⁰	SD		Height	Z coord.	Radius ¹¹
		mm	mm	mm	mm	mm		mm	mm	mm
c01	exterior	Ø61.285±1.174	1.783	0.595	0.188	0.316	162	0.200	130.027	30.642
c02	exterior	Ø84.293±1.362	2.279	0.603	0.272	0.391	144	0.200	113.564	42.146
c03	exterior	Ø102.632±2.047	3.598	1.058	0.400	0.494	172	0.200	87.878	51.316
c04	exterior	Ø104.354±1.390	2.563	0.715	0.282	0.363	185	0.200	61.934	52.177
c05	exterior	Ø90.522±1.090	1.857	0.483	0.169	0.344	125	0.200	33.154	45.261
c06	interior	Ø54.865±1.382	2.498	0.876	0.213	0.343	173	0.200	126.417	27.432
c06_s	interior sep.	Ø54.173±1.643	1.837	0.673	0.080	0.526	321	0.200	126.417	27.087
c07	interior	Ø72.356±1.720	2.700	0.885	0.386	0.550	262	0.200	113.564	36.178
c07_s	interior sep.	Ø73.154±0.259	0.464	0.122	0.051	0.063	267	0.200	113.564	36.577
c08	interior	Ø80.519±2.081	2.692	0.933	0.275	0.654	418	0.200	97.005	40.259
c08_s	interior sep.	Ø82.331±0.720	1.229	0.263	0.087	0.159	380	0.200	97.005	41.165

Table 8: Detailed circularity measurements at selected samples perpendicular to vessel curvature, vessel MV016c.

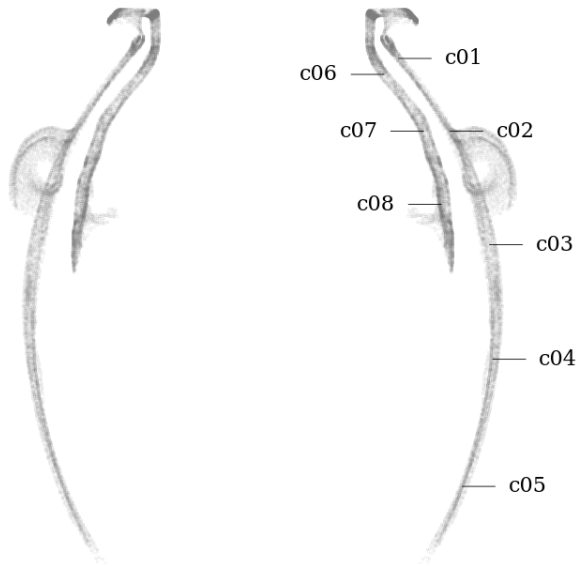


Figure 66: Circularity measurement sample locations, full mesh aligned to exterior surface

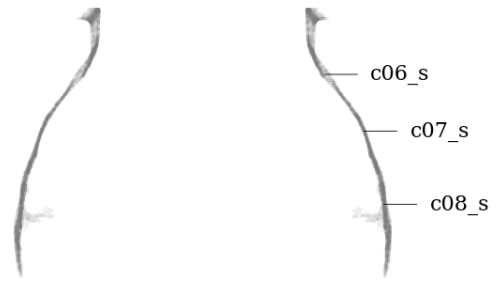


Figure 67: Circularity measurement sample location, separately aligned interior mesh

Samples perpendicular to the surface curvature

Tag	Area	Measured deviation ⁸	Residuals				Sam-ple size	Slice		
			Range	RMSD ⁹	MAD ¹⁰	SD		Height	Z coord.	Radius ¹¹
		in	in	in	in	in		in	in	in
c01	exterior	Ø2.4260±0.0277	0.0487	0.0165	0.0053	0.0071	90	0.0079	5.1192	1.2130
c02	exterior	Ø3.3463±0.0456	0.0781	0.0223	0.0056	0.0106	96	0.0079	4.4710	1.6732
c03	exterior	Ø4.0521±0.0858	0.1402	0.0387	0.0155	0.0182	147	0.0079	3.4598	2.0261
c04	exterior	Ø4.1101±0.0556	0.1004	0.0289	0.0115	0.0146	188	0.0079	2.4383	2.0550
c05	exterior	Ø3.5647±0.0394	0.0679	0.0169	0.0083	0.0114	116	0.0079	1.3053	1.7823
c06	interior	Ø2.1710±0.0388	0.0748	0.0280	0.0066	0.0098	151	0.0079	4.9771	1.0855
c06_s	interior sep.	Ø2.1763±0.0338	0.0572	0.0195	0.0052	0.0086	176	0.0079	4.9771	1.0881
c07	interior	Ø2.8768±0.0521	0.1010	0.0315	0.0107	0.0137	251	0.0079	4.4710	1.4384
c07_s	interior sep.	Ø2.8804±0.0080	0.0147	0.0041	0.0018	0.0022	216	0.0079	4.4710	1.4402
c08	interior	Ø3.1934±0.0778	0.1141	0.0325	0.0068	0.0187	366	0.0079	3.8191	1.5967
c08_s	interior sep.	Ø3.2337±0.0247	0.0467	0.0108	0.0041	0.0062	376	0.0079	3.8191	1.6169

Table 9: Detailed circularity measurements at selected samples in z-plane, vessel MV016c.

Samples in the Z-plane

Tag	Area	Measured deviation ⁸	Residuals				Sam-ple size	Slice		
			Range	RMSD ⁹	MAD ¹⁰	SD		Height	Z coord.	Radius ¹¹
		in	in	in	in	in		in	in	in
c01	exterior	Ø2.4128±0.0462	0.0702	0.0234	0.0074	0.0124	162	0.0079	5.1192	1.2064
c02	exterior	Ø3.3186±0.0536	0.0897	0.0237	0.0107	0.0154	144	0.0079	4.4710	1.6593
c03	exterior	Ø4.0406±0.0806	0.1417	0.0417	0.0157	0.0195	172	0.0079	3.4598	2.0203
c04	exterior	Ø4.1084±0.0547	0.1009	0.0282	0.0111	0.0143	185	0.0079	2.4383	2.0542
c05	exterior	Ø3.5639±0.0429	0.0731	0.0190	0.0066	0.0135	125	0.0079	1.3053	1.7819
c06	interior	Ø2.1600±0.0544	0.0983	0.0345	0.0084	0.0135	173	0.0079	4.9771	1.0800
c06_s	interior sep.	Ø2.1328±0.0647	0.0723	0.0265	0.0031	0.0207	321	0.0079	4.9771	1.0664
c07	interior	Ø2.8487±0.0677	0.1063	0.0348	0.0152	0.0217	262	0.0079	4.4710	1.4243
c07_s	interior sep.	Ø2.8801±0.0102	0.0183	0.0048	0.0020	0.0025	267	0.0079	4.4710	1.4400
c08	interior	Ø3.1700±0.0819	0.1060	0.0367	0.0108	0.0258	418	0.0079	3.8191	1.5850
c08_s	interior sep.	Ø3.2414±0.0283	0.0484	0.0103	0.0034	0.0062	380	0.0079	3.8191	1.6207

Table 10: Detailed circularity measurements at selected samples perpendicular to vessel curvature, vessel MV016c.

Comparison of circularity on the full vessel surface

Metric

Samples perpendicular to the surface curvature

Area	Range			Standard Deviation			RMSD			Slices	Slice height
	Median	Min.	Max.	Median	Min.	Max.	Median	Min.	Max.		
	mm	mm	mm	mm	mm	mm	mm	mm	mm		mm
Exterior	2.343	1.185	3.571	0.318	0.132	0.548	0.672	0.215	1.063	405	0.200
Interior	2.270	1.277	9.686	0.298	0.173	1.428	0.670	0.330	2.249	192	0.200
Interior separate	1.009	0.362	8.364	0.129	0.046	1.341	0.241	0.081	2.168	221	0.200

Table 11: Detailed circularity measurements at selected samples in z-plane, vessel MV016c.

Samples in the z-plane

Area	Range			Standard Deviation			RMSD			Slices	Slice height
	Median	Min.	Max.	Median	Min.	Max.	Median	Min.	Max.		
	mm	mm	mm	mm	mm	mm	mm	mm	mm		mm
Exterior	2.381	1.515	3.656	0.350	0.202	0.681	0.667	0.305	1.112	517	0.200
Interior	2.764	1.560	9.676	0.469	0.241	2.126	0.895	0.528	2.815	226	0.200
Interior separate	1.103	0.440	8.400	0.144	0.057	2.059	0.255	0.103	2.621	226	0.200

Table 12: Detailed circularity measurements at selected samples perpendicular to vessel curvature, vessel MV016c.

Imperial

Samples perpendicular to the surface curvature

Area	Range			Standard Deviation			RMSD			Slices	Slice height
	Median	Min.	Max.	Median	Min.	Max.	Median	Min.	Max.		
	in	in	in	in	in	in	in	in	in		in
Exterior	2.343	1.185	3.571	0.318	0.132	0.548	0.672	0.215	1.063	405	0.200
Interior	2.270	1.277	9.686	0.298	0.173	1.428	0.670	0.330	2.249	192	0.200
Interior separate	1.009	0.362	8.364	0.129	0.046	1.341	0.241	0.081	2.168	221	0.200

Table 13: Detailed circularity measurements at selected samples in z-plane, vessel MV016c.

Samples in the z-plane

Area	Range			Standard Deviation			RMSD			Slices	Slice height
	Median	Min.	Max.	Median	Min.	Max.	Median	Min.	Max.		
	in	in	in	in	in	in	in	in	in		in
Exterior	2.381	1.515	3.656	0.350	0.202	0.681	0.667	0.305	1.112	517	0.200
Interior	2.764	1.560	9.676	0.469	0.241	2.126	0.895	0.528	2.815	226	0.200
Interior separate	1.103	0.440	8.400	0.144	0.057	2.059	0.255	0.103	2.621	226	0.200

Table 14: Detailed circularity measurements at selected samples perpendicular to vessel curvature, vessel MV016c.

Circularity analysis of exterior surface - perpendicular to surface curvature

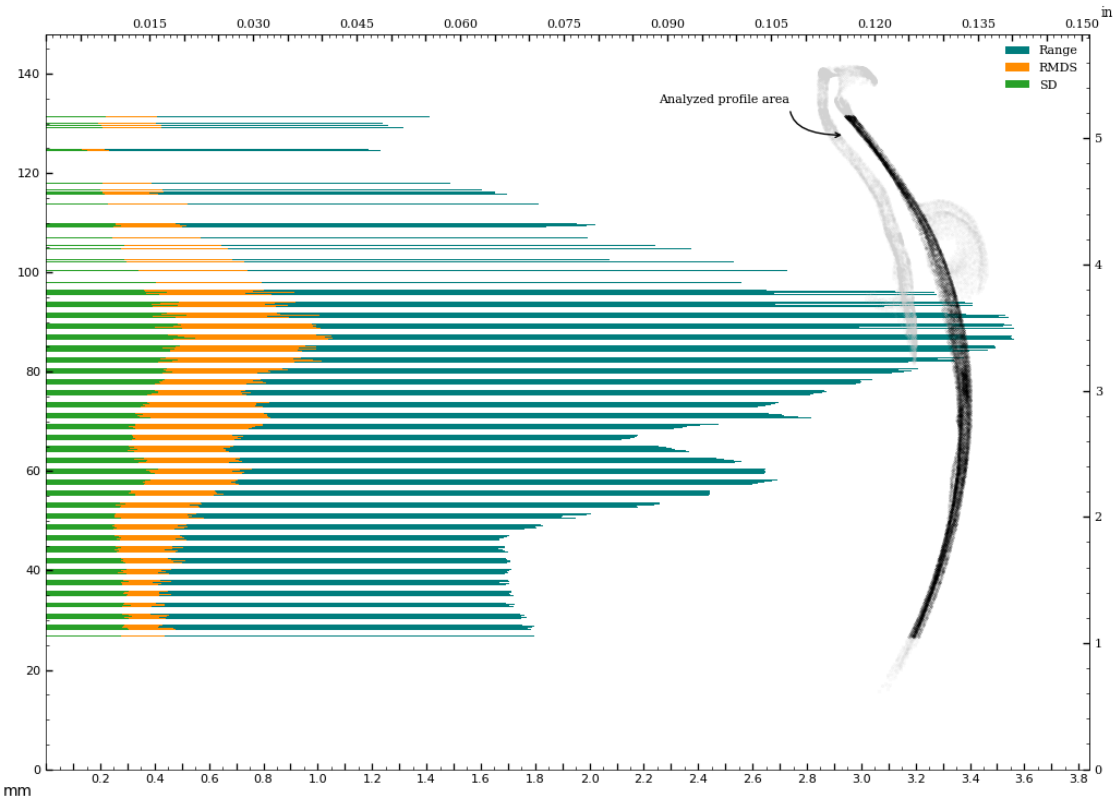


Figure 68: Circularity of exterior surface - perpendicular to surface curvature.

Circularity analysis of exterior surface - in z-plane

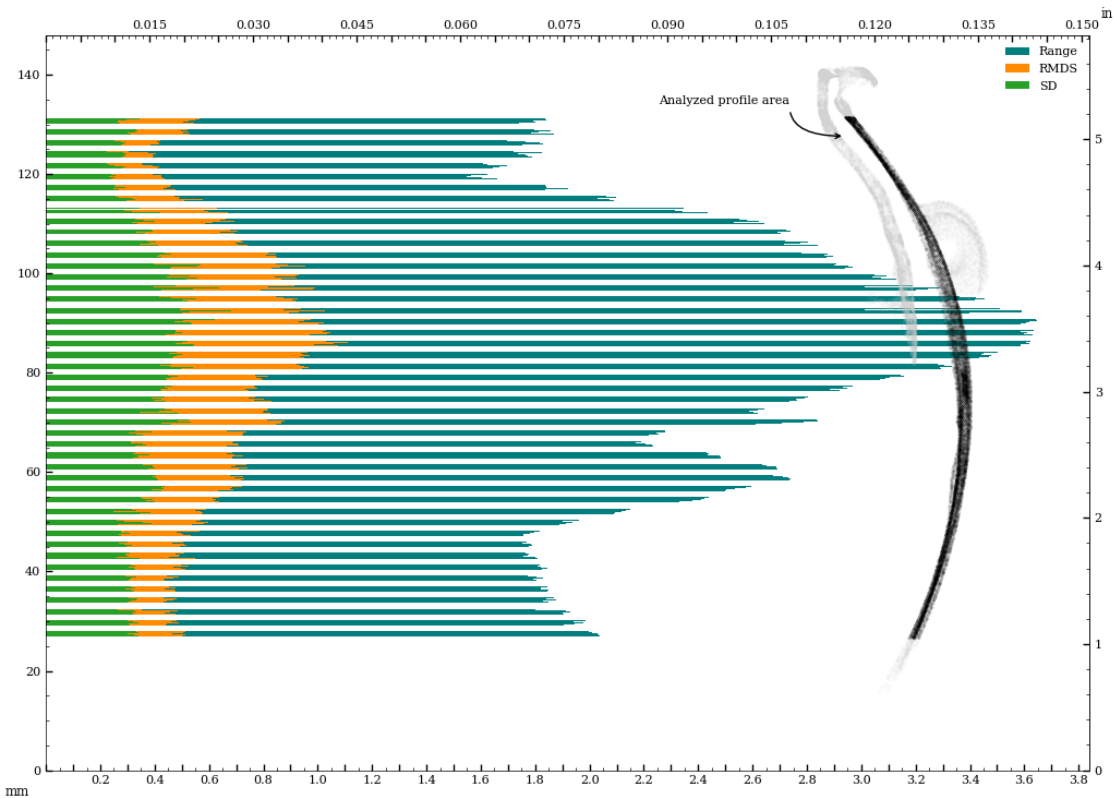


Figure 69: Circularity of exterior surface - in z-plane.

Circularity analysis of exterior surface, perpendicular to surface curvature, Standard Deviation and Root Mean Squared Deviation

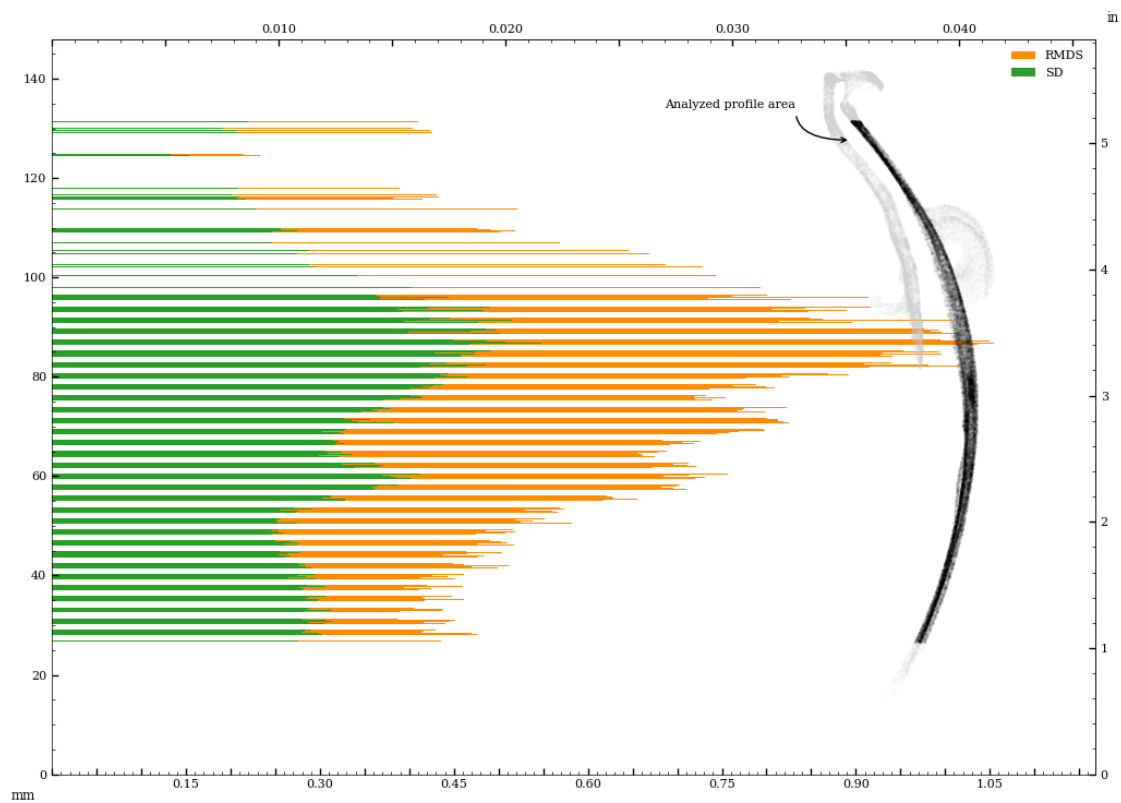


Figure 70: Vessel circularity of exterior surface, perpendicular to surface curvature, standard deviation and median absolute deviation.

Circularity analysis of exterior surface, in z-plane, Standard Deviation and Root Mean Squared Deviation

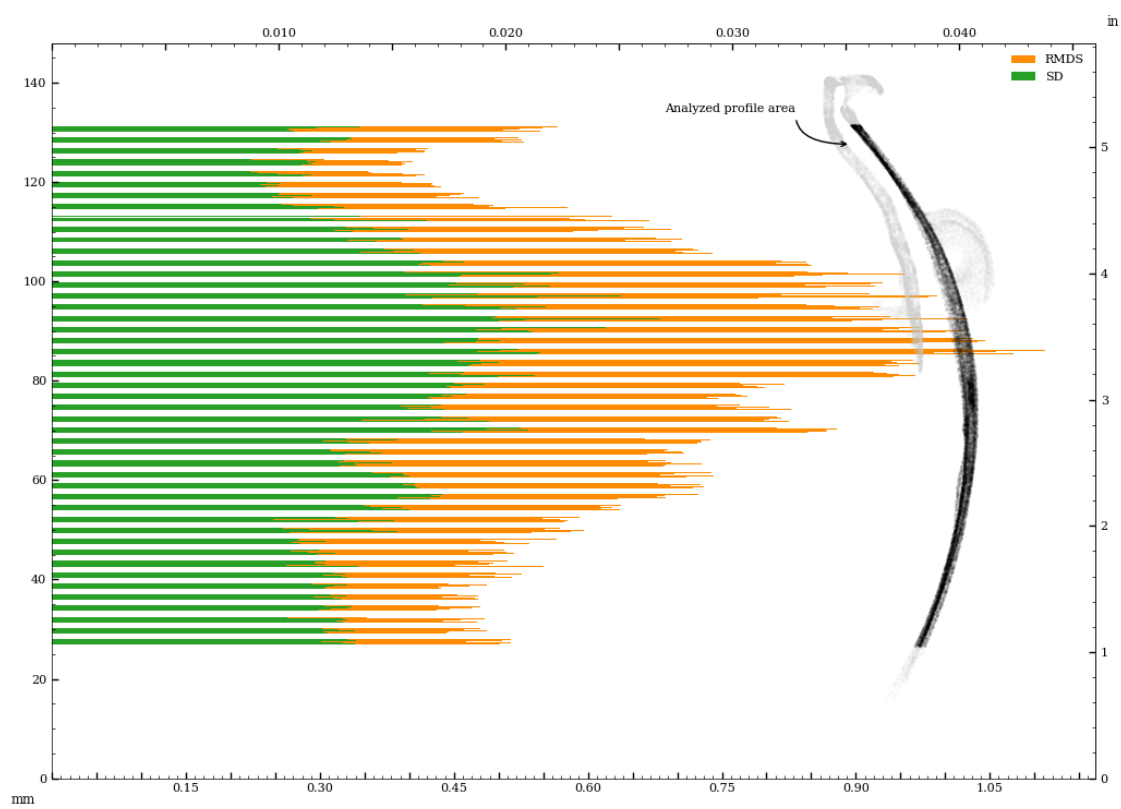


Figure 71: Vessel circularity of exterior surface, in z-plane, standard deviation and median absolute deviation.

Circularity analysis of interior surface - perpendicular to surface curvature

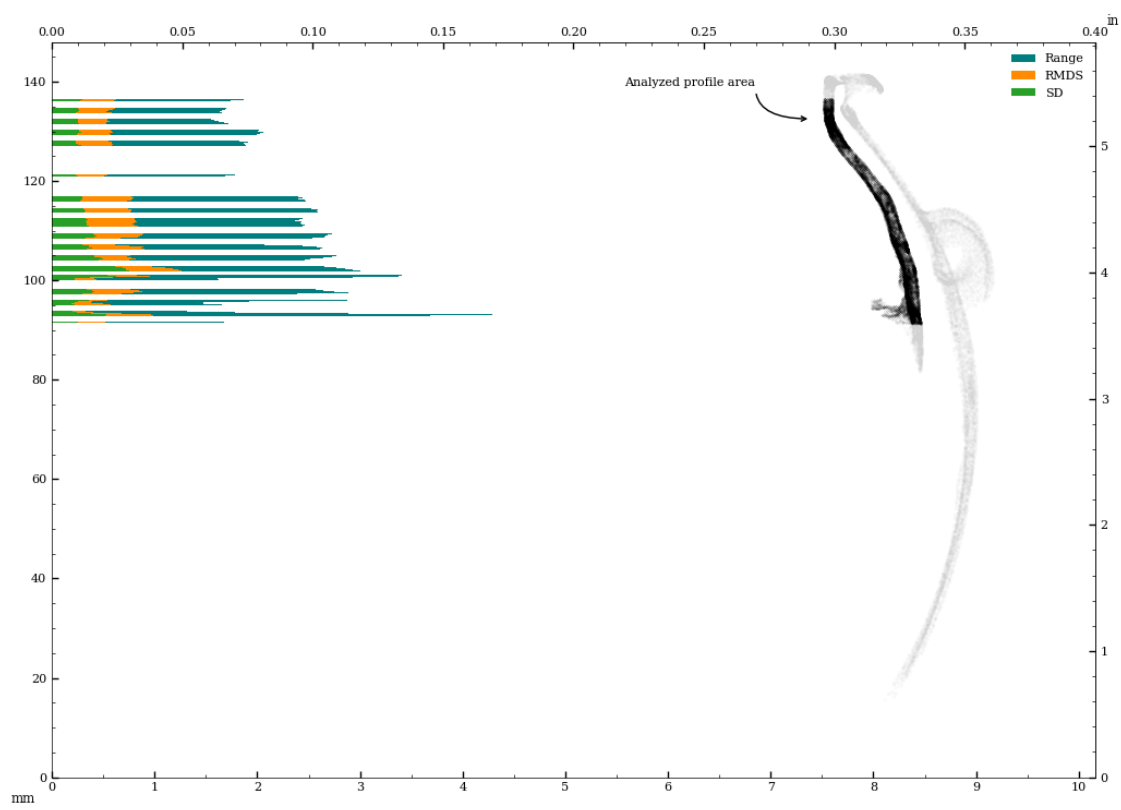


Figure 72: Circularity of interior surface - perpendicular to surface curvature.

Circularity analysis of interior surface - in z-plane

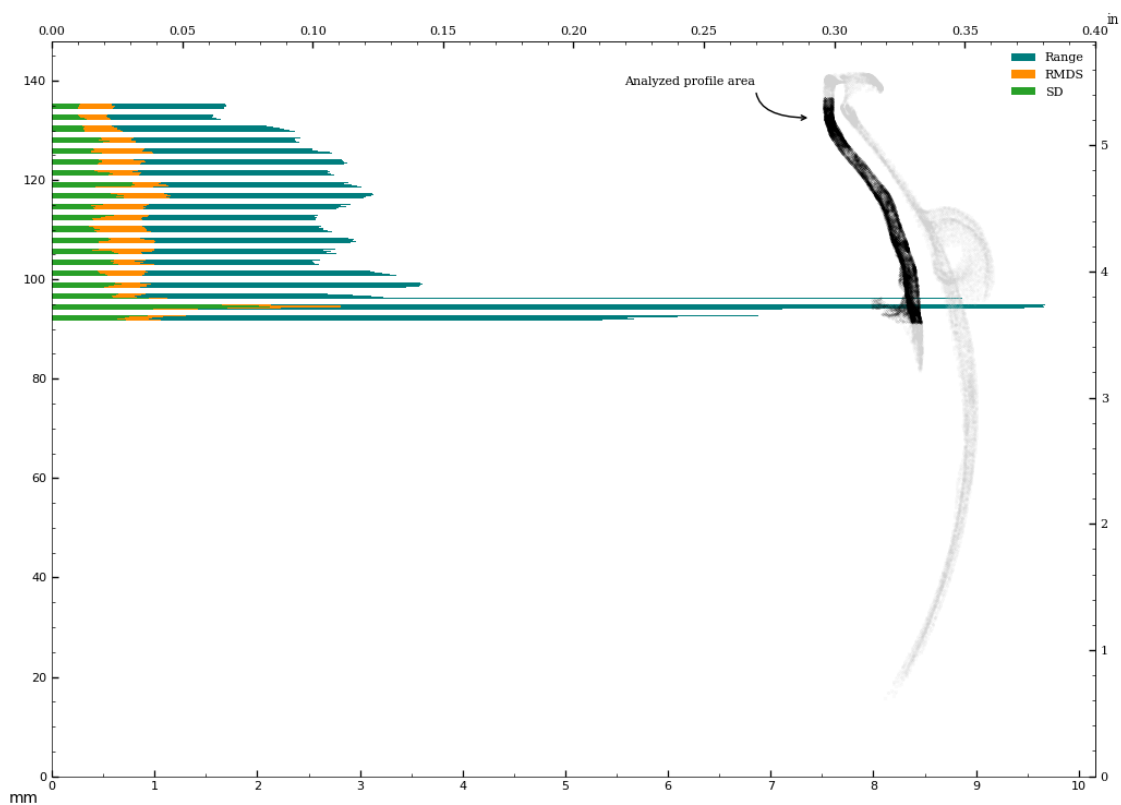


Figure 73: Circularity of interior surface - in z-plane.

Circularity analysis of interior surface, perpendicular to surface curvature, Standard Deviation and Root Mean Squared Deviation

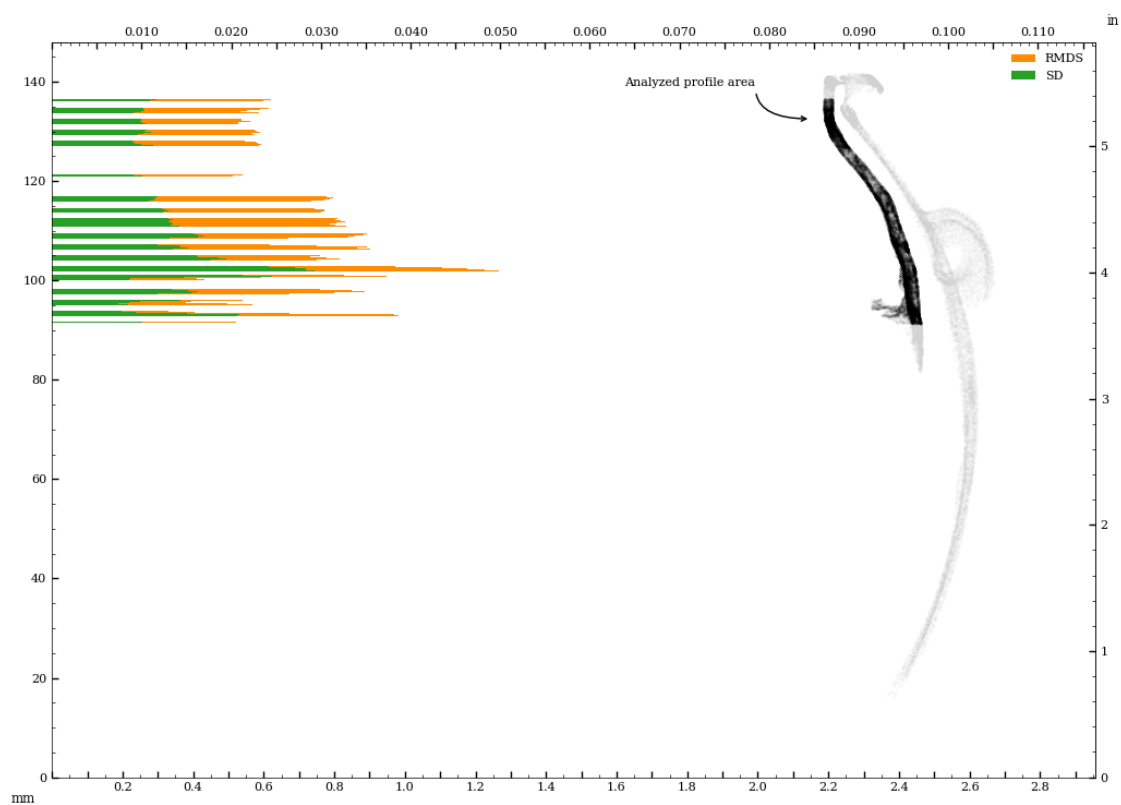


Figure 74: Vessel circularity of interior surface, perpendicular to surface curvature, standard deviation and median absolute deviation.

Circularity analysis of interior surface, in z-plane, Standard Deviation and Root Mean Squared Deviation

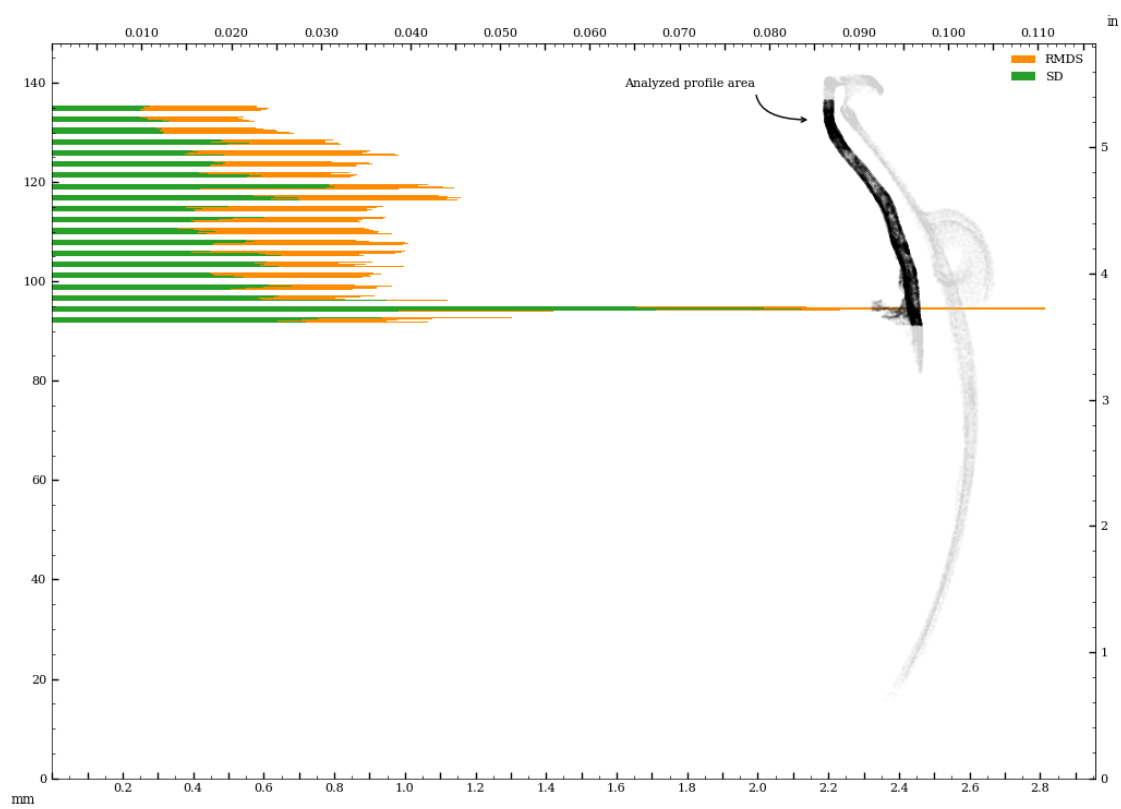


Figure 75: Vessel circularity of interior surface, in z-plane, standard deviation and median absolute deviation.

Circularity analysis of interior separately aligned surface - perpendicular to surface curvature

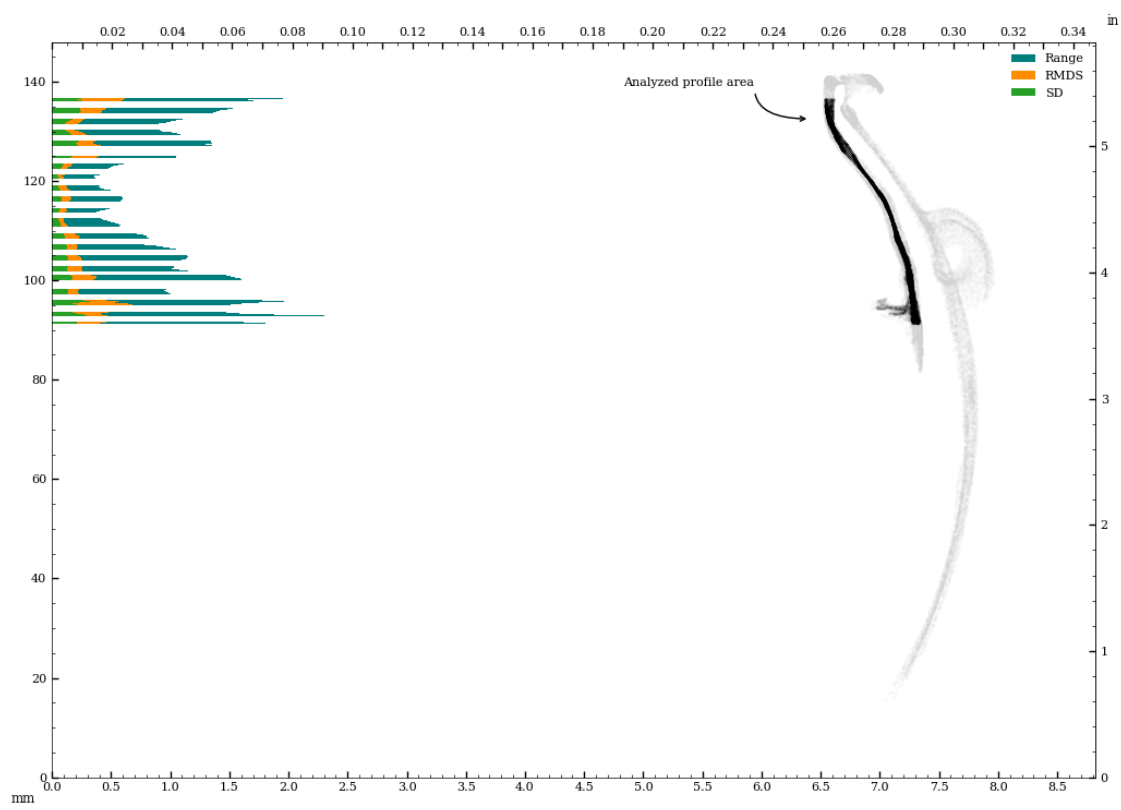


Figure 76: Circularity of interior_separate surface - perpendicular to surface curvature.

Circularity analysis of interior separately aligned surface - in z-plane

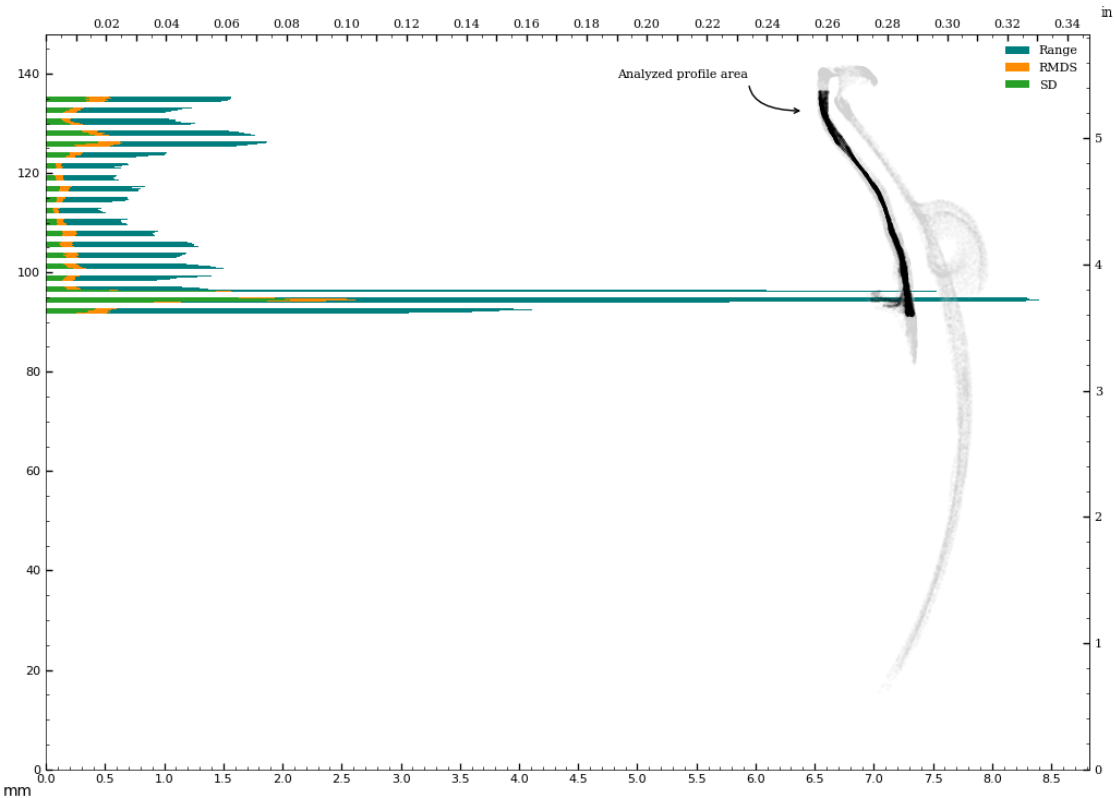


Figure 77: Circularity of interior_separate surface - in z-plane.

Circularity analysis of interior separately aligned surface, perpendicular to surface curvature, Standard Deviation and Root Mean Squared Deviation

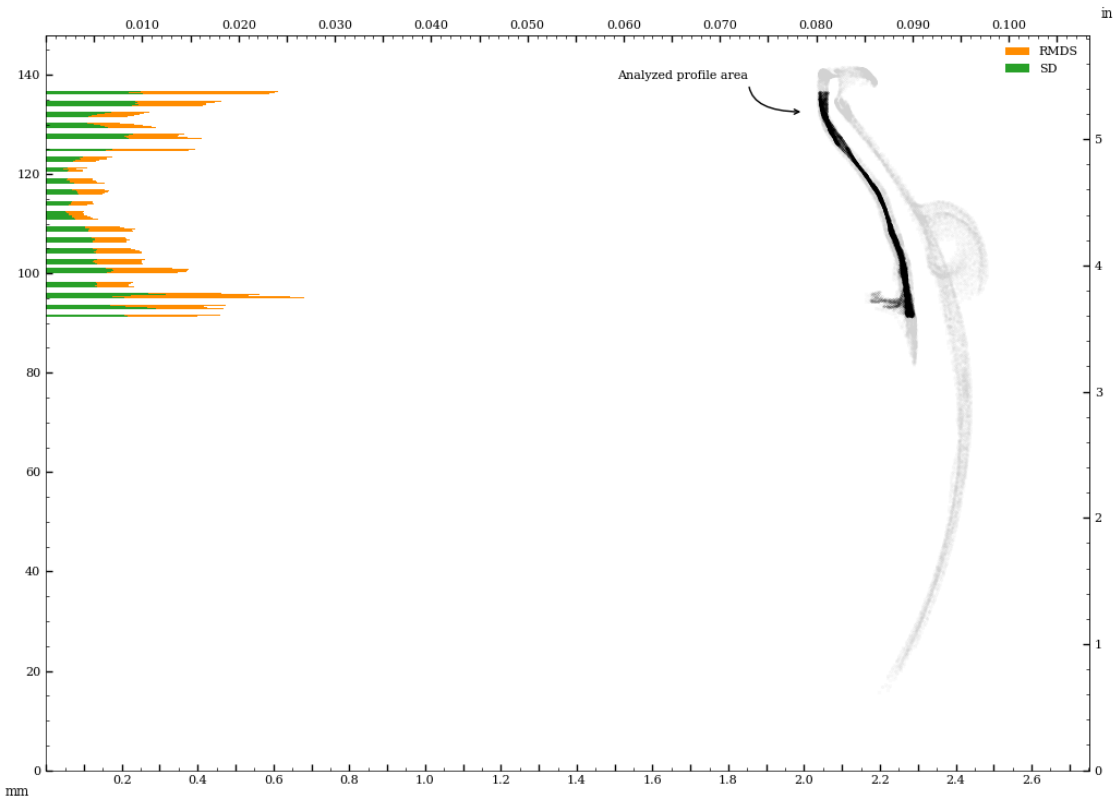


Figure 78: Vessel circularity of interior_separate surface, perpendicular to surface curvature, standard deviation and median absolute deviation.

Circularity analysis of interior separately aligned surface, in z-plane, Standard Deviation and Root Mean Squared Deviation

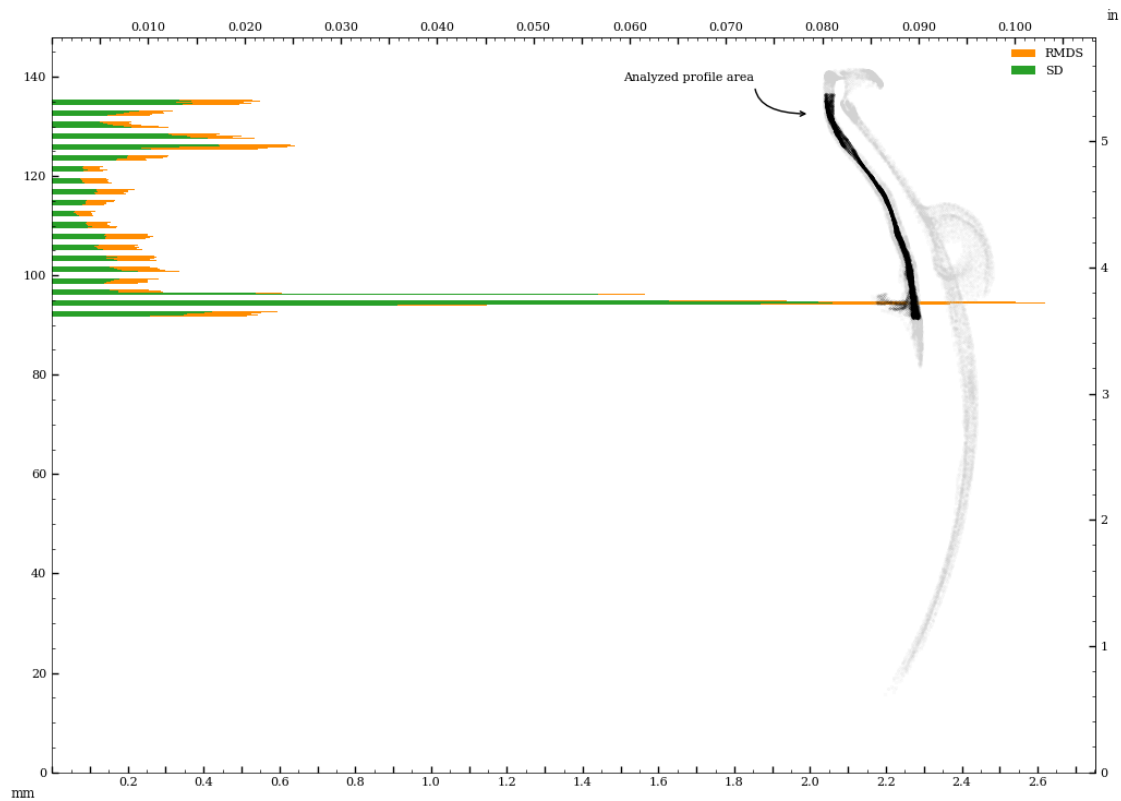


Figure 79: Vessel circularity of interior_separate surface, in z-plane, standard deviation and median absolute deviation.

Appendix B - Comparison Of Concentricity Measurements (Z-plane vs. surface-perpendicular)

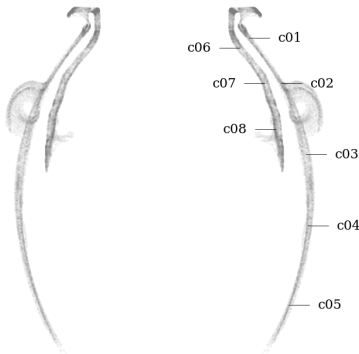


Figure 80: Circularity measurement sample locations, full mesh aligned to exterior surface

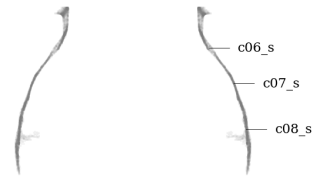


Figure 81: Circularity measurement sample location, separately aligned interior mesh

Concentricity measurements perpendicular to surface curvature

Tag	Reference	Deviation	Sample size	Circle fit residuals analysis for sample listed in Tag column						
				Range full	Range inliers	RMSD full	RMDS inliers	SD full	SD inliers	Center (x,y)
		mm		mm	mm	mm	mm	mm	mm	μm
c01	z-axis	0.762	162	2.381	2.381	0.637	0.637	0.330	0.330	−641, 412
c02	z-axis	0.401	144	2.805	2.805	0.735	0.735	0.370	0.370	323, 239
c03	z-axis	0.389	172	3.682	3.682	1.112	1.112	0.565	0.565	234, −310
c04	z-axis	0.242	185	2.907	2.907	0.753	0.753	0.388	0.388	−192, −146
c05	z-axis	0.413	125	2.619	2.619	0.752	0.752	0.404	0.404	59, 409
c06	z-axis	1.181	173	2.406	2.406	0.875	0.875	0.363	0.363	−1180, 49
c06_s	z-axis	0.843	321	3.416	3.416	1.135	1.135	0.505	0.505	−372, 756
c07	z-axis	1.279	262	5.452	5.452	1.756	1.756	0.734	0.734	−810, −990
c07_s	z-axis	0.048	267	0.463	0.463	0.122	0.122	0.059	0.059	−48, −3
c08	z-axis	1.217	418	5.687	5.687	2.056	2.055	0.782	0.784	−569, −1076
c08_s	z-axis	0.204	380	1.230	1.065	0.282	0.274	0.157	0.154	202, 30
c02	c07	1.671								1133, 1228

Concentricity measurements in z-plane

Tag	Reference	Deviation	Sample size	Circle fit residuals analysis for sample listed in Tag column						
				Range full	Range inliers	RMSD full	RMDS inliers	SD full	SD inliers	Center (x,y)
		mm		mm	mm	mm	mm	mm	mm	μm
c01	z-axis	0.762	162	2.381	2.381	0.637	0.637	0.330	0.330	−641, 412
c02	z-axis	0.401	144	2.805	2.805	0.735	0.735	0.370	0.370	323, 239
c03	z-axis	0.389	172	3.682	3.682	1.112	1.112	0.565	0.565	234, −310
c04	z-axis	0.242	185	2.907	2.907	0.753	0.753	0.388	0.388	−192, −146
c05	z-axis	0.413	125	2.619	2.619	0.752	0.752	0.404	0.404	59, 409
c06	z-axis	1.181	173	2.406	2.406	0.875	0.875	0.363	0.363	−1180, 49
c06_s	z-axis	0.843	321	3.416	3.416	1.135	1.135	0.505	0.505	−372, 756
c07	z-axis	1.279	262	5.452	5.452	1.756	1.756	0.734	0.734	−810, −990
c07_s	z-axis	0.048	267	0.463	0.463	0.122	0.122	0.059	0.059	−48, −3
c08	z-axis	1.217	418	5.687	5.687	2.056	2.055	0.782	0.784	−569, −1076
c08_s	z-axis	0.204	380	1.230	1.065	0.282	0.274	0.157	0.154	202, 30
c02	c07	1.671								1133, 1228

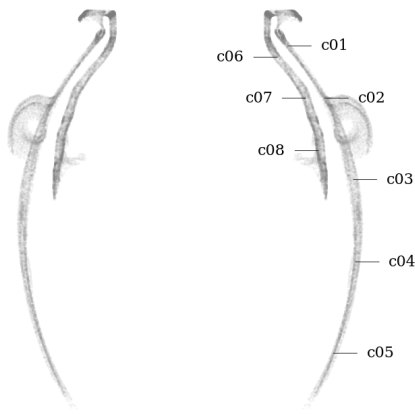


Figure 82: Circularity measurement sample locations, full mesh aligned to exterior surface



Figure 83: Circularity measurement sample location, separately aligned interior mesh

Concentricity measurements perpendicular to surface curvature

Tag	Reference	Deviation	Sample size	Circle fit residuals analysis for sample listed in Tag column						
				Range full	Range inliers	RMSD full	RMDS inliers	SD full	SD inliers	Center (x,y)
		in		in	in	in	in	in	in	thou
c01	z-axis	0.0300	162	0.0938	0.0938	0.0251	0.0251	0.0130	0.0130	−25.2, 16.2
c02	z-axis	0.0158	144	0.1104	0.1104	0.0289	0.0289	0.0146	0.0146	12.7, 9.4
c03	z-axis	0.0153	172	0.1450	0.1450	0.0438	0.0438	0.0222	0.0222	9.2, −12.2
c04	z-axis	0.0095	185	0.1144	0.1144	0.0297	0.0297	0.0153	0.0153	−7.6, −5.8
c05	z-axis	0.0163	125	0.1031	0.1031	0.0296	0.0296	0.0159	0.0159	2.3, 16.1
c06	z-axis	0.0465	173	0.0947	0.0947	0.0344	0.0344	0.0143	0.0143	−46.5, 1.9
c06_s	z-axis	0.0332	321	0.1345	0.1345	0.0447	0.0447	0.0199	0.0199	−14.7, 29.8
c07	z-axis	0.0503	262	0.2147	0.2147	0.0692	0.0692	0.0289	0.0289	−31.9, −39.0
c07_s	z-axis	0.0019	267	0.0182	0.0182	0.0048	0.0048	0.0023	0.0023	−1.9, −0.1
c08	z-axis	0.0479	418	0.2239	0.2239	0.0809	0.0809	0.0308	0.0309	−22.4, −42.3
c08_s	z-axis	0.0080	380	0.0484	0.0419	0.0111	0.0108	0.0062	0.0061	8.0, 1.2
c02	c07	0.0658								44.6, 48.4

Concentricity measurements in z-plane

Tag	Reference	Deviation	Sample size	Circle fit residuals analysis for sample listed in Tag column						
				Range full	Range inliers	RMSD full	RMDS inliers	SD full	SD inliers	Center (x,y)
		in		in	in	in	in	in	in	thou
c01	z-axis	0.0300	162	0.0938	0.0938	0.0251	0.0251	0.0130	0.0130	−25.2, 16.2
c02	z-axis	0.0158	144	0.1104	0.1104	0.0289	0.0289	0.0146	0.0146	12.7, 9.4
c03	z-axis	0.0153	172	0.1450	0.1450	0.0438	0.0438	0.0222	0.0222	9.2, −12.2
c04	z-axis	0.0095	185	0.1144	0.1144	0.0297	0.0297	0.0153	0.0153	−7.6, −5.8
c05	z-axis	0.0163	125	0.1031	0.1031	0.0296	0.0296	0.0159	0.0159	2.3, 16.1
c06	z-axis	0.0465	173	0.0947	0.0947	0.0344	0.0344	0.0143	0.0143	−46.5, 1.9
c06_s	z-axis	0.0332	321	0.1345	0.1345	0.0447	0.0447	0.0199	0.0199	−14.7, 29.8
c07	z-axis	0.0503	262	0.2147	0.2147	0.0692	0.0692	0.0289	0.0289	−31.9, −39.0
c07_s	z-axis	0.0019	267	0.0182	0.0182	0.0048	0.0048	0.0023	0.0023	−1.9, −0.1
c08	z-axis	0.0479	418	0.2239	0.2239	0.0809	0.0809	0.0308	0.0309	−22.4, −42.3
c08_s	z-axis	0.0080	380	0.0484	0.0419	0.0111	0.0108	0.0062	0.0061	8.0, 1.2
c02	c07	0.0658								44.6, 48.4